Design, synthesis, and biological evaluation of 1,8-naphthyridine derivatives as RSK4 inhibitors for the treatment of lung cancer

A Thesis Submitted by

Luiza dos Reis Cruz

In partial fulfilment of the requirements for the degree of

Doctor of Philosophy

Supervisors:

Prof. Anthony G M Barrett, FRS, FMedSci

Prof. Matthew J Fuchter

Department of Chemistry

Imperial College London

October 2018

Declaration of Originality

I, Luiza dos Reis Cruz, certify that the research described in this manuscript was carried out under the supervision of Professor Anthony G. M. Barrett and Professor Matthew Fuchter, Imperial College London, and Doctor Deborah Lanigan, Vanderbilt University. Except where specific reference is made to the contrary, it is original work produced by the author and neither the whole nor any part had been submitted before for a degree in any other institution

Copyright Declaration

Abstract

Lung cancer is the most common cause of cancer death worldwide and it has one of the lowest survival rates among tumours, thus the need to develop new drugs to treat the disease is clear. Among the different kinases involved in cancer pathologies in general, and in lung cancer, we focused our efforts on the validation of RSK4 as a tumour promoter in the lungs. Preliminary unpublished results suggested the antibiotics trovafloxacin and moxifloxacin inhibit RSK4 activation and as consequence increase chemosensitisation to cisplatin, decreasing cell survival and preventing cell invasion and migration. To validate these findings and try to establish the necessary features for compound activity, trovafloxacin was successfully synthesised in gram scale, along with 47 analogues to allow for structure-activity relationship studies.

To do so, a biochemical assay was envisioned to study the ability of our compounds to inhibit RSK activation by its upstream kinase ERK. To this end, both kinases were recombinantly expressed and purified, and we have ongoing efforts to achieve the necessary conditions for compound assessment. Additionally, we were able to develop a HEK-293 cell line stably overexpressing RSK4 for a cell-based assay aimed at the measurement of RSK4 phosphorylation levels, and preliminary results show that some of our analogues were able to decrease RSK4 activation in comparison to the controls used. This assay was supported by analyses by tandem mass spectrometry.

Finally, *in vivo* studies using trovafloxacin in a xenograft mouse model highlighted the ability of the antibiotic to prevent cell survival, invasion and migration, and to enhance cisplatin effects.

Acknowledgements

First, I would like to thank my supervisors, Professors Tony Barrett and Matt Fuchter. They have helped me to be a better medicinal chemist and scientist, and for this I will always be extremely grateful.

I would also like to thank Doctor Deborah Lannigan for being my scientific mentor when I was at Vanderbilt University. Postdoctoral fellows Jochen, Ainoa, and Harry at Imperial and Kasia and Shinji at Vanderbilt have all taught me so much in the laboratory throughout these four years. Without them, this thesis would not exist. In addition, I would like to thank the Coordenação de Pessoal de Nivel Superior, CAPES/Brasil, for my funding throughout these four years.

I am also thankful for the supportive staff at Imperial College, especially Pete Haycock and Lisa Haigh, and Professors Chris Braddock and Alan Spivey, and Dr. Peter DiMaggio. In addition, Professor Phil Parsons and Virginia have made my days so much brighter in the department.

To all my friends that I have shared uncountable hours in the lab, Hannah, Alex, Katie, Melis, James, Josh, René, Sara, Linda, Freeman, Frances, and Zach. And to all past and current members of Barrett, Fuchter and Parsons groups. Sorry if you did not like my musical taste. And to all my friends in London, thank you for being my extended family for four years. You made everything much easier.

Finally, none of this would be possible without my parents, Mauricio and Eleni, and my sister, Mariane. They supported me in every possible way in this crazy adventure and this work is for them.

However, for practical purposes, in a hopelessly practical world…

The God of Small Things, Arundhati Roy

Abbreviations

Throughout this manuscript, abbreviations and acronyms recommended by the American Chemical Society in the Organic Chemistry and Medicinal Chemistry areas have been employed (revised in the *Journal of Organic Chemistry* and *Journal of Medicinal Chemistry* on August 2018; http://pubs.acs.org/paragonplus/submission/joceah/joceah_abbreviations.pdf and http://pubs.acs.org/paragonplus/submission/jmcmar/jmcmar_abbreviations.pdf). In addition, those indicated below have also been used.

AGC	Protein Kinase A, G, and C Family
BLAST	Basic Local Alignment Search Tool
CAMK	Ca^{2+}/calmodulin-dependent Protein Kinase
CBB	Coomassie Brilliant Blue
CDX	Cell Line-Derived Xenograft
CHO	Chinese Hamster Ovary cells
CTKD	C-Terminal Kinase Domain
ERα	Estrogen Receptor α
FACS	Fluorescence-Activated Cell Sorting
GFP	Green Fluorescent Protein
HEK293	Human Embryonic Kidney cells
HTRF	Homogenous Time Resolved Fluorescence
IDILI	Idiosyncratic Drug-Induced Liver Injury
IPTG	Isopropyl β-D-1-thiogalactopyranoside
LUAD	Lung Adenocarcinoma
LUSC	Lung Squamous Cell Carcinoma
KRAS	Kirsten rat sarcoma
MEK	MAPK/ERK Kinase

MIRC	Michael-Initiated Ring Closure
MOI	Multiplicity of Infection
MSK	Mitogen- and Stress-Activated Protein Kinase
mTOR	Mechanistic Target of Rapamycin
Ni-NTA	Nickel Nitrilotriacetic Acid
NSCLC	Non-Small Cell Lung Cancer
NTKD	N-Terminal Kinase Domain
PDK1	Phosphoinositide-Dependent Kinase-1
PK	Protein Kinases
rpS6	Ribosomal protein S6
RSK	Ribosomal S6 Kinase
Sf9	*Spodoptera frugiperda* cells
S_NAr	Nucleophilic Aromatic Substitution
SCLC	Small Cell Lung Cancer
TNBC	Triple-Negative Breast Cancer
TP53	Tumour Protein 53

Table of Contents

1. General Introduction

1.1. Lung Cancer

1.1.1. Key facts and statistics

Cancer is one of the leading causes of morbidity and mortality worldwide, accounting for approximately 14 million new cases and 8 million related deaths in 2012. From those, approximately 1.8 million cases and 1.6 million deaths are caused by lung cancer, making it the most common cause of cancer death.[1]

According to Cancer Research UK, lung cancer is the second most common cancer diagnosed in women (after breast cancer) and in men (after prostate cancer) in the UK. Over the last decade, incidence rates have decreased by around 10% among males, whereas rates in females increased by around 18%. Moreover, incidence rates are highest in people aged 85 to 89. In England and Wales, the survival rates after one, five and ten or more years are 32, 10 and 5%, respectively. This may be because almost 75% of patients are diagnosed at a late stage when curative treatment is not viable. Around 46,000 people were diagnosed with lung cancer in the UK in 2015 and in the same year, over 35,000 people have died from it.

Tobacco use is the most important risk factor for lung cancer, causing about 80 to 90% of cases in the United States.[2] Additionally, other lifestyle factors have been linked to lung cancer, such as ionising radiation, air pollution, and diesel engine exhaust.

1.1.2. Cellular and molecular origins

Lung tumours can be classified into two main histopathological groups: small cell lung cancer (SCLC) and non-small cell lung cancer (NSCLC), the latter accounting for 85% of all cases.[3] NSCLC can be subdivided into lung adenocarcinoma (LUAD) and lung squamous cell carcinoma (LUSC). These subtypes generally follow a proximal-to-distal distribution pattern: LUSC arising mostly in the upper airways, whereas LUAD and SCLC have origins in the lower airways. Thus, it is suggested that these subclasses arise from distinct cellular origins localised within a defined epithelium niche.[4]

Lung carcinogenesis, like most malignancies, is a complex, molecularly heterogeneous process characterized by the accumulation of numerous alterations. Abnormal signalling pathways, insensitivity to growth-inhibitory signals, abnormalities in cell cycle regulation, evasion of programmed cell death, limitless cell division, ability to develop new blood vessels, and tissue invasion and metastasis are some of the cellular defects caused by genetics damages associated with cancer.[5] The most common of these aberrant pathways for NSCLC are shown in **Figure 1**.

In LUAD, the two most common mutations are found in Kirsten rat sarcoma (KRAS) and epidermal growth factor receptor (EGFR) genes. In addition, tumour protein p53 (TP53) alterations are present in more than 46% of LUAD and 90% of LUSC.[3] Some of these alterations might play different roles during different stages of carcinogenesis, some accounting for early initiation, like KRAS, while other are responsible for tumour progression, like TP53. Interestingly, molecular markers are considerably distinct between smokers and non-smokers. More importantly however, the identification of these genetic alterations is paramount in the selection of the right treatment.

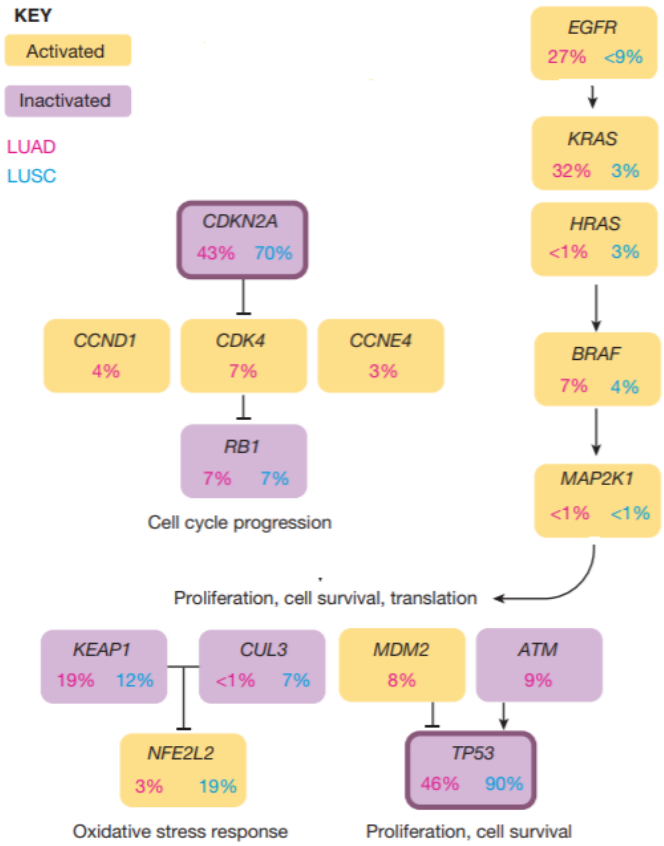

Figure 1 – Common genetic alterations in NSCLC involving key pathway components. EGFR: epidermal growth factor receptor; KRAS: Kirsten rat sarcoma; HRAS: GTPase transforming protein p21; BRAF: proto-oncogene B-Raf; MAP2K1: dual specificity mitogen-activated protein kinase 1; CDKN2A: cyclin-dependent kinase inhibitor 2A; CCND1: cyclin D1; CDK4: cyclin-dependent kinase 4; CCNE4: cyclin E4; RB1: retinoblastoma protein 1; KEAP1: Kelch-like ECH-associated protein 1; CUL3: cullin 3; MDM2: mouse double minute 2 homolog; ATM: ataxia-telangiectasia mutated protein; NFE2L2: nuclear factor (erythroid-derived 2)-like 2; TP53: tumour protein p53. Adapted from Herbst et al.[3].

1.1.3. Current treatments and unmet needs

Platinum-based doublet therapy (two chemotherapy drugs given together) has been the standard therapy combination for NSCLC patients, especially during early stages of the disease. Most commonly, cisplatin is used in combination with vinca alkaloids, like vindesine, vinblastine, vinorelbine, or docetaxel, the latter also being used as a single-agent second-line therapy.[6] Surgical intervention has also been proved to be most effective for initial stages.

However, platinum-based therapy only offers symptomatic relief and modest survival increase, between 7 to 10 months across all combinations. Moreover, chemotherapy is palliative at best in patients, with advanced disease and significant toxicity being often an issue due to the inability of these drugs to target cancer cells versus healthy ones.

To overcome this challenge, molecularly targeted therapies started around 20 years ago, with gefitinib, an oral EGFR tyrosine kinase inhibitor, being introduced as a monotherapy for NSCLC. Erlotinib, another EGFR inhibitor, is also available as second- and third-line treatment options. Monoclonal antibody cetuximab directed against the extracellular domain of EGFR was also developed and can be used in combination with standard chemotherapy.[7] In addition, crizotinib, an oral small-molecule that inhibits the anaplastic lymphoma kinase present in 3 to 5% of NSCLCs, is also available.[8]

Unfortunately, even though targeted drugs overcome some of the side effects associated with traditional therapies, they can only be used in small sub-sets of patients. In addition, resistance has been widely reported.[9] Therefore, there is an urgent need to find new targets for the development of novel targeted therapies for the treatment of lung cancer.

1.2. Protein Kinases

1.2.1. Overview of kinase biology

Protein phosphorylation is one of the most significant signal transduction mechanisms by which intercellular signals regulate crucial processes such as cell proliferation and differentiation. Approximately, 20% of all the 32,000 human genes encode proteins involved in signal transduction. Among these are 518 protein kinases (PKs), enzymes that regulate the phosphorylation of specific amino acids using adenosine triphosphate (ATP) as the source of phosphate.[10] As exemplified by the EGFR family, some PKs (and

their associated messengers) are involved in many pathologies and therefore are considered the largest druggable gene family.[11]

Briefly, PKs work by transferring a γ-phosphate from ATP to specific substrates. This phosphorylation may modify the conformation, catalytic properties, and/or interactions of the phosphorylated substrate with other proteins and targets, thus mediating signalling pathways on cell machinery. There are two main classes of PKs: Ser/Thr- and Tyr-specific kinases. Some PKs might also phosphorylate other residues, like histidine, and aspartate or glutamate. In addition, tyrosine kinases can be subdivided into two groups, transmembrane and cytoplasmic kinases, the former named receptor tyrosine kinases. These have an extracellular domain able to bind to specific ligands and play an important role in cell division and differentiation.

All PKs share a similar two-lobe structure: one consisting of β-sheets (N-terminal) and a large lobe comprising α-helices (C-terminal).[12] The ATP-binding pocket is located between these two lobes, where the adenine ring of ATP establishes hydrogen bond interactions with the residues in the kinase hinge. The ribose and phosphate groups bind in a hydrophilic channel extending to the substrate binding site. Moreover, PKs also share a conserved activation loop, that controls their activity. When this activation loop is phosphorylated by an upstream kinase, the enzyme adopts an active conformation while in the absence of the phosphate group, the PK remains in an inactive form, that blocks the substrate binding site.

1.2.2. ERK1/2 and the MAP kinase pathway

As previously stated, PKs are often responsible for signal transduction within the cell machinery, integrating environmental signals and translating them into the cell control system. Moreover, activating mutations (upregulation) of key signalling pathways are

often present in many solid tumours. One important example is the Ras-dependent extracellular signal-regulated kinases 1 and 2 (ERK1/2) cascade of the generic mitogen-activated protein kinase (MAPK) pathway (**Figure 2**).[13,14] Indeed, by promoting cell proliferation, kinases present in this pathway are considered good therapeutic cancer targets.

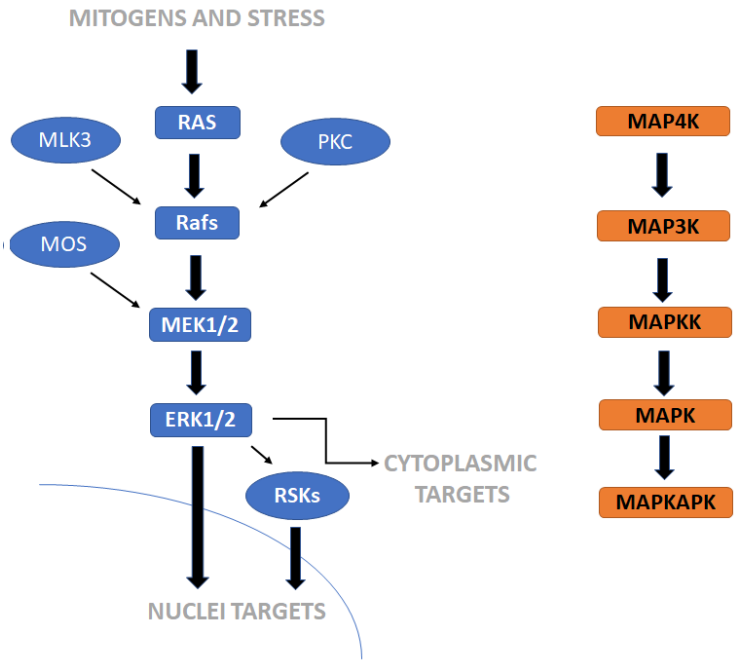

Figure 2 – The MAP kinase pathway.

This pathway is triggered by mitogenic factors, differentiation stimuli and cytokines, that will eventually produce active Ras, which is a small GTPase in charge of cellular signal transduction. Once bound to guanosine-5'-triphosphate (GTP), Ras activates Raf, which in turn phosphorylates the MAPK kinases MEK1/2, finally leading to ERK activation. There are two known ERK genes, ERK1 and 2. The activation of both kinases is initiated by the phosphorylation of a conserved Thr-Glu-Tyr peptide found in the activation loop (Thr183 and Tyr185 in human ERK2). ERKs are ubiquitous proteins that, once activated, phosphorylate a range of regulatory substrates in all cellular compartments. These

include other PKs, signalling effectors, receptors, cytoskeletal proteins, and nuclear transcriptional regulators (**Figure 3**).[13,14]

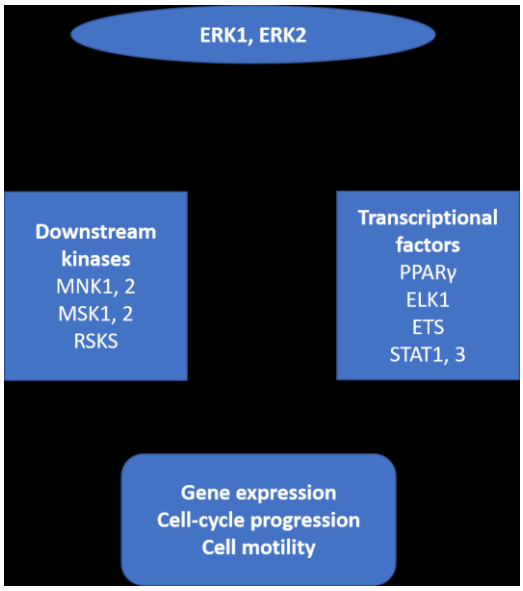

Figure 3 – Downstream effects of ERK activation.

ERK1 and 2 are intrinsically involved in cell growth regulation. This could be through global mRNA translation (via enhancement of mammalian target of rapamycin, mTOR), direct regulation of ribosomal gene transcription, and pyrimidine synthesis. In addition, it has been suggested that ERKs might be involved in the regulation of G2/M transition and mitosis.[15]

1.2.3. PKs and their role in drug discovery

Having so many roles under physiological conditions, it is not surprising that abnormal kinase activity is directly connected to many diseases, especially those involving inflammatory and proliferative responses.[16]

There are three types of aberrant kinase functions linked to cancer proliferation and survival. The first type includes kinases that have become resistant to normal regulatory

mechanisms and are oncogenic. Their constitutive functionalisation is essential for cancer cells in a so-called oncogene addiction, making these malignancies extremely susceptible to kinase inhibitors. The second type consists of synthetic lethal kinases. They are usually not mutated nor oncogenic but are in key pathways downstream of oncogenes. Inhibition of these kinases creates a lethal phenotype when paired with a non-lethal mutation in the tumour cells. The third class of kinases are required for different stages in carcinogenesis and maintenance, such as the vascular endothelial growth factor receptor (VEGFR) kinase, responsible for developing and sustaining blood supply to cancer cells.[17]

There are different types of kinase inhibitors, namely ATP-competitive, covalent inhibitors, allosteric modulators, and inhibitors of kinase activation.

Most commonly, kinase inhibitors bind to the ATP binding site of PKs. These ATP-competitive inhibitors recognise the active conformation of the kinase and typically consist of a heterocyclic ring (to mimic the purine in ATP) and side chains that will sit at the adjacent hydrophobic regions (**Figure 4**).

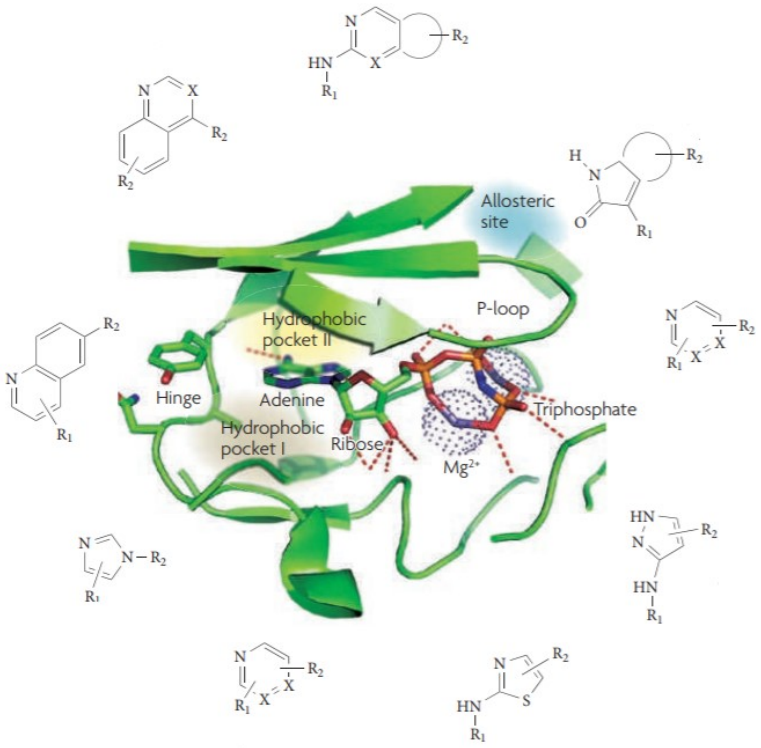

Figure 4 – The ATP binding site of AKT with key regions and bonds. Commonly used heterocyclic core scaffolds (X = C, N). From Zhang et al.[17].

In addition, ATP-competitive inhibitors can bind to an active (type I inhibitors) or inactive (type II inhibitors) conformation, depending on the position of the conserved region Asp-Phe-Gly (called DFG). This motif at the N terminus of the activation loop is flipped out (DFG out) when the kinase is in a catalytically inactive state if compared to an active state (DFG in).

There a few challenges however. ATP binds to a very conserved region of PKs and finding an inhibitor that is selective for only one kinase can be difficult. Furthermore, these inhibitors must present high potency to compete with ATP's millimolar concentrations inside cells.[18]

A second type of inhibitors bind to a different region than the ATP-binding site and are called allosteric inhibitors. Ligands that bind to an allosteric site can stabilise either an active (promotes target activation) or inactive (blocks further target binding) conformation

of the target receptor. In the case of kinases, these different conformations can either promote or block the binding of ATP or protein substrate. Allosteric inhibitors usually have the highest degree of kinase selectivity, since allosteric sites are less conserved.[19]

Another drug discovery strategy for allosteric inhibitors is the development of compounds that inhibit kinase activation. These are molecules that by binding to an allosteric region of a specific kinase prevent it from being phosphorylated by the next upstream kinase in the cascade. The few examples of these inhibitors display exquisite specificity since they can bind to unique sites and are not ATP competitors.[18] To identify these molecules, it is necessary to set up screens including two consecutive kinases in a given cascade and then identify whether the tested compounds are direct kinase inhibitors of either of them or if they act by preventing kinase activation of the downstream component.

Furthermore, a third type of inhibitors can form irreversible bonds with the kinase active site. Frequently, these covalent inhibitors are developed by structure-guided incorporation of an electrophilic subunit that can react with the highly nucleophilic thiol group of cysteine and, more recently, to lysine residues.[20] By permanently binding to kinases, enzymatic activity is only restored with protein biosynthesis. One major concern of covalent inhibitors is toxicity, specially through haptenization.[21]

1.3. Ribosomal S6 Kinase (RSK) family

1.3.1. RSK family

The ribosomal S6 kinase (RSK) family of proteins is one of the many ERK substrates (**Figure 5**).

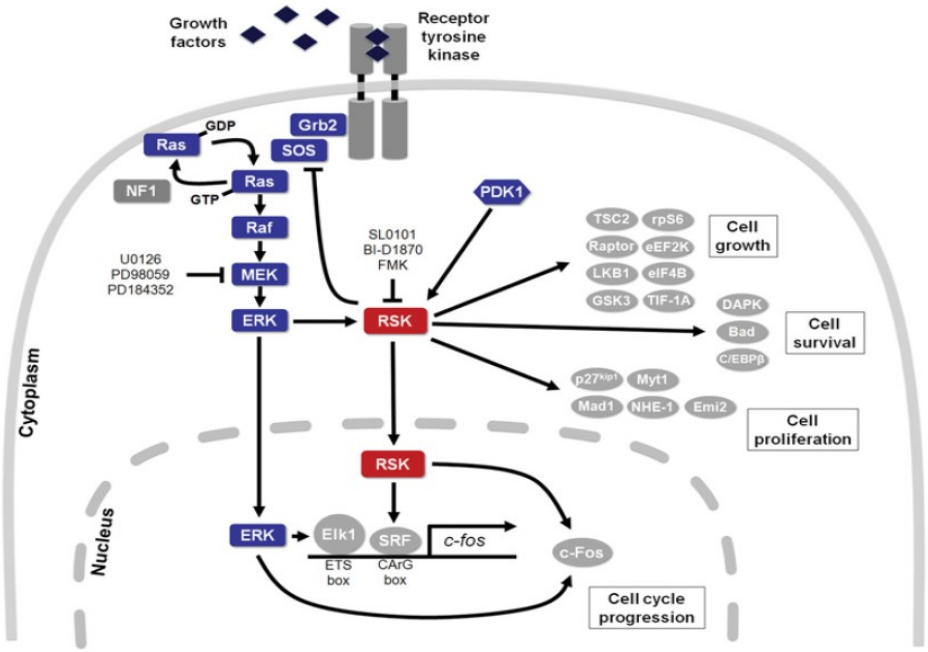

Figure 5 – RSK family in the MAP kinase pathway. U0126, PD98059, and PD184352 are MEK inhibitors. SL0101, BI-D1870, and FMK are RSK inhibitors. From Romeo et al.[22]

They are cytoplasmic Ser/Thr kinases that phosphorylate the ribosomal protein S6 (rpS6), among other substrates. rpS6 is a component of the 40S ribosomal subunit and therefore is involved in translational regulation. In humans, four RSK isoforms (RSK1–4) and two structurally related homologues (mitogen- and stress-activated kinases, MSK1/2) have been identified. RSK2 is the best characterised isoform and most of its substrates have been identified.[22–24] However, these may be shared with other isoforms or even with other AGC family members since most studies have not addressed substrate selectivity.[25]

The RSK family is involved in important processes within the cell. As effectors of ERK, they mediate global transcription control and RNA translation as well as regulation of mediators of the cell cycle, and many other physiological functions.[26] Moreover, the gene encoding RSK2 has also been implicated in the Coffin-Lowry syndrome, which is associated with mental retardation, and skeletal and cardiac effects.[27]

Except for RSK4, mRNA expression of RSK isoforms has been confirmed to be ubiquitous in all tested human tissues (**Figure 6**). Nevertheless, it has been shown that at least some functions found in different tissues and developmental phases are isoform-specific. For instance, RSK1 and RSK3 have a temporal regulation pattern in the nervous system, RSK1 being important in early development stages and RSK3 in later stages.[22]

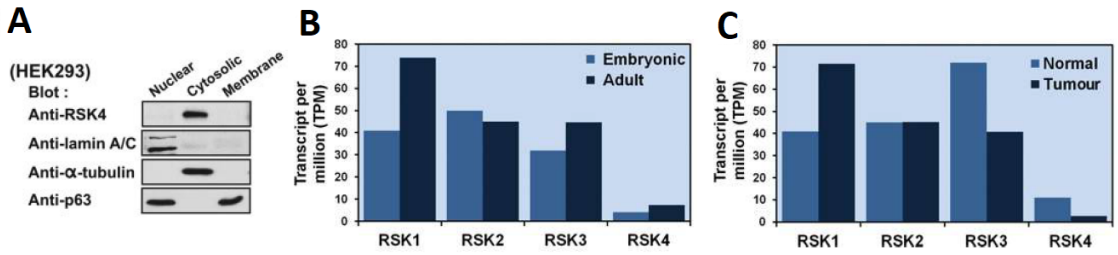

Figure 6 – Subcellular localization (A) of RSK4 and expression pattern (B and C) of RSK isoforms. Adapted from Dummler et al.[28] and Romeo et al.[22]

The four RSK isoforms display high homology, especially in their N- and C-terminal kinase domains, NTKD and CTKD, respectively (**Figure 7A**).[22,25,29] Indeed, the presence of two different catalytic domains within the same polypeptide is the most impressive feature about the family. The NTKD, which is responsible for substrate phosphorylation, is homologous to the catalytic domains of AGC kinases whereas the CTKD (autophosphorylation) is related to the kinase domains found in the calcium/calmodulin-dependent protein kinase (CAMK) family. The two domains are connected by a linker region of about 100 amino acids (**Figure 7B**).

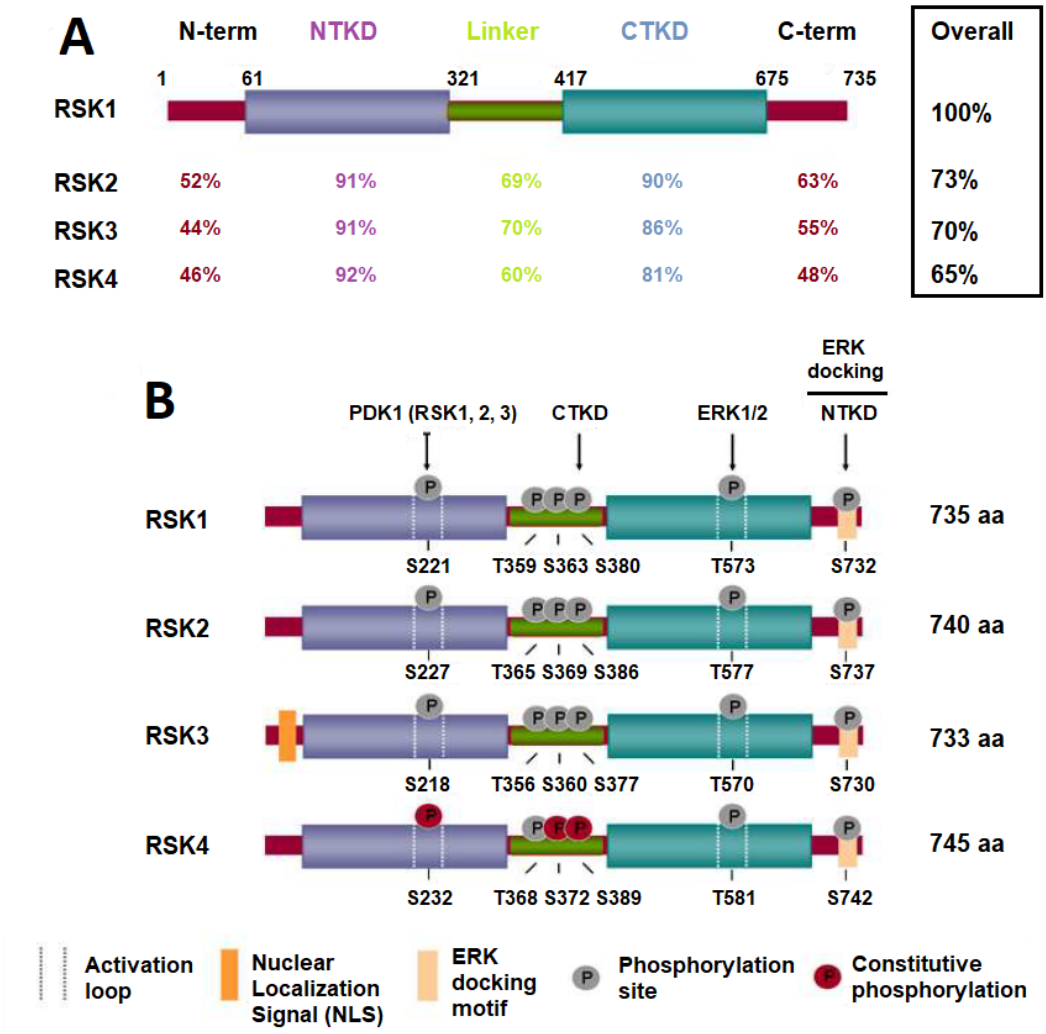

Figure 7 – Schematic representation of members of the RSK family. **A**. Homology percentage between RSK1 and the other human RSKs. **B**. Functional domains and phosphorylation sites of the RSK isoforms. Adapted from Carriere et al.[25]

Moreover, RSK1–3 also require the 3-phosphoinositide-dependent protein kinase 1 (PDK1), besides ERK1/2, for their complete activation. PDK1 is a constitutively active kinase that is broadly expressed. It has been shown that it is responsible for basal RSK phosphorylation in cells, whereas upon stimulation by growth factors, RSK activation requires both PDK1 and ERK1/2.[30]

Activation of the RSKs is initiated after mitogenic stimulation, promoting the recruitment of ERK1/2 for the transfer of the phosphate group. In the case of RSK1, ERK1/2 phosphorylates Thr573 in the activation loop of CTKD, and Thr359 and Ser363 in the

linker region. The activated CTKD then proceeds to the autophosphorylation of Ser380 (hydrophobic motif in the linker). This event creates a docking site for PDK1 which, in turn, phosphorylates Ser221 in the activation loop of NTKD, leading to a fully active RSK1 ready for the phosphorylation of downstream substrates (**Figure 8**).

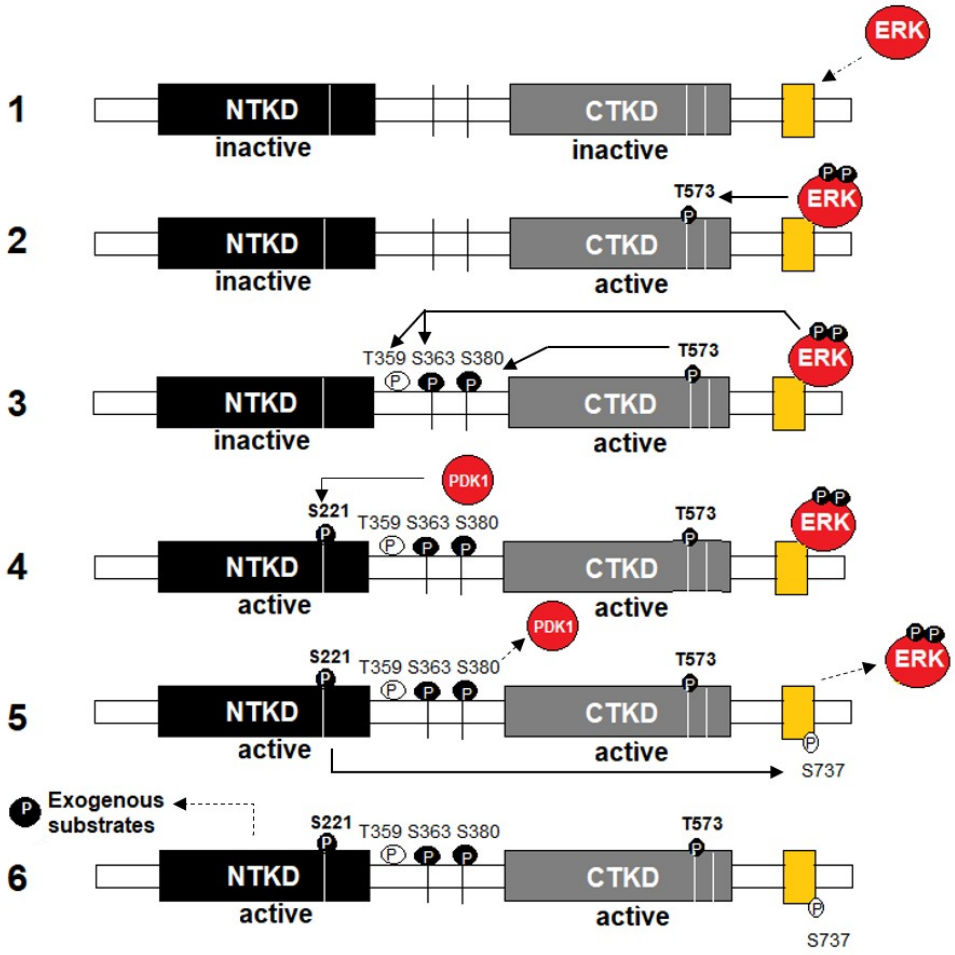

Figure 8 – Model of RSK1 activation. Adapted from Romeo et al.[22]

This process occurs in a similar way for RSK1–3. However, other mechanisms of activation have been studied. For example, RSK2 can also be phosphorylated in response to the fibroblast growth factor (FGF) and Src activation. In addition, it has been suggested that residue Ser380 can also be phosphorylated without the participation of CTKD, since when this domain is inactivated by mutagenesis, the phosphorylation of the NTKD is only partially inhibited.[22]

However, activation of RSK4 follows a slightly different process. Unlike RSK2 for example, which needs the presence of a growth factor (for instance, epidermal growth factor, EGF) to be active, endogenous RSK4 is thought to be constitutively activated. In **Figure 9A**, the white columns in the left panel show only a 25% increase in phosphorylation in the presence of EGF, whereas in the right panel, RSK2 kinase activity increases almost 100% when EGF is present.[28] Recombinant RSK4 displays a different pattern however. In **Figure 9B**, an increase of 50% can be seen for RSK4, while RSK2 increase is maintained at high levels. In addition, **Figure 9** also shows that RSK4 activity can be inhibited by U0126, a known MEK1 inhibitor[31].

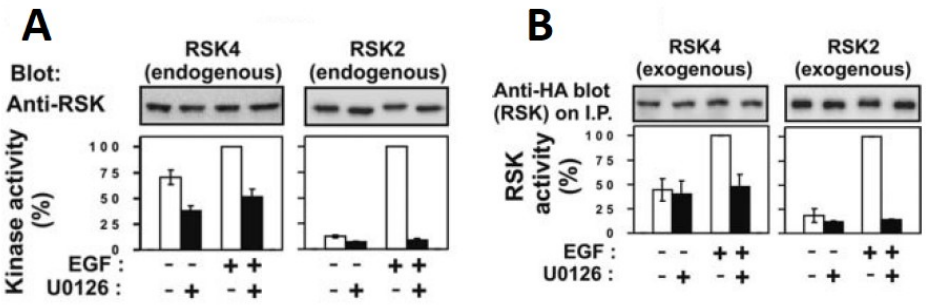

Figure 9 – Endogenous and recombinant RSK4 activity. Adapted from Dummler et al.[28]

Supporting these findings, the same group has also shown that RSK4 has similar levels of phosphorylation in Ser232, Ser 372, and Ser389 (RSK4 specific phosphorylation sites, **Figure 10**) in serum-starved and EGF-stimulated cells. Regarding the 40-50% decrease in activity, seen in **Figure 9**, it is believed that U0126 could reduce global phosphorylation across all kinase sites.

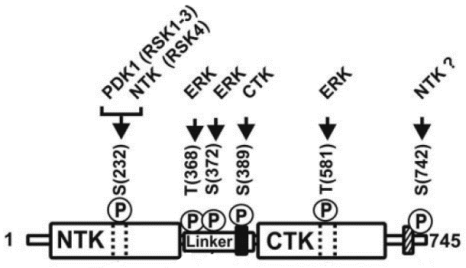

Figure 10 – RSK4 docking sites. From Dummler et al.[28]

Moreover, it has also been shown that mutation in the PDK1 docking site or indeed complete deletion of PDK1 gene does not affect phosphorylation of Ser232. This shows that, differently from the other RSKs, RSK4 does not require PDK1 for its activation.

Conversely, a different activation pathway for endogenous RSK4 has been proposed. Constant activation of Ser232 and Ser389 contribute to keep the NTKD in the active conformation and a low basal ERK activity is responsible for further phosphorylation of Ser372 and Thr581. A mixture of autophosphorylation by the NTKD and CTKD as well as by other kinases contribute to these.

1.3.2. RSK in cancer and drug discovery

RSK isoforms have been correlated to different diseases. In malignancies, RSK1 and RSK2 are believed to be tumour promoters.[32] For instance, RSK2 has been found to be active in 70% of patients with locally advanced breast cancers[33] and in 85% of triple-negative breast cancer (TNBC) tumours[34]. Moreover, overexpression of RSK1 and RSK2 was found in breast cancer when compared to normal tissues.[35] In addition, RSK2 has been shown to be an important regulator in cell proliferation in prostate cancer.[36] RSK2 has also been associated with skin cancer[37] and head and neck tumours[38].

However, RSK3 and RSK4 have more divergent correlations in tumorigenesis. For example, it has been shown that RSK4 gene is down-regulated in various carcinoma (renal and colon) and adenoma (colon) cell lines.[39,40] Interestingly, RSK4 overexpression induced cell arrest and senescence in normal fibroblasts and malignant carcinoma cell lines. Moreover, RSK4 may play a role in the development or progression in breast cancer[41], which was further proved when exogenous RSK4 expression decreased cell proliferation and supressed invasive and migratory activities[42]. Other studies however

have suggested that RSK3/4 overexpression enhances proliferation upon P13K inhibition and that MEK- and RSK-specific inhibitors can overcome this proliferation.[43] It was also found that RSK4 overexpression in renal cell carcinoma could promote cell cycle progression and increase invasive and metastatic activity.[44]

In lung cancer however, the available data regarding the role of RSKs isoforms is not clear. While silencing RSK1 increases metastasis in xenograft models, silencing RSK2 and RSK4 impaired this process, and downregulating both RSK1 and RSK4 increases cell lung invasion and migration.[45] In contrast, inhibition of RSK4 activity was correlated to decreased cell migration and invasion in lung tumours.[46]

1.3.3. RSK4 and lung cancer

Interestingly, the group of Professor Michael Seckl and Dr. Olivier Pardo at the Hammersmith Hospital of Imperial College has identified RSK4 as a potential oncogene in lung tumours (Chrysostomou et al., submitted manuscript). They have shown that silencing RSK4 decreases cell survival in A549 cell lines when in combination with taxol and cisplatin (**Figure 11A**). Moreover, silencing RSK4 enhances cisplatin and taxol potency, as it can be observed from the reduction in cell numbers in the presence of these chemotherapeutic agents in RSK4-silenced cells when compared to normal cancer cells. In the case of cisplatin this fact is believed to be associated with enhanced apoptosis and DNA damage. To prove this, the authors assessed caspase 3/7 activation, since caspases are known to play an essential role in programmed cell death events (**Figure 11B**). Additionally, other mediators of apoptosis, such as anti-apoptotic proteins BCL2 and cIAP1, were also supressed when RSK4 was silenced (**Figure 11C**). Finally, RSK4 downregulation also decreases cell migration and cell invasion in lung malignancies (**Figure 11D** and **E**).

In addition, they have also shown that nearly 60% of primary lung cancers are positive for RSK4, being highest in LUAD and lowest in SCLC cases. Moreover, RSK4 seems to control the invasiveness of LUAD cells and is present in higher levels in 52% of metastatic lesions from LUAD patients. Supportive results were found in RSK4 knockout mice, which showed delayed tumour growth and decreased dissemination.

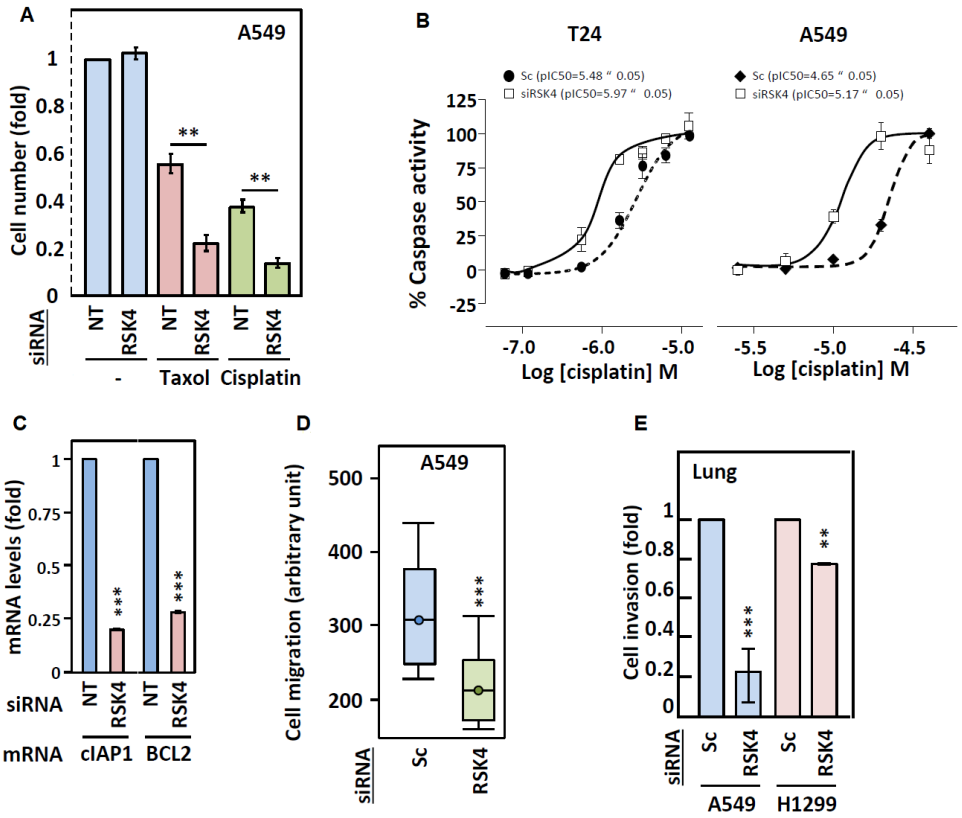

Figure 11 – RSK4 downregulation in lung cell lines. **A**. Decreased cell survival with cisplatin. **B**. Increased caspase activity with cisplatin. **C**. Decreased expression of anti-apoptotic proteins, cIAP1 and BCL2. **D**. Decreased cell migration and **E**. invasion when RSK4 is downregulated. From Chrysostomou et al. (submitted manuscript).

Taking these findings into context, it would be very interesting to find specific inhibitors to validate RSK4 as a tumour promoter in the lung. In this sense, five RSK-specific inhibitors have been identified to date: fmk (irreversible inhibitor),[47] SL0101,[48] BI-D1870,[49] and LJH685 and LJI308[50] (**Figure 12**) (For more information, see reviews by Ludwik and Lannigan[32] and Nguyen[51]).

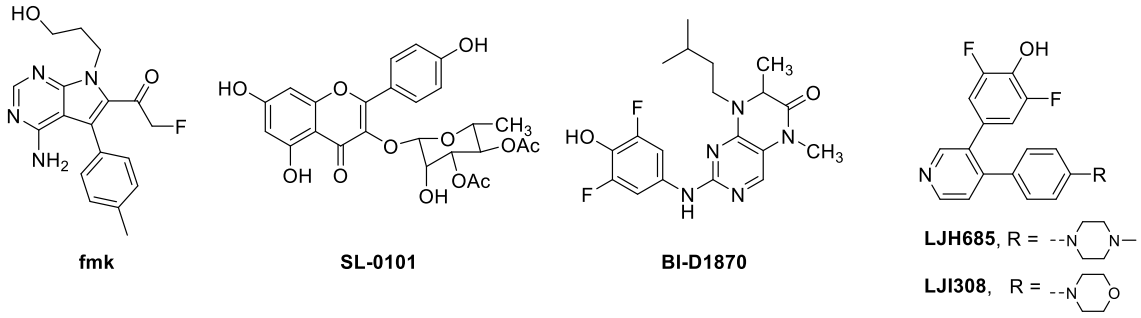

Figure 12 – Known RSK-specific inhibitors.

These inhibitors do not show any specificity towards different RSK isoforms. Moreover, considering that RSK1 is believed to be a tumour suppressor in lung tumours,[45] the use of pan-RSK inhibitors to study the effects of RSK4 in the lung is limited. This highlights the importance of finding specific inhibitors for RSK4.

In this regard, the group of Prof. Seckl and Dr. Pardo has performed a range of screening assays to identify possible inhibitors. They have developed a high through-put Homogenous Time Resolved Fluorescence (HTRF)-based assay to identify compounds that modulate RSK activation by ERK. Using this assay, they have identified moxifloxacin and trovafloxacin, among other antibiotics and fragments, as possible inhibitors, with IC_{50} values under 10 μM (**Figure 13A** and **B**).

In addition, trovafloxacin showed chemosensitisation with cisplatin (**Figure 13C**). Noteworthy, trovafloxacin treatment reproduced RSK4 silencing: increased apoptosis in correlation with decreased BCL2 and cIAP1 (**Figure 13D**) and decreased cell migration and invasiveness (**Figure 13E**). They have also shown through molecular modelling and mathematical modelling of free energy propagation that trovafloxacin binds to the inactive/dephosphorylated NTKD, supporting the hypothesis that trovafloxacin is an allosteric RSK4 NTKD activation inhibitor.

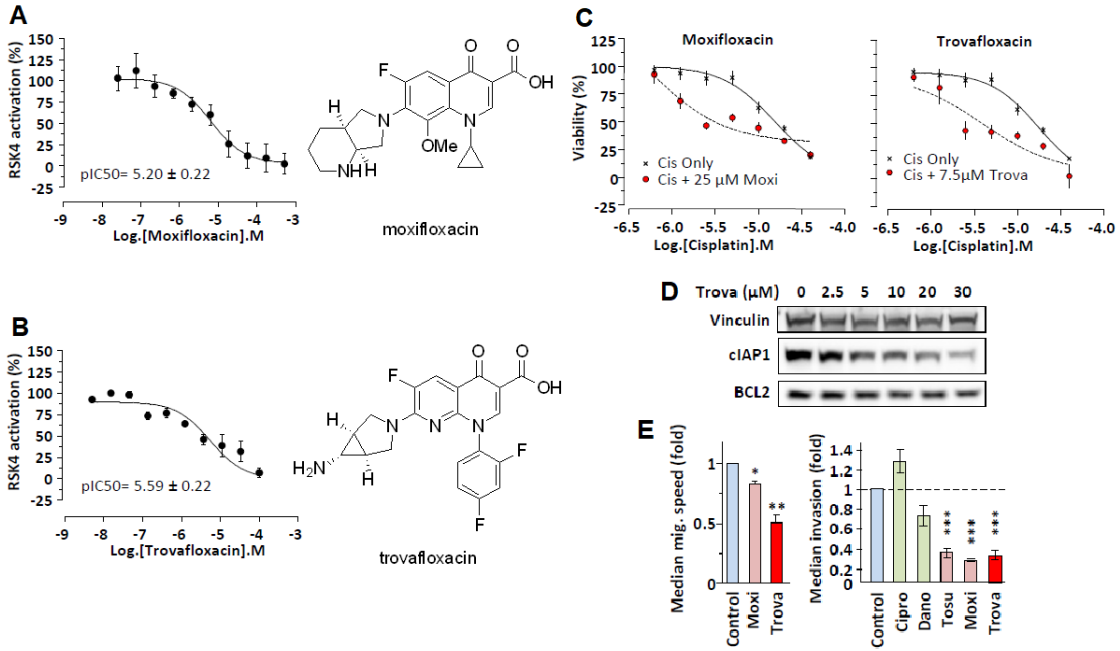

Figure 13 – Floxacin experiments. Increasing concentrations of moxifloxacin (**A**) and trovafloxacin (**B**) inhibit RSK4 activation. **C**. Increasing concentrations of moxifloxacin and trovafloxacin sensitise cells to cisplatin. **D**. Lysates of A549 cells treated with trovafloxacin were analysed by SDS-PAGE/Immunoblotting for anti-apoptosis proteins. **E**. Cell migration speed and invasiveness were monitored after treatment with 10 uM of the indicated drugs. Moxi: moxifloxacin; Trova: trovafloxacin, Cipro: ciprofloxacin; Dano: danofloxacin; Tosu: tosufloxacin. From Chrysostomou et al. (submitted manuscript).

Finally, they have also retrospectively analysed patient data from a clinical trial that used levofloxacin with regular chemotherapy (floxacins are commonly used in the clinic to limit infections in cancer patients). These results showed clinical evidence that such combination does improve patient survival.

Together, these findings show that floxacins are a good starting point for a medicinal chemistry programme aimed at finding inhibitors of RSK4 activation.

1.4. Project Aims

Considering that lung cancer is the most common cause of cancer death worldwide and that it has one of the lowest survival rates, it is clear the need to develop new drugs to treat this disease. In this regard, taking into account the role of kinases in tumour origin

and progression, and the possible role of RSK4 as a lung tumour promoter mentioned above, the use of small molecule inhibitors of RSK4 could provide a good starting point for a new lung cancer drug discovery programme.

In this context, and bearing in mind the preliminary results obtained by Prof. Seckl and Dr. Pardo's group showing the ability of fluoroquinolones to prevent cell invasion by inhibiting RSK4 activation and not its activity, which suggests they behave as allosteric modulators of RSK4 NTKD activation, the goal of this project is the development of the first selective, non-ATP-competitive inhibitors of RSK4 activation for the treatment of lung cancer using trovafloxacin as a starting point (**Figure 14**).

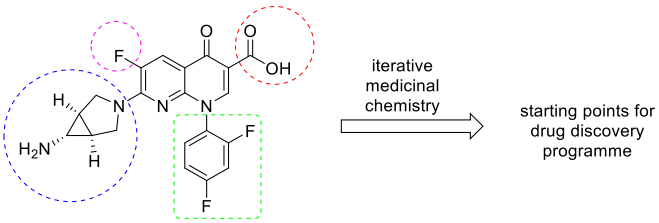

Figure 14 – Medicinal chemistry early strategy.

The achievement of this goal requires the fulfilment of the following specific aims: design and synthesis of fluoroquinolone analogues and development of biochemical and cell-based assays to allow for the evaluation of the synthesised compounds and the study of their mode of action

Additionally, considering that RSK4 silencing produced an increase in the IC_{50} value of drugs such as cisplatin, trovafloxacin will be synthesised and, in collaboration with the group of Prof. Seckl and Dr. Pardo at the Hammersmith Hospital, further studied in terms of its ability to produce a synergistic response with such chemotherapeutic agents.

2. Results and Discussion

2.1. Development of fluoroquinolone analogues

2.1.1. Background of fluoroquinolone as antibiotics

The first reference to the quinolone class[1] as antibacterial agents was made by Lesher et al. in 1962.[52,53] In this short communication, a series of 1-alkyl-1,8-naphthyridines-4-one-carboxilic acid derivatives was prepared and evaluated against a variety of microorganisms. Nalidixic acid (**Table 1**) was found to be the most potent compound in the series, presenting very good activity against the more challenging Gram-negative bacteria. Indeed, it was the first drug introduced into the market for the treatment of uncomplicated urinary tract infections.

Other first-generation quinolones were developed by the 1970s (**Table 1**).

However, it was only in the early 1980s that 2nd generation fluoroquinolones were introduced. The major modifications were the introduction of a fluorine atom at position C6 and a large ring substituent at C7. These allowed to target specific groups of bacteria and to improve pharmacokinetics and pharmacodynamics.[54–56] Selected quinolones are shown in **Table 1**.

[1] Commonly, 1,8-naphthyridines are also considered to be part of the antibiotic class of quinolones and fluoroquinolones.

Table 1 – Selected quinolones and fluoroquinolones antimicrobials.

1st Generation	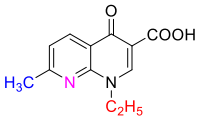 nalidixic acid	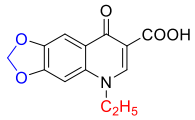 oxolinic acid
2nd Generation	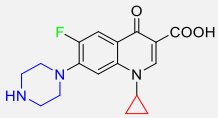 ciprofloxacin	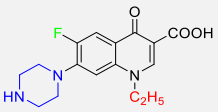 norfloxacin 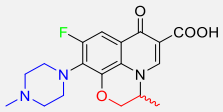 ofloxacin
3rd Generation	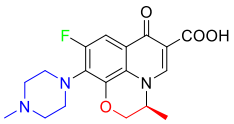 levofloxacin	
4th Generation	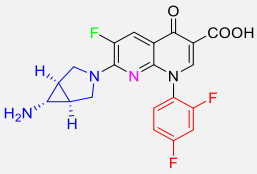 trovafloxacin	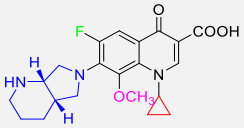 moxifloxacin 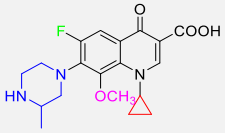 gatifloxacin

Quinolones act by converting two bacterial enzymes, DNA gyrase and DNA topoisomerase IV, into toxic enzymes that fragment the bacterial chromosome. Both enzymes modulate the topology of DNA in bacteria by generating double-stranded breaks in the bacterial chromosome. Shortly after binding at the enzyme-DNA interface, quinolones induce an enzymatic conformational change, forcing the enzyme to break the DNA and preventing re-ligation of the broken DNA strands. Interestingly, quinolones cannot bind to human gyrases, which provides quinolones with a successful therapeutic window.[57]

The structure-activity relationship (SAR) of quinolones as antimicrobials is well understood.[58,59] Briefly, a keto acid at positions C3 and C4 is required for quinolone activity and therefore cannot be changed. Modifications at N1, C5, C7, and X8 have been extensively studied over the last 40 years and are summarised below in **Figure 15**.

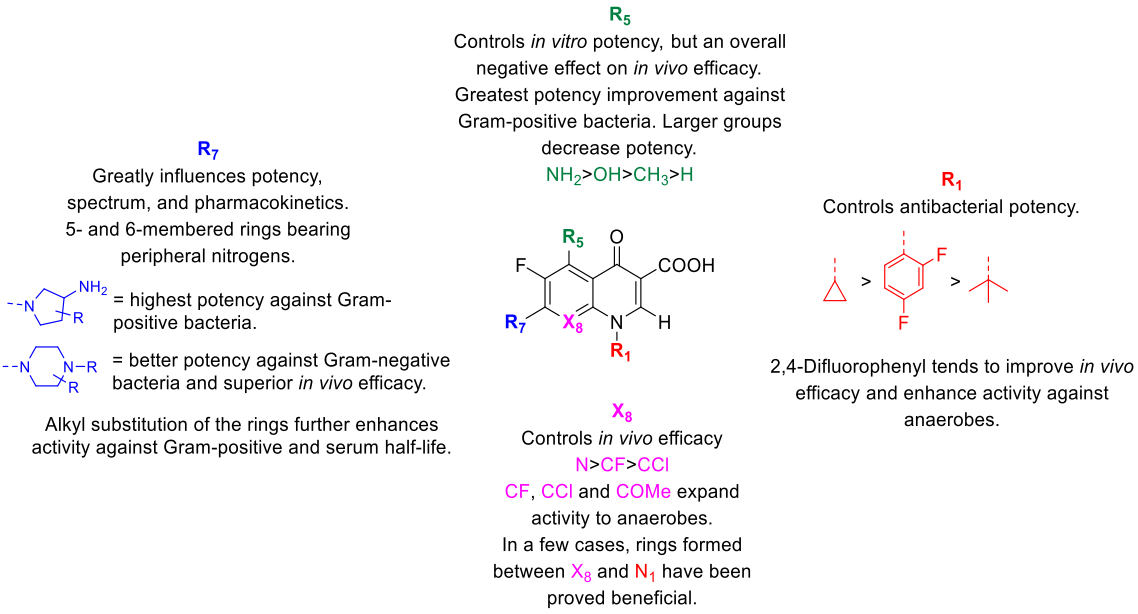

Figure 15 – Structure-activity relationship of fluoroquinolones. Adapted from work by Domagala[58].

The first publications of trovafloxacin date back to the early 1990s. Continuing work done at Pfizer (New York, USA), Brighty et al. described 7-azabicyclo-substituted quinolones with the general structure shown in **Figure 16**.[60,61]

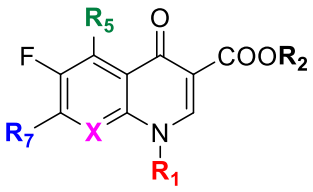

X= CH, CF, CCl, $COCH_3$, CCH_3, CCN, or N;

R_1= ethyl, *t*-butyl, vinyl, cyclopropyl, 2-fluoroethyl, 4-fluorophenyl, or 2,4-difluorophenyl;

R_2= H, a pharmaceutically acceptable cation, or (C1-C6) alkyl;

R_5= H, F, Cl, Br, C1-C4 alkyl, C1-C4 alkoxy, NH_2, or $NHCH_3$;

R_7= 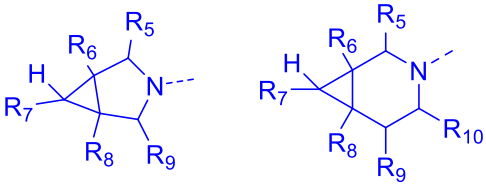

R_5, R_6, R_7, R_8, R_9, R_{10}= independently H, CH_3, CH_2NH_2, CH_2NHCH_3, **or** $CH_2NHC_2H_5$.

Figure 16 – General structure of the first published 7-azabicyclo substituted quinolone analogues.

In vitro antimicrobial activity was first shown by Gooding and Jones in 1993.[62] In these preliminary tests, trovafloxacin (published as CP-99,219) showed a wide spectrum of activity and a high potential for use against strains resistant to other fluoroquinolones. Other papers later showed great activity against Gram-positives,[63,64] and anaerobes[65]. Pharmacokinetics and safety properties were published in 1996.[66–68] However, it was not until 1998 that trovafloxacin was launched as a broad-spectrum antimicrobial with extended half-life allowing a once-a-day dose.

However, in June of 1999, its use was severely restricted due to liver toxicity. This action was in response to the strong association of trovafloxacin in 14 cases of hepatotoxicity, including six deaths and four patients who required liver transplants.[69] It was later confirmed by Shaw et al. that trovafloxacin causes idiosyncratic drug-induced liver injury (IDILI).[70–73] IDILI encompasses a range of clinical diseases that show a variety of symptoms, from biochemical abnormalities to acute liver failure.

2.1.2. Design of fluoroquinolone analogues

Despite the toxicity issues associated with the use of trovafloxacin, and in the absence of any other RSK4 activation inhibitors, it was decided to use the structure of the antibiotic as a starting point for the medicinal chemistry efforts, encouraged by the interesting preliminary results reported by Chrysostomou et al. (submitted manuscript).

Considering their initial findings suggesting that trovafloxacin and related compounds behave as allosteric inhibitors of RSK4 activation and that there was no information whatsoever regarding their binding site within the enzyme, initial efforts were focused on the co-crystallisation of RSK4 with trovafloxacin, in collaboration with the group of Prof. Seckl and Dr Pardo. However, all attempts to obtain structural information of the fluoroquinolone's binding site for rational drug design purposes failed.

Although the mode of action of fluoroquinolones as RSK4 inhibitors is necessarily different from the molecular basis behind their antibiotic properties, it was decided to maintain the main features of this family of compounds and to focus on the development of an initial series of analogues bearing modifications at the C7 position of the core scaffold. This type of modification has already been published for various fluoroquinolones[74–76] and it would be a good starting point for the development of an initial SAR.

In addition, taking into account that moxifloxacin, bearing a cyclopropyl group at the N1 position instead of the 2,4-difluorophenyl group found in trovafloxacin, had the second-best results regarding chemosensitisation towards chemotherapeutic agents, it was decided to maintain both N1 substituents for the exploration of the C7 position using commercially available alkyl amines, both cyclic and acyclic (**Figure 17**).

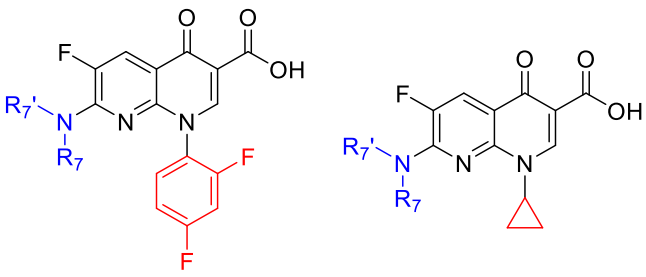

Figure 17 – General scaffold structures for planned analogues.

2.1.3. Synthesis of trovafloxacin and related analogues

Generally, 7-substituted fluoroquinolones (or naphthyridines) are synthesised by coupling the quinolone core to the amine via a nucleophilic aromatic substitution, S_NAr.[74–76] Accordingly, **Figure 18** depicts the general retrosynthetic analysis needed to

obtain the quinolone core of trovafloxacin analogues bearing a 2,4-difluorophenyl group (**1**) and a cyclopropyl ring (**2**) at position N1.

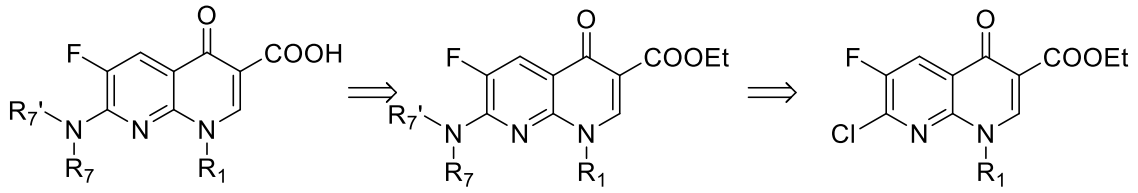

1, R_1= 2,4-difluorophenyl
2, R_1= cyclopropyl

Figure 18 – Retrosynthetic analysis of 1,8-naphthyridines.

1,8-Naphthyridone **1** was synthesized in four steps following experimental procedures previously reported by Chu et al., albeit with some modifications, starting from commercial 2,6-dichloro-5-fluoronicotinic acid (**Scheme 1**).[74] Its treatment with thionyl chloride provided acid chloride **3**, which was used without further purification in the next step. Reaction of **3** with the dilithio dianion of monoethyl malonate gave ethyl 2,6-dichloro-5-fluoronicotinyl acetate **4** (as a mixture with the corresponding enol) in 88% yield after recrystallization. Treatment of **4** with triethyl orthoformate in acetic anhydride gave the one carbon homologue enol ether intermediate, which was then allowed to react with 2,4-difluoroaniline in dichloromethane (DCM) to give **5** (as a mixture with the correspondent enol) in 78% yield. Finally, **1** was synthesised in excellent yield by cyclisation of **5** with potassium carbonate in acetonitrile as described by Remuzon et al.,[77] after a failed attempt using sodium hydride in tetrahydrofuran (THF)[74].

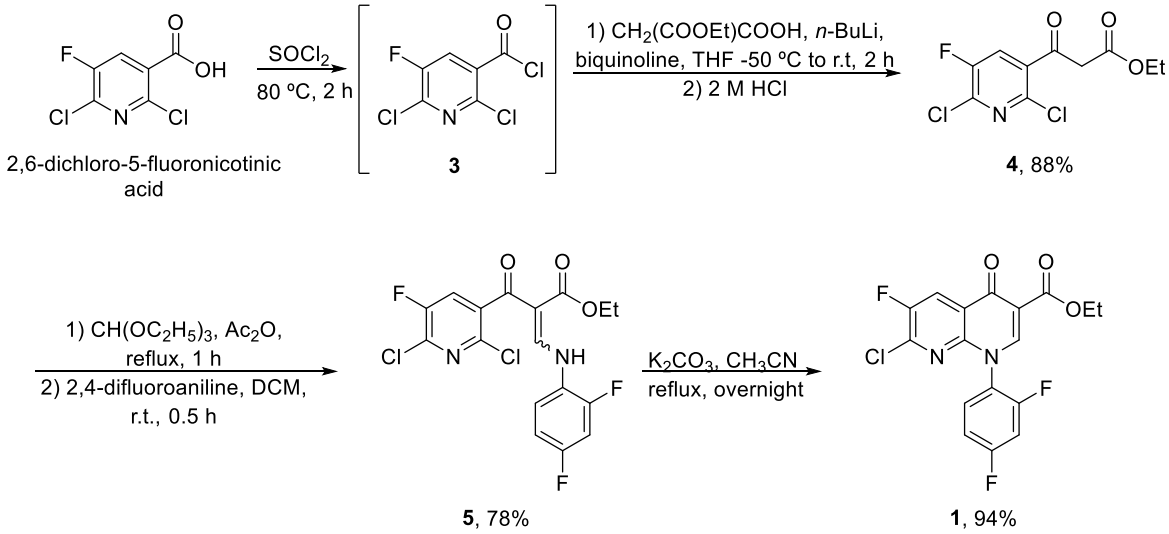

Scheme 1 – Synthesis of intermediate **1**.

Using these conditions, **1** could easily be synthesised in multigram scale and in over 60% yield over 4 steps.

With the synthesis of **1** already optimised, cyclopropyl intermediate **2** was prepared from **4** following a similar strategy (**Scheme 2**).

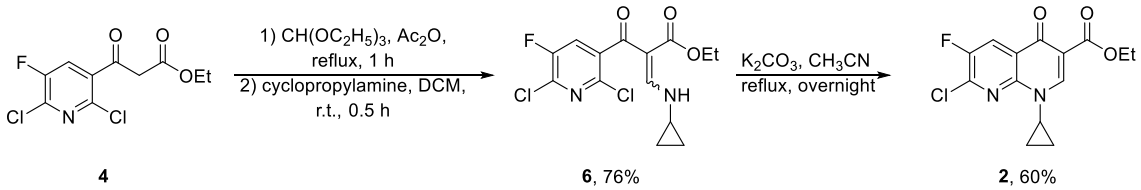

Scheme 2 – Synthesis of intermediate **2**.

Once the necessary quinolone intermediates **1** and **2** had been obtained, their coupling with the corresponding commercially available amines would furnish the first library of analogues. For the case of trovafloxacin itself, preparation of the necessary bicyclic amine was required first. Amine **11** was prepared as described by Norris et al.,[78] with some adjustments (**Scheme 3**).

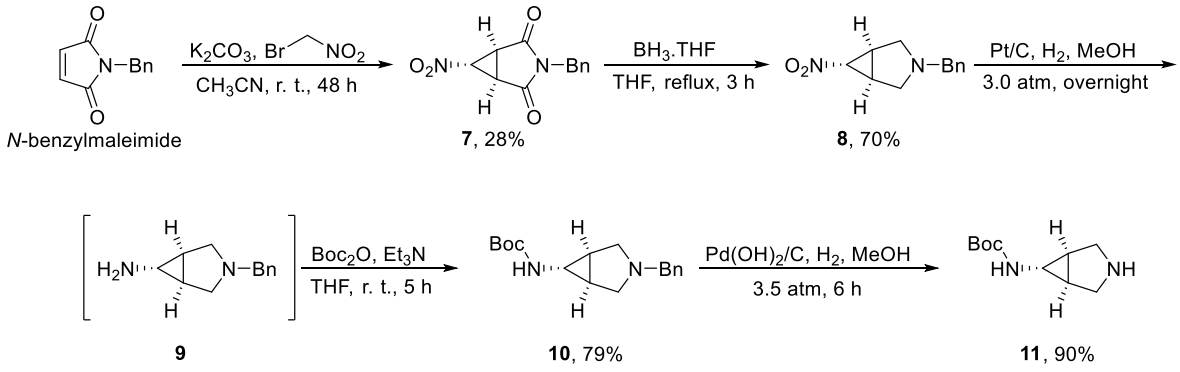

Scheme 3 – Synthesis of amine **11**.

The first and critical step is the cyclopropanation of *N*-benzylmaleimide by a nucleophilic addition-ring closure sequence as depicted in **Figure 19A**. This kind of cyclopropanation reaction, involving conjugate addition of an anionic carbon to an electrophilic alkene, is defined as Michael-initiated ring closure (MIRC) reaction.[79] Several bases have been tested in the past for the formation of the anionic species that initiates the sequence, such as guanidines, amidines, phenoxides, and potassium carbonate, the latter giving the best results.[78,80–82]

Moreover, the stereoselectivity of this reaction is not completely understood. Steric hindrance alone is not thought to be a complete barrier in this type of reaction, with others reporting ratios as low as *exo* : *endo* 2:1 in similar scaffolds.[83] However, Norris et al. reported an almost exclusive synthesis of the *exo* product, with a relative yield of 98.5 to 99.5% after epimerization of the *endo* product in the presence of potassium carbonate.[78] Regarding the low yield of the reaction, one possible explanation is that the *endo* product decomposes more rapidly than the *exo* product.

Accordingly, **7** was synthesised from *N*-benzylmaleimide and bromonitromethane in the presence of potassium carbonate in 28% yield (**Figure 19B**).[78]

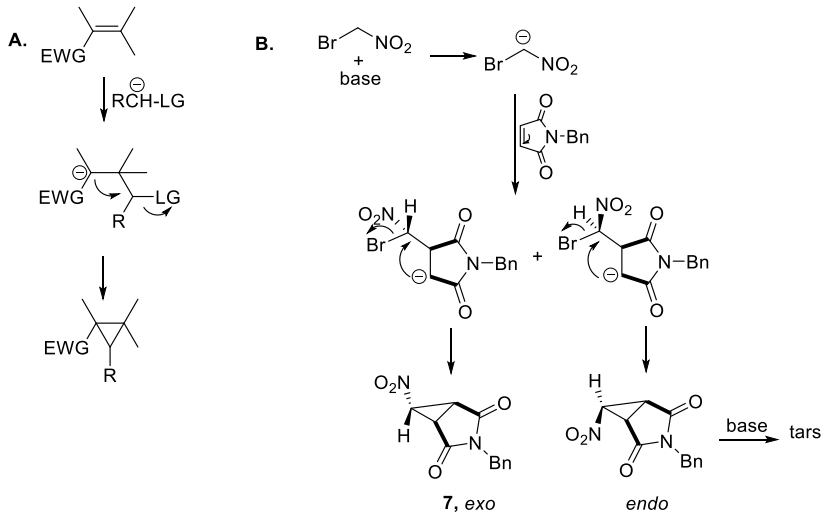

Figure 19 – **A**. Michael-initiated ring closure reaction scheme. **B**. Proposed route of tars formation. Adapted from Norris et al.[78].

After the cyclopropanation, a series of reductions and protections took place. First, the imide functionality of **7** was reduced using borane in THF complex, giving **8** in 70%. The nitro group was then reduced using catalytic hydrogenation over platinum on carbon, giving the free amine **9** in quantitative yield. **9** was then protected with di-*t*-butyl-dicarbonate, giving **10** in 79% yield. Finally, the benzyl group was removed via catalytic hydrogenolysis over palladium hydroxide and the desired secondary amine **11** was synthesised in 90% yield.

Finally, S_NAr of naphthyridone **1** with amine **11** in the presence of triethylamine gave the protected trovafloxacin **12** in 89% yield. Further removal of both ethyl ester and Boc groups with methanesulfonic acid[80] provided the desired product as a mesylate salt (**Scheme 4**). It has been published that this salt could be substantially hygroscopic and pick up water from the air to form a hydrate. It has been reported however that refluxing this hygroscopic salt with organic solvents (i.e. 2-propanol, *n*-propanol, dimethylsulfoxide, tetrahydrofuran or *n*-butanol) could induce a change in the polymorphic form of the salt, yielding an anhydrate instead.[84] Following this, the resulted salt was refluxed in 2-propanol for 20 h to provide the anhydrous form (from the X-ray powder diffraction below

and elemental analysis) of trovafloxacin mesylate salt **13**. Combined reactions resulted in more than 1 g of **13**.

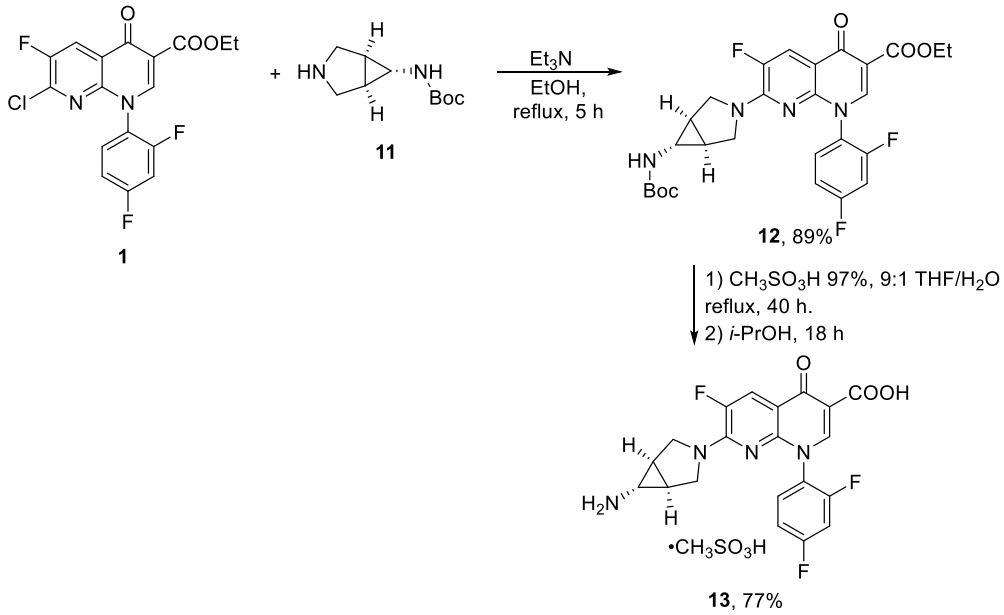

Scheme 4 – Synthesis of trovafloxacin mesylate **13**.

Having in mind that solubility issues could arise from using different crystalline forms of a salt, an X-ray powder diffraction experiment was carried out to compare the diffraction pattern of the synthesised trovafloxacin salt **13** and a commercial sample (Sigma-Aldrich®), used in previous biological experiments. As shown in **Figure 20**, the commercial sample (red) exhibits better resolved peaks, suggesting a higher crystallinity, in comparison to the synthesised sample (blue). However, both salts display a similar diffraction pattern (number of peaks) indicating that both correspond to the same crystalline form.

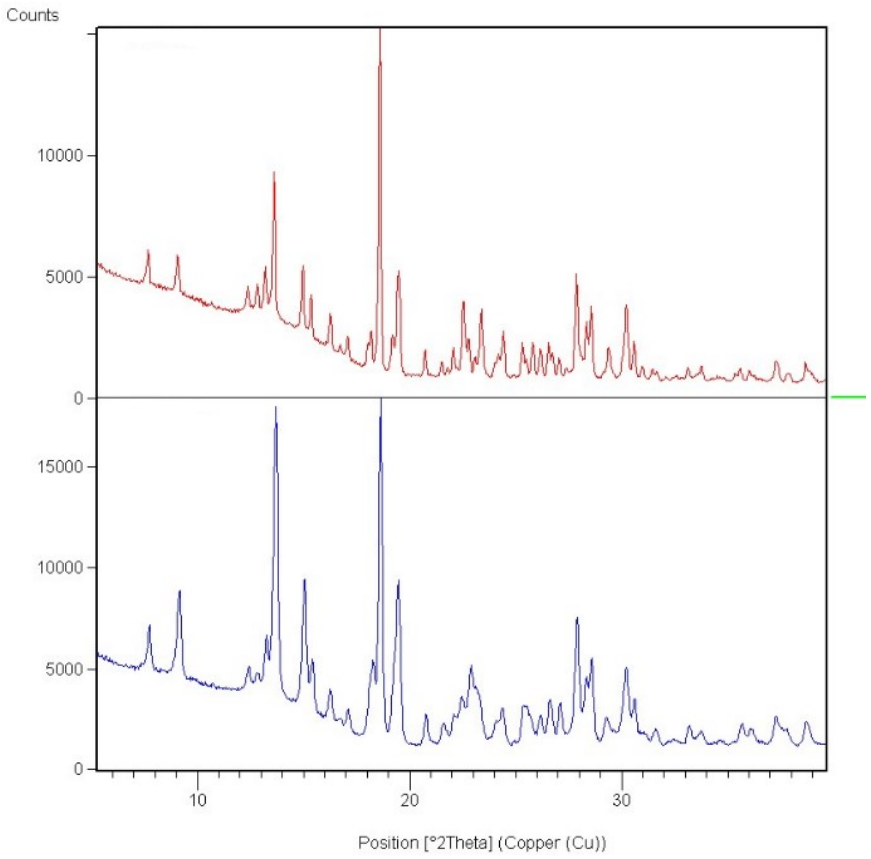

Figure 20 – X-ray powder diffraction pattern from the Sigma-Aldrich® (above) sample and the synthesised trovafloxacin mesylate salt (below).

In the absence of any representative SAR information, cyclic and non-cyclic examples of primary and secondary aliphatic amines were selected for the preparation of trovafloxacin analogues, primarily due to their commercial availability.

Thus, trovafloxacin analogues **29–43** were successfully synthesised from intermediates **1** and **2** following the protocol published by Chu et al. (**Table 2**).[74]

Table 2 – Synthesis of first series of analogues of fluoroquinolones.

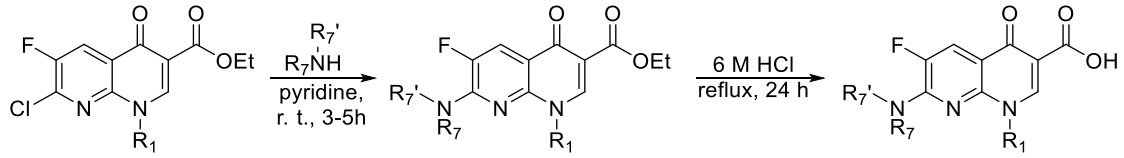

1, R_1= 2,4-difluorophenyl
2, R_1= cyclopropyl

14 - 28

29 - 43

R_1	NHR_7R_7'	**Entry**, yield (protected)	**Entry**, yield (deprotected)
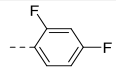	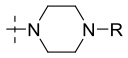	**14** (R= Boc)**,** 34%	**29** (R= H), 56%
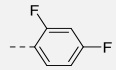	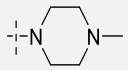	**15**, 40%	**30**, 71%
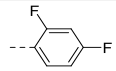		**16**, 73%	**31**, 35%
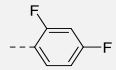	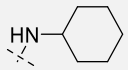	**17**, 23%	**32**, 36%
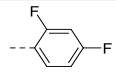		**18**, 43%	**33**, 38%
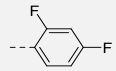	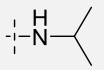	**19**, 59%	**34**, 48%
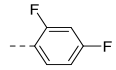	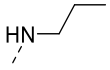	**20**, 49%	**35**, 34%
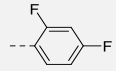	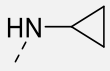	**21**, 81%	**36**, 23%
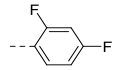		**22**, 62%	**37**, 53%
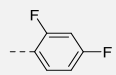	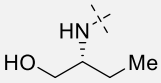	**23**, 50%	**38**, 59%
	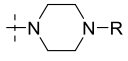	**24** (R= Boc), 63%	**39** (R= H), 52%
	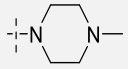	**25**, 60%	**40**, 80%
		**26**, 77%	**41**, 38%
		**27**, 52%	**42**, 41%
	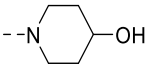	**28**, 74%	**43**, 26%

2.1.4. Other analogues using a tertiary butyl ester group protecting group

Since the yield of the deprotection step for most analogues was only moderate, it was decided to change the carboxylic acid protecting group to a *tert*-butyl substituent for the preparation of further derivatives, since cleavage of *tert*-butyl esters under milder conditions has been previously described.[85–87] Naphthyridines **47** and **48** were then synthesised, using the same strategy as for the preparation of the corresponding ethyl ester derivatives **1** and **2** (**Scheme 5**).

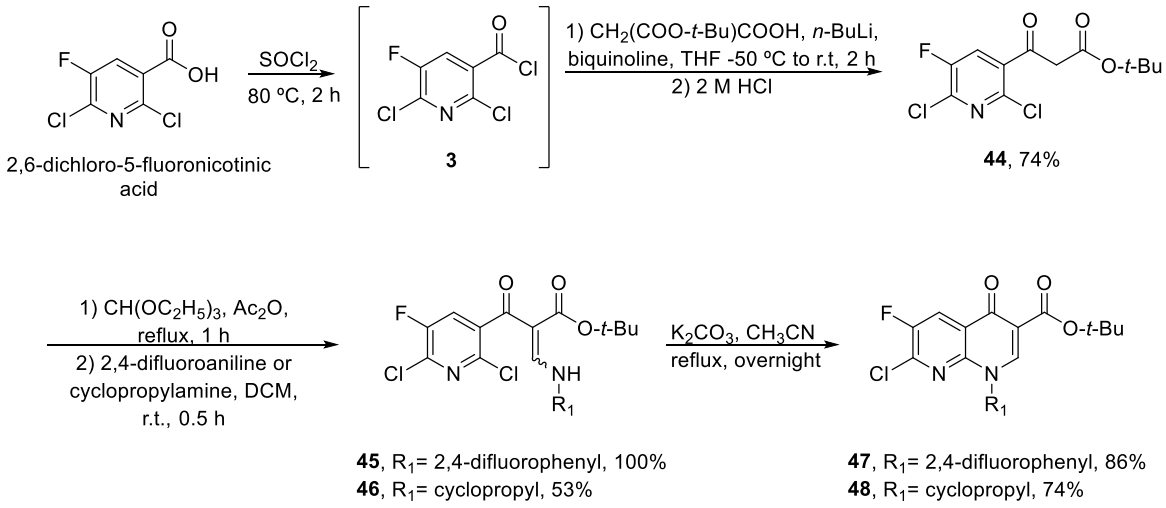

Scheme 5 – Synthesis of naphthyridines **47** and **48**.

A second series of analogues was synthesised using these new intermediates to provide final compounds **62**–**74** after deprotection of the *tert*-butyl ester of the corresponding intermediates **49**–**61** (**Table 3**). However, no significant difference could be observed in the yields of the deprotection step between both esters (**Table 3**).

Table 3 – Synthesis of second series of analogues of fluoroquinolones.

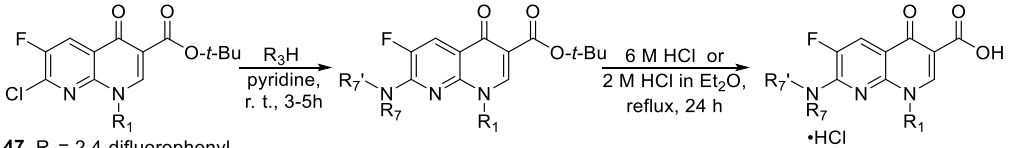

47, R_1= 2,4-difluorophenyl
48, R_1= cyclopropyl

49 - 61

62- 74

R_1	NHR_7R_7'	**Entry**, yield (protected)	**Entry**, yield (deprotected)
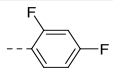	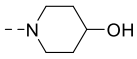	**49**, 69%	**62**, 48%
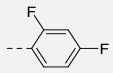	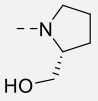	**50**, 77%	**63**, 28%
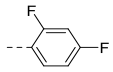	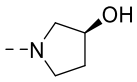	**51**, 76%	**64**, 30%
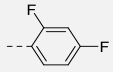	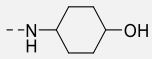	**52**, 70%	**65**, 46%
	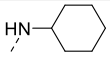	**53**, 40%	**66**, 50%
		**54**, 70%	**67**, 39%
	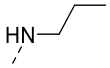	**55**, 60%	**68**, 47%
	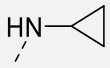	**56**, 67%	**69**, 56%
	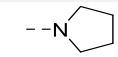	**57**, 52%	**70**, 73%
		**58**, 55%	**71**, 20%
	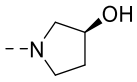	**59**, 51%	**72**, 49%
	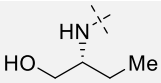	**60**, 72%	**73**, 55%
	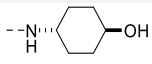	**61**, 32%	**74**, 52%

2.1.5. Solubility issues and attempt to solve them

Containing both amine and carboxylic acid moieties, fluoroquinolones are often found in an equilibrium of several protolytic forms depending on the pH. This leads to an intrinsic low solubility in aqueous solutions. Unfortunately, almost all analogues presented very

low solubility in many solvents, including dimethyl sulfoxide (DMSO) and aqueous media, which could hamper their biological assessment.

In order to address this issue, we first aimed at the study of the counter ion effect in the aqueous solubility of our derivatives, since this has been proved to be useful for some fluoroquinolones.[88] Since trovafloxacin was already synthesised as a mesylate salt instead of the hydrochloride one, methanesulfonic acid was used for the final deprotection step of representative analogues to obtain the corresponding mesylate salts. At this point, *tert*-butyl ester intermediates **47** and **48** were chosen as starting point purely because intermediate **44** had been successfully prepared in large scale (intermediates **14**, **16**, **24**, and **25** had already been synthesised using an ethyl ester protecting group) (**Table 4**).

Table 4 – Deprotection of analogues using methanesulfonic acid.

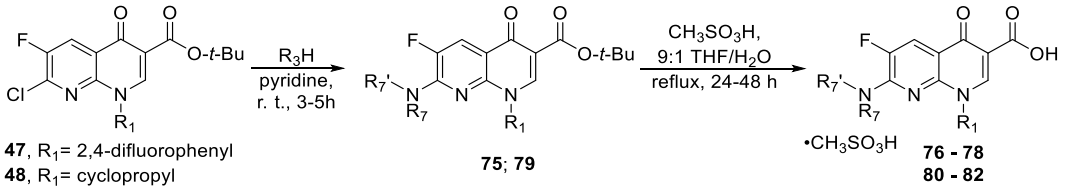

47, R_1= 2,4-difluorophenyl
48, R_1= cyclopropyl

75; **79**

76 - 78
80 - 82

R_1	NHR_7R_7'	**Entry**, yield (protected)	**Entry**, yield (deprotected)
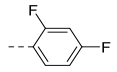	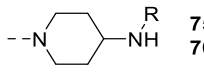 **75**, R= Boc **76**, R= H	**75**, 90%	**76**, 30%
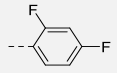	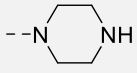	**14**, 34% (Table 2)	**77**, 65%
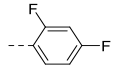	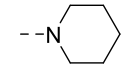	**16**, 73% (Table 2)	**78**, 65%
	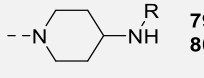 **79**, R= Boc **80**, R= H	**79**, 58%	**80**, 92%
	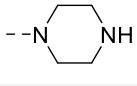	**24**, 63% (Table 2)	**81**, 100%
	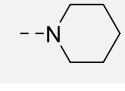	**25**, 77% (Table 2)	**82**, 66%

Analogues **76**–**78** and **80**–**82** were successfully synthesised. They present better visible solubility in DMSO than previous analogues, being able to be solubilised at 50 μM, an acceptable concentration for initial assays.

Encouraged by the slight improvement in the solubility of the mesylate salts, it was decided to prepare one last analogue that combined the main features of both trovafloxacin and moxifloxacin. Therefore, analogue **84** was synthesised bearing the C7 substituent of trovafloxacin, while keeping the N1 substituent of moxifloxacin (**Scheme 6**) and indeed it was soluble at the desirable concentration.

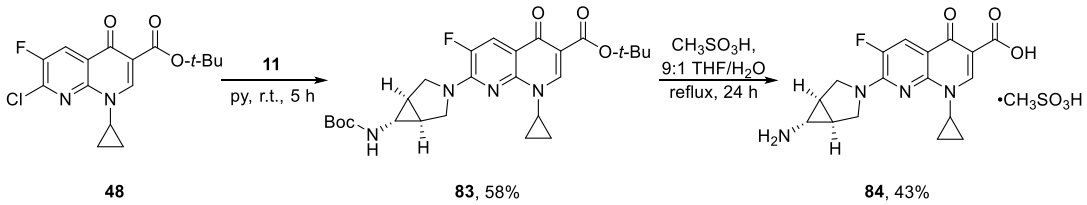

48 **83**, 58% **84**, 43%

Scheme 6 – Synthesis of analogue **84**.

A second strategy to increase solubility was the study of a different heterocycle. Hoegenauer et al. have suggested that lipophilicity can be improved by modifications of the central bicyclic core of quinoline-, cinnoline- and 1,5-naphthyridine-based analogues.[89] Thinking forward, solubility of the fluoroquinolone analogues could be modulated by rearranging or adding new heteroatoms within the naphthyridine core. Having that in mind, analogues with the following general structure were planned (**Figure 21**).

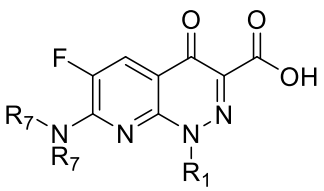

R_1= 2,4-difluorophenyl or cyclopropyl
NHR_7R_7'= commercial secondary and terciary amines

Figure 21 – Planned new analogues.

These derivatives could be prepared in a similar manner to that employed for the synthesis of intermediates **1** and **2** but using a diazonium salt as an electrophile for the α-alkylation of the keto ester (**Figure 22**).

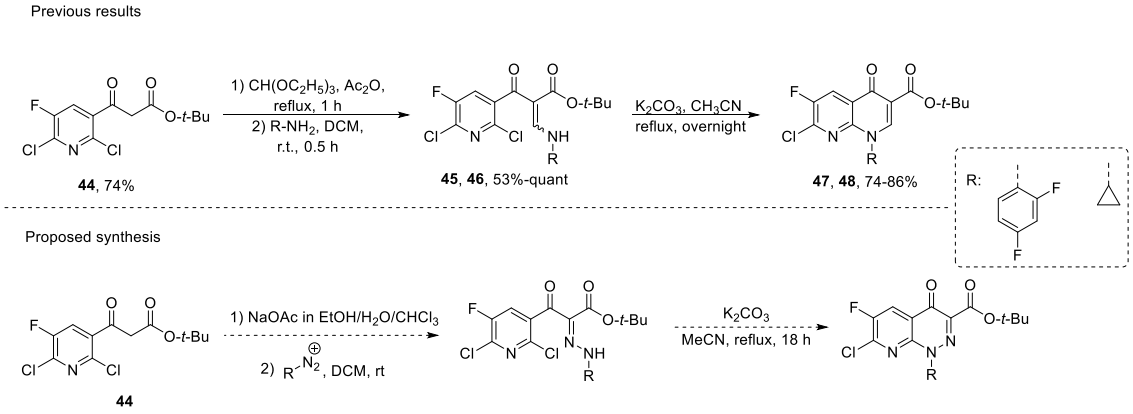

Figure 22 – Previous achievements in naphthyridine derivatives synthesis and proposed preparation of the new analogues.

Intermediate **86** was prepared by enolate formation of ketoester **44**, followed by nucleophilic attack to diazonium salt **85**, prepared in situ from 2,4-difluoroaniline using conditions published by Miyamoto et al.[90]. Finally, cyclised product **87** was obtained using previously optimised conditions in 80% yield (**Scheme 7**).

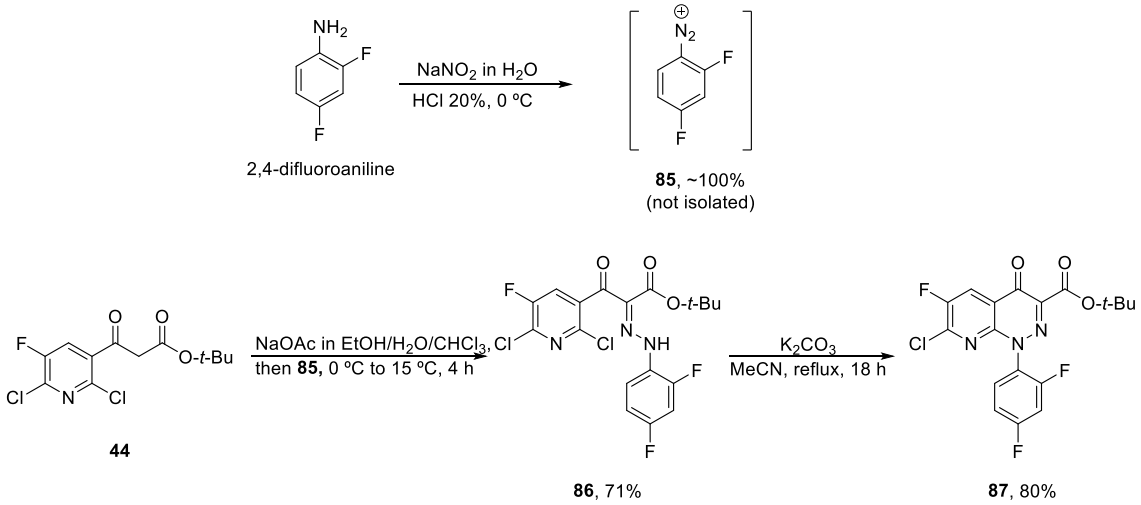

Scheme 7 – Synthesis of intermediate **87**.

Using **87**, two new analogues were synthesised (**Table 5**). These analogues were chosen to be synthesised for being representative examples of the naphthyridine series: a cyclic, secondary amine and a primary hydroxylamine.

Table 5 – Third series of analogues with new heterocyclic core **87**.

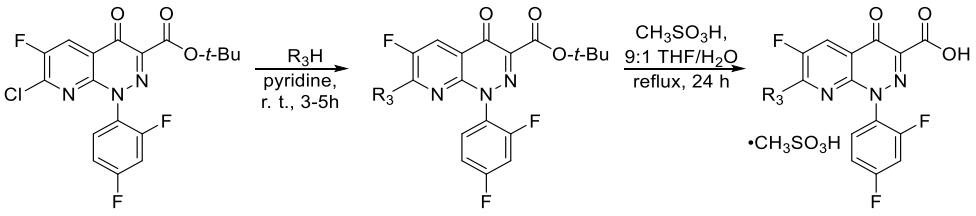

87 **88 - 89** **90 - 91**

R_3	**Entry**, yield	**Entry**, yield
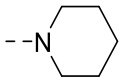	**88**, 80%	**90**, 38%
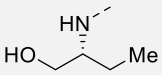	**89**, 55%	**91**, 70%

Unfortunately, the corresponding cyclopropyl intermediate could not be synthesised using the proposed pathway. The reaction to form the equivalent diazonium salt **92** was unsuccessful due to the decomposition of the starting material (**Scheme 8**).

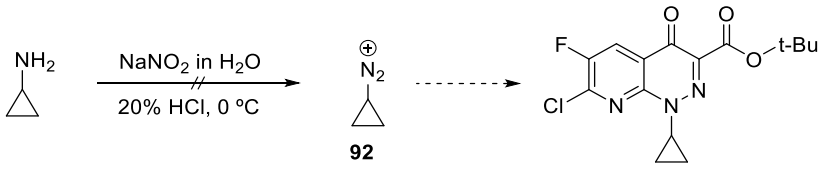

92

Scheme 8 – Failed synthesis of **92**.

2.1.6. Summary of chemistry efforts

In summary, over 1 g of trovafloxacin was synthesised to undergo a variety of biological studies in collaboration with Prof Seckl and Dr. Pardo's team to shed some light on the mechanism of action of this antibiotic as a RSK4 inhibitor.

Moreover, 47 analogues of both trovafloxacin and moxifloxacin were designed and successfully prepared (**Figure 23**). These derivatives have a good structural range to allow an initial SAR study, presenting a variety of C7 and N1 substituents as well as a different core scaffold (represented by **87**).

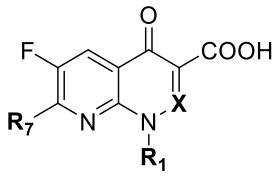

47 analogues

X = C or N

$\mathbf{R_1}$ = 2,4-difluorophenyl or cyclopropyl

$\mathbf{R_7}$ = primary or secondary amines

Figure 23 – Summary of chemistry efforts.

2.2. Biological evaluation of trovafloxacin analogues

As stated in Chapter One, the group of Professor Seckl and Dr. Pardo have identified RSK4 as a potential tumour promoter in the lungs and progress is being made to further prove this hypothesis and to initiate a drug discovery programme.

The aims of the first stages of a drug discovery programme are to identify hit molecules and targets (**Figure 24**). A phenotype-based approach seeks first to identify hit molecules by looking at the desired response in live cells followed by elucidation of the molecular targets responsible for such phenotype. A target-based approach on the other hand focuses on specific targets of interest, which will then be used in assays and screens to optimise lead molecules able to bind the target with high potency.

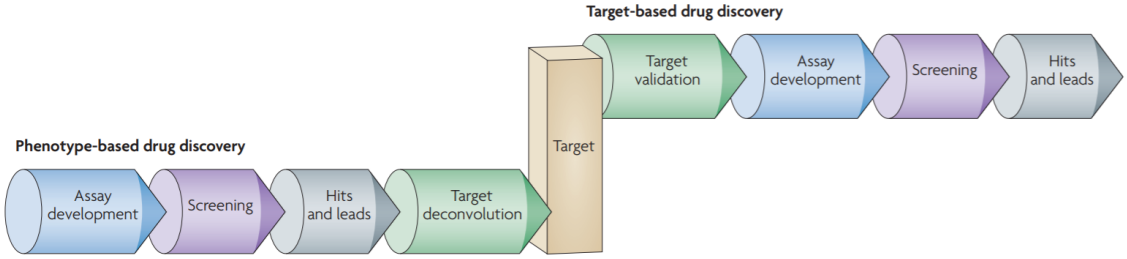

Figure 24 – Phenotype-based drug discovery versus target-based drug discovery. From Terstappen et al.[91].

From 1999 to 2013, 70% of first-in-class drugs approved by the Food and Drug Administration (FDA) were discovered using a target-based approach. The remaining 30% were discovered on systems-based methods.[92]

Although all synthesised derivatives were sent to our collaborators to be evaluated in terms of their ability to inhibit RSK4 activation using the original HTRf assay, the obtained results were unreliable due to a lack of reproducibility. For instance, trovafloxacin was found to be ten-fold less potent in these last experiments and analogues were reported

to have picomolar efficacy. This fact highlighted the importance of having solid biological assays in place for medicinal chemistry purposes, and the need to develop such assays in the interest of this research project.

In order to assess the ability of our trovafloxacin derivatives to inhibit RSK4 activation, it was decided to set up a biochemical assay that could allow us to obtain SAR information about the necessary features for compound activity. Additionally, considering the complexity of the signalling pathways in which RSK4 is involved, we also envisioned the development of a cell-based assay specifically tailored to detect RSK4 activation.

To that end, I conducted a placement within the group of Dr. Deborah Lannigan at Vanderbilt University (Nashville, US) for six months. Her group is specialised in breast cancer biology and physiological functions of the RSK family in breast tissues. The group has also discovered SL0101, a specific inhibitor of the RSK proteins.[35]

2.2.1. Biochemical assay

In order to set up such an appropriate biochemical assay to evaluate the ability of the floxacin analogues to inhibit RSK4 activation, purified RSK4 and the upstream kinase ERK2 were required.

2.2.1.1. ERK2 expression

Although prokaryotic systems are not normally used as host cells when post-translational modifications like phosphorylation are necessary in the purified enzymes, the group of Melanie Cobb has developed a method to synthesise active kinases of the MAPK pathway, including ERK2, in *Escherichia coli*.[93]

They have shown that if the upstream activator is present in its constitutively active form, the downstream component will be expressed in its active form as well. This is achieved by using modified plasmids that encode two or more protein kinases that will be transformed into the same host cells.

Thus, in the case of ERK2, they prepared a plasmid encoding an untagged, constitutively active mutant of MEK1 (the upstream activator of ERK2) and the ERK2 gene tailored with a histidine tag for further purification (**Figure 25**). A ribosomal binding site was introduced between each gene to synthesise both kinases separately. Additionally, an ampicillin resistance gene was also included in the plasmid. Ampicillin is a generic antibiotic, and therefore, the bacteria not carrying the resistance gene can be eliminated upon treatment with the drug.

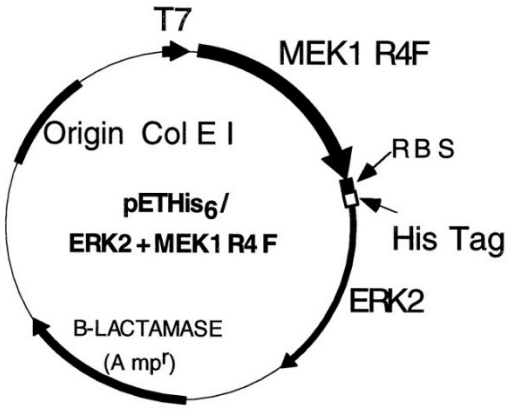

Figure 25 – Plasmid pET-His6-MEK1-R4F_ERK2 used for expression of two proteins: constitutively active MEK1 and tagged-ERK2. RBS: Ribosome Binding Site. From Addgene.

Phosphorylated ERK2 was expressed in *E. coli*, using the method developed by Cobb's laboratory and explained above.[93] The customised plasmid made by Cobb, containing both MEK1 and ERK2 genes, was bought from Addgene. The use of this plasmid allowed the expression of both proteins in bacteria. His-tagged ERK2 was purified using affinity chromatography with an agarose resin containing nickel-nitriloacetic acid (Ni-NTA) that binds to the histidine.

Briefly, the plasmid was cloned and subsequently DNA was isolated from bacteria cells (from individual colonies that generated liquid bacterial cultures) using the QIAprep Spin Miniprep Kit®. Purified plasmid DNA was then transformed into BL21(DE3) cells, a competent strain of *E. coli*, for storage and propagation. Protein expression was induced by adding isopropyl β-D-1-thiogalactopyranoside (IPTG, 0.25 mM final concentration), a lactose-mimic metabolite that triggers gene transcription under the control of a lac operator. On day 4, cells were harvested and ERK2 was purified by means of the histidine tag using Emulsiflex and Ni-NTA agarose (full method described in the Experimental session).

Roughly, 100 mg of active ERK2 (42 kDa) were obtained after 4 elution steps (E1-4), and identity was confirmed by Western Blot analysis using commercially available anti-phosphorylation ERK1/2 antibody (**Figure 26**). The two bands correspond to doubly phosphorylated ERK1 and ERK2.

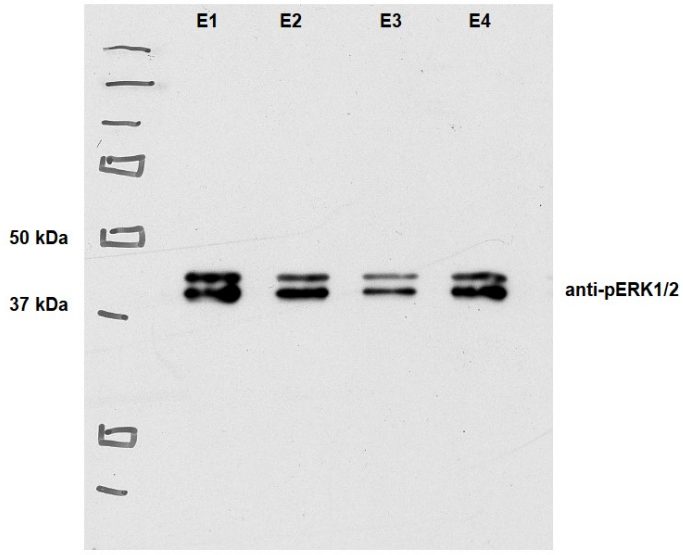

Figure 26 – Western analysis of elution fractions E1 – E4 after purification with Ni-NTA agarose seen with anti-phosphorylation antibody to ERK1 and 2.

To further confirm that ERK2 had been successfully expressed in the active state needed for the RSK4 activation assay, a kinase assay developed in house was performed using

a known ERK1/2 inhibitor, GDC-0994, with a reported IC_{50} for ERK2 of 0.3 nM.[94] As depicted in **Figure 27**, the IC_{50} values obtained for the recombinantly expressed and purified ERK2 in two independent experiments carried out in triplicate (0.27 and 0.32 nM) were consistent with the reported value.

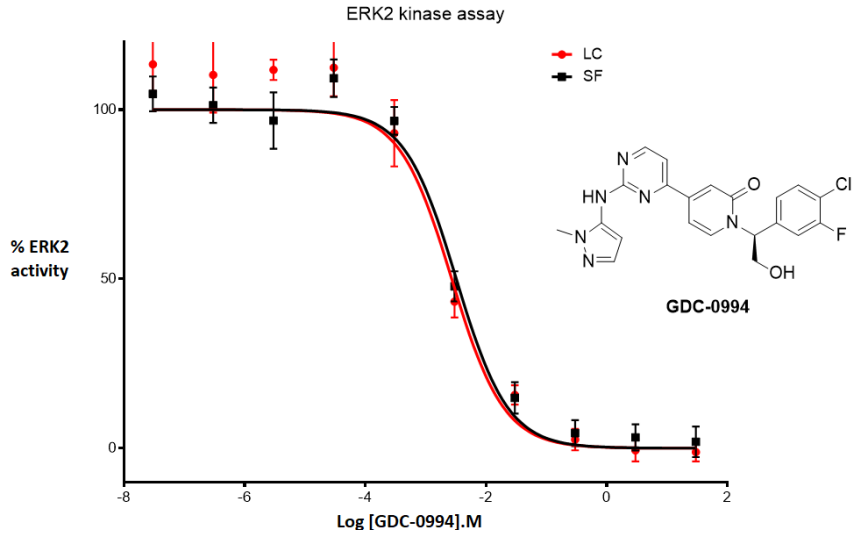

Figure 27 - ERK2 inhibition with GDC-0994, a known ERK1/2 inhibitor. Curves in red and black show the results from two independent experiments carried out in triplicate.

2.2.1.2. Expression of RSK4

E. coli is the most common host used for heterologous protein production. Its main advantage is a fast growth in inexpensive medium, giving high yields of protein in an economical production. However, not every gene can be expressed using *E. coli*, the most common problems being unique structural features, stability and translational efficiency of mRNA, protein folding, degradation by host cell proteases, and toxicity.[95]

RSK4 is a larger, more complex protein than ERK2 and therefore a eukaryotic system was needed for expression. Among the different host cells available (namely mammalian and insect cells), the use of a baculovirus expression insect cell-based system was envisioned.

There are different ways to produce a baculovirus encoding a protein of interest.[96] In the case of RSK4, an *in vitro* transposition system was selected. This method relies on the use of a purified transposase to insert the RSK4 gene from a donor plasmid into the viral DNA receptor. The donor plasmid contains also a herpes gene that upon treatment with the antiviral drug ganciclovir will be eliminated (negative selection), leaving only the recombinant viral DNA.

To this end, commercially available BaculoDirect™ Baculovirus Expressing System kit (Life Technologies) was used. This kit uses the Gateway® cloning technology to produce the baculovirus from an entry clone containing RSK4 gene and the BaculoDirect™ Linear DNA in a recombination reaction, catalysed by a clonase enzyme (**Figure 28**).

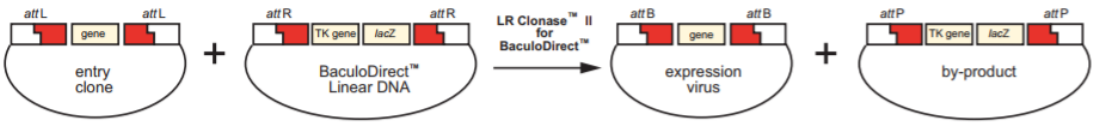

Figure 28 – General scheme of a LR recombinant reaction. From Life Technologies.

The first step is to isolate the necessary entry clone. Thus, a plasmid containing the gateway entry clone of RSK4 containing a V5-tag for easier visualisation and a His tag for purification (without stop codon, for C-terminal fusions) was purchased from Addgene. The plasmid DNA was isolated from bacteria cells using QIAprep Spin Miniprep Kit®, sequenced and cross-checked with known references using Basic Local Alignment Search Tool (BLAST), to ensure the plasmid had been generated successfully. The clone was then transformed into DH5α cells for further expression and purification of a larger quantity of entry clone. Using NucleoBond Xtra Midi Macherey-Nagel Kit®, the clone was purified, giving a final concentration of 3248.1 ng/μL, and recombined into the BaculoDirect™ Linear DNA using the LR Clonase™ II Enzyme Mix provided in the expression kit. The recombinant reaction was then analysed by polymerase chain reaction (PCR). In **Figure 29**, lane 2 shows DNA amplified using the reverse primer of

the V5 tag, this is, the partner DNA strand of the one present in the baculovirus. Likewise, lane 3 shows the DNA resulting from amplification using in this case the reverse strand of the RSK4 gene used, the main band corresponding to RSK4 and the fainted one to the reaction by-product, depicted in **Figure 28**.

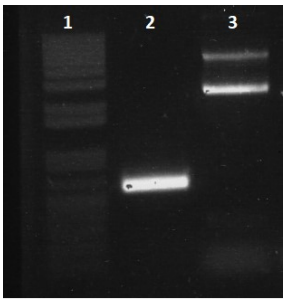

Figure 29 – PCR analysis. 1. Marker 2. Recombinant DNA-V5 reverse primer 3. Recombinant DNA-hRSK4-int1R (the faint band represent the by-product showed in the previous figure).

With the RSK4 baculovirus successfully obtained, insect cells were next infected to allow for the recombinant expression of the kinase. Thus, *Spodoptera frugiperda* cells (Sf9 cells) were selected for RSK4 expression, using the BaculoDirect™ Baculovirus Expressing System (BaculoDirect™ C-Term Expression Kit from Life Technologies). **Figure 30** shows an overview of the experiment.

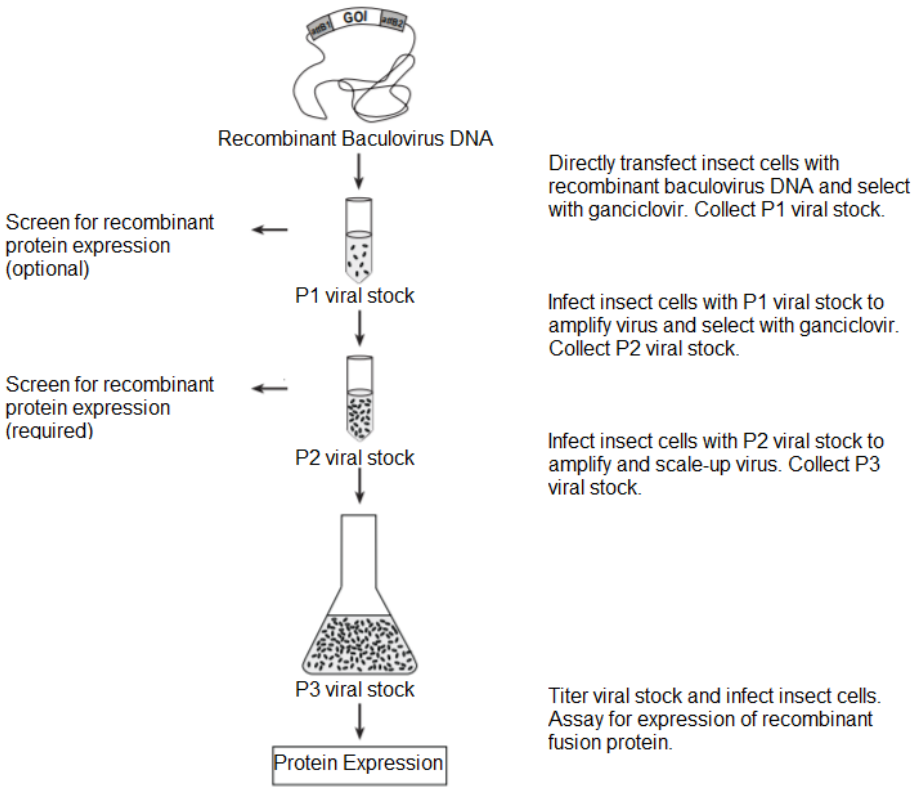

Figure 30 – Experimental summary of RSK4 expression using baculovirus. From Life Technologies.

Sf9 cells were then transfected with recombinant baculovirus DNA using the Cellfectin® II reagent provided with the expression kit. After 72 h, cells were showing signs of infection and the supernatant medium was collected (P1 viral stock). Cells were harvested and lysed to verify protein expression of recombinant RSK4 by western analysis. **Figure 31** shows the detected RSK4 in the lysates at different dilutions (1, 1:2, 1:4 and 1:10 for lanes 1, 2, 3, and 4 respectively) using anti-V5 antibody.

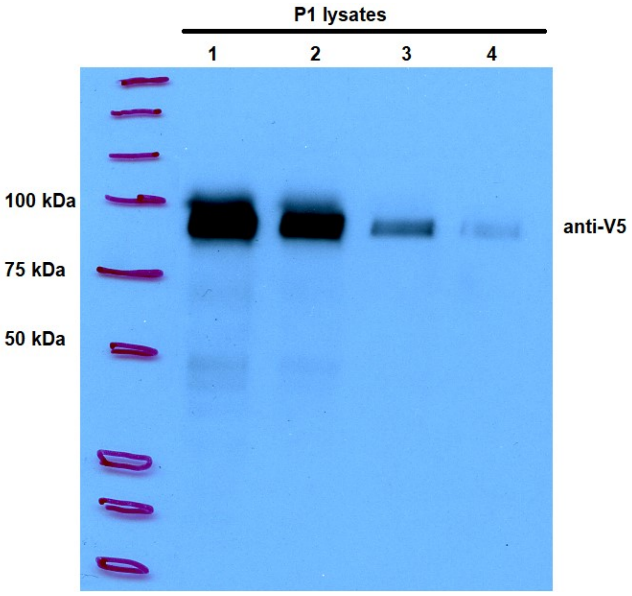

Figure 31 – Western analysis of P1 cell lysate using an anti-V5 antibody. Lanes 1 to 4 represent serial dilutions of cell lysates.

Following confirmation of RSK4 expression, higher titer stocks (P2 and P3) were prepared as shown above in **Figure 30**. Before starting protein production, the titer of P3 viral stock was verified to decide on the multiplicity of infection (MOI). For this experiment, MOIs of 1, 2, 5, 10 and 100 were chosen. Cells were plated in a 6-well tissue culture plate and incubated for 1 h to allow them to fully attach to the bottom of the plate surface. After that time, P3 viral stock was added to each well at the desired MOIs and cells were harvested after 48 h incubation. Cells were then stained using anti-V5 (green) for RSK4 detection and Hoescht (blue) for the visualisation of the cell nucleus. The results obtained for the different MOIs are shown in **Figure 32**.

The best infection attending to amount of labelling was obtained when a MOI of 10 (100µL) was used (**Figure 32E**), corresponding to the minimum amount of viral stock necessary to infect all cells. This condition was therefore selected to infect cells for protein production.

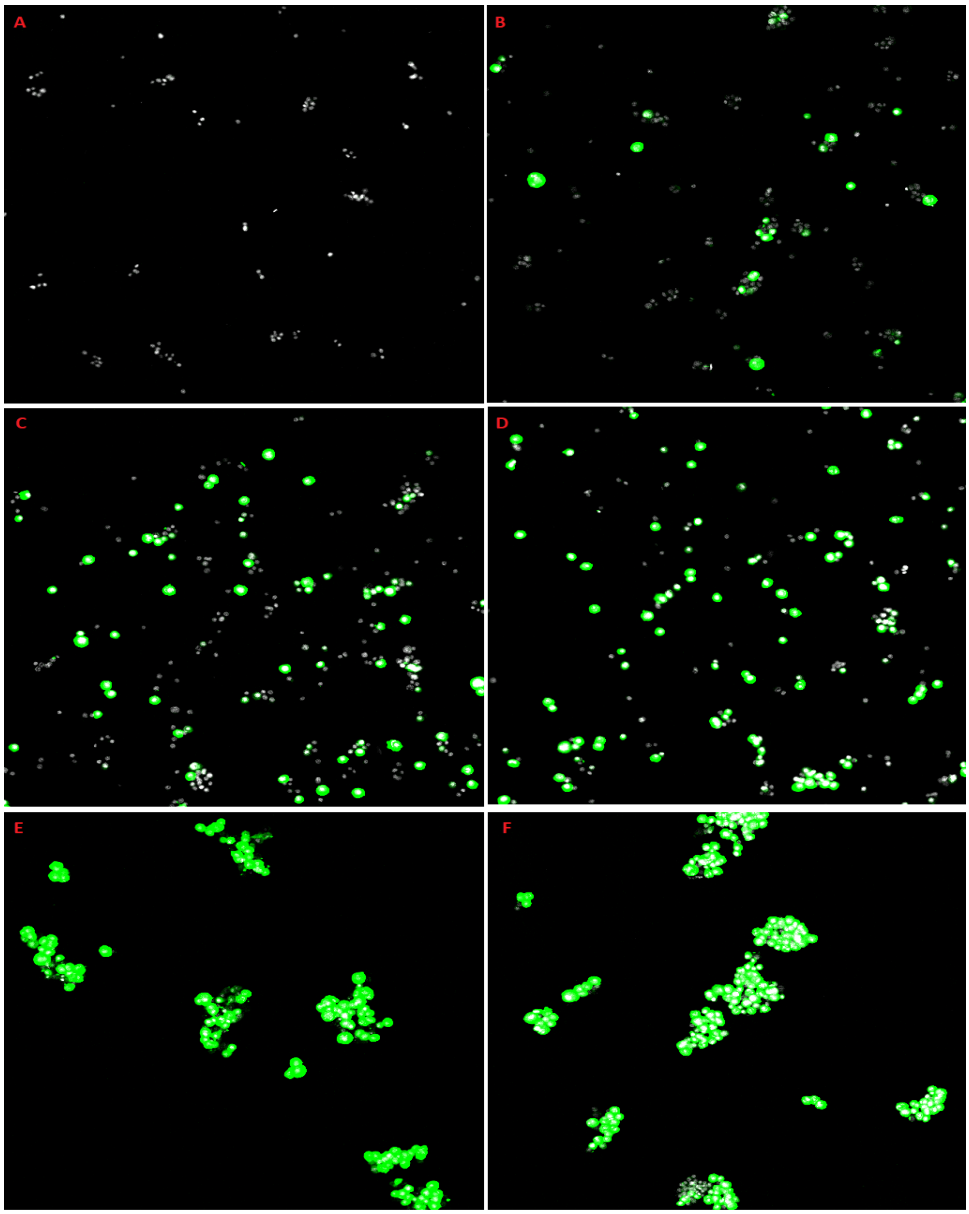

Figure 32 – Cells stained with anti-V5/Hoechst after MOI experiment. A. Negative control; B. 10 µL of P3 viral stock; C. 20 µL of P3 viral stock; D. 50 µL of P3 viral stock; E. 100 µL of P3 viral stock; F. 200 µL of P3 viral stock.

For protein production, Sf9 cells were incubated for 48 h. P3 viral stock was then added and cells incubated for further 48 h. Two hours before harvesting, the mixture was split into two spinner flasks and U0126, a MEK inhibitor, was added into one of them at a final concentration of 10 µM. This would inhibit ERK2 and consequently RSK4 phosphorylation, giving the desired inactivated protein. Cells were then harvested and RSK4 was purified using Emulsiflex and Ni-NTA agarose as previously described for ERK2 (full method described in the Experimental section).

RSK4 identity was verified by western blot analysis using anti-phosphorylation RSK and anti-V5 antibodies (**Figure 33**). As it can be seen, treatment with U0126 (E1-T) did not seem to change the phosphorylation state of RSK4 in comparison to untreated cells (E1-UT).

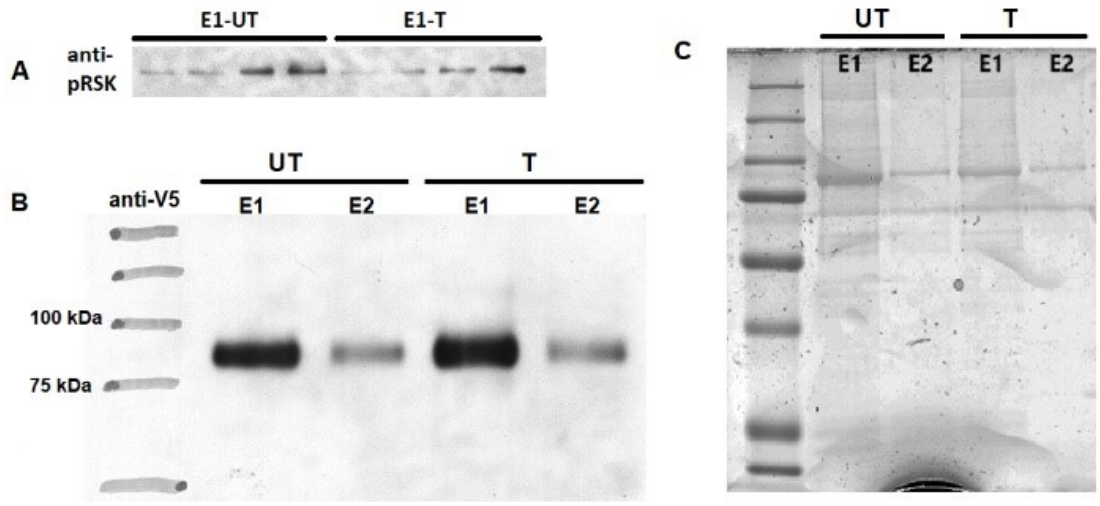

Figure 33 – Western analyses and Coomassie Brilliant Blue (CBB) stains of RSK4 protein production after purification. A. Serial dilutions of E1 fractions with anti-pRSK; B. E1 and E2 with anti-V5 antibody; C. CBB of E1 and E2. UT: untreated and T: treated with 10 μM U0126.

Next, the purity of RSK4 was analysed using Coomassie Brilliant Blue (CBB) as stain, which is a dye commonly used in biochemistry for protein detection. As it can be seen in **Figure 34**, only one band corresponding to RSK4 can be seen in lane 4. Lane 1 shows the molecular weight markers, and lanes 2 and 3 were loaded with pure RSK1 and 2, respectively, as control.

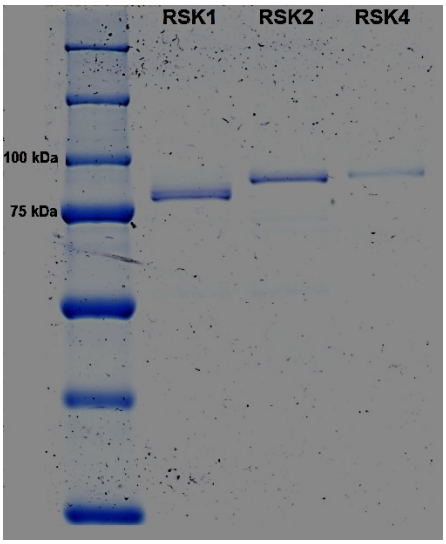

Figure 34 – Coomassie Brilliant Blue (CBB) staining of purified RSK1, RSK2, and RSK4.

2.2.1.3. Biochemical assays - development

With expressed and purified ERK2 and RSK4, the next step was to develop the kinase assay necessary for the biological assessment of our compound library. A general scheme of the pathway is outlined in **Figure 35**.

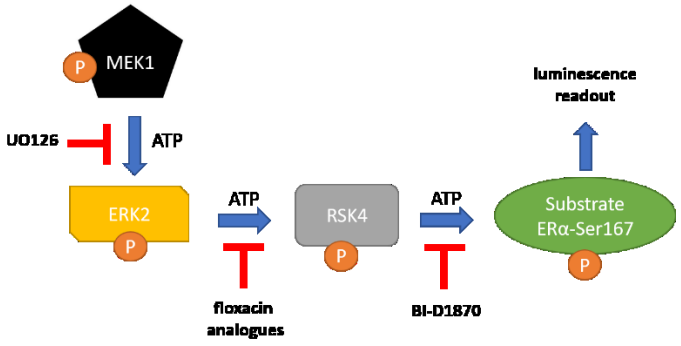

Figure 35 – Outline of RSK4 signalling pathway.

Estrogen receptor α (ERα) phosphorylation was chosen as the readout of the experiment. ERα is a substrate of the RSK family[97] and it has been used as substrate for RSK activity kinase assays in the past.[98] However, as previously mentioned, substrate phosphorylation can be prevented not only by inhibiting RSK4 activity directly, but also by preventing its activation. In the first case the experiment readout provides a direct

measure of drug inhibition, while in the second instance the result will be an indirect measure. Additionally, the ERα phosphorylation read out would also be affected by ERK2 and MEK1 inhibitors. Therefore, to prevent false positive results in the search of RSK4 inhibitors, constitutively active ERK2 was used, to avoid the use of MEK1.

For those compounds showing the ability to inhibit ERα phosphorylation, further studies will be needed to assign mechanism of action. Since the focus of this project is the development of inhibitors of RSK4 activation, a control experiment without ERK2 must be in place to rule out inhibitors of RSK4 activity, and an additional kinase experiment of ERK2 will have to be carried out to discard ERK2 inhibitors.

Since unpublished results by Seckl and Pardo's group showed that floxacin analogues do not bind to the active enzyme, to be able to assess the compound library in a RSK4 activation assay, RSK4 needs to be in its inactivated state, or at least only partially phosphorylated. Western blot analysis of purified RSK4 showed some degree of phosphorylation (**Figure 33A**). This is consistent with the constitutive phosphorylation in positions Ser232, Ser372, and Ser389 found in native RSK4, but could also mean that recombinant RSK4 is already fully active. To confirm this and investigate the optimal conditions of the assay, a series of preliminary kinase assays were carried out.

Firstly, a normal activity assay was performed using recombinant RSK4 at two different concentrations (5 and 25 nM), from both treated and untreated with MEK inhibitor U0126 (in theory, dephosphorylated and phosphorylated samples, respectively). RSK2 (5 nM) was included as a positive control for the phosphorylation of ERα. The effect of the pan-RSK inhibitor BI-D1870 (IC_{50} of 24 and 15 nM for RSK2 and RSK4, respectively, with 100 μM ATP)[49] was also studied. Phosphorylation of ERα was measured at time 0, immediately after adding ATP (10 μM) followed by addition of ethylenediaminetetraacetic acid (EDTA), when no phosphorylation should be detected, representing the negative

control (as for all subsequent assays), and 20 and 40 min after reaction start. As shown in **Figure 36,** no phosphorylation could be detected at time 0 for any of the assayed conditions (as expected), while the luminescence detected after 20 and 40 min reaction time was comparable, suggesting a maximum response after 20 min already. Furthermore, similar responses were obtained for both RSK4 concentrations, indicating that phosphorylation of the substrate is already maximised when RSK4 is at 5 nM. Similarly, same level of substrate phosphorylation was found regardless of treatment with U0126, suggesting that both samples are in the same state of activation. As expected, RSK2 was able to phosphorylate the substrate, and this event could be prevented in the presence of BI-D1870, showing that the obtained results are reliable in these conditions. Interestingly, RSK4 activity could also be hindered in the presence of the known inhibitor, albeit to a less extent than RSK2. Overall, these results highlight the fact that recombinant RSK4 had been obtained in an active state.

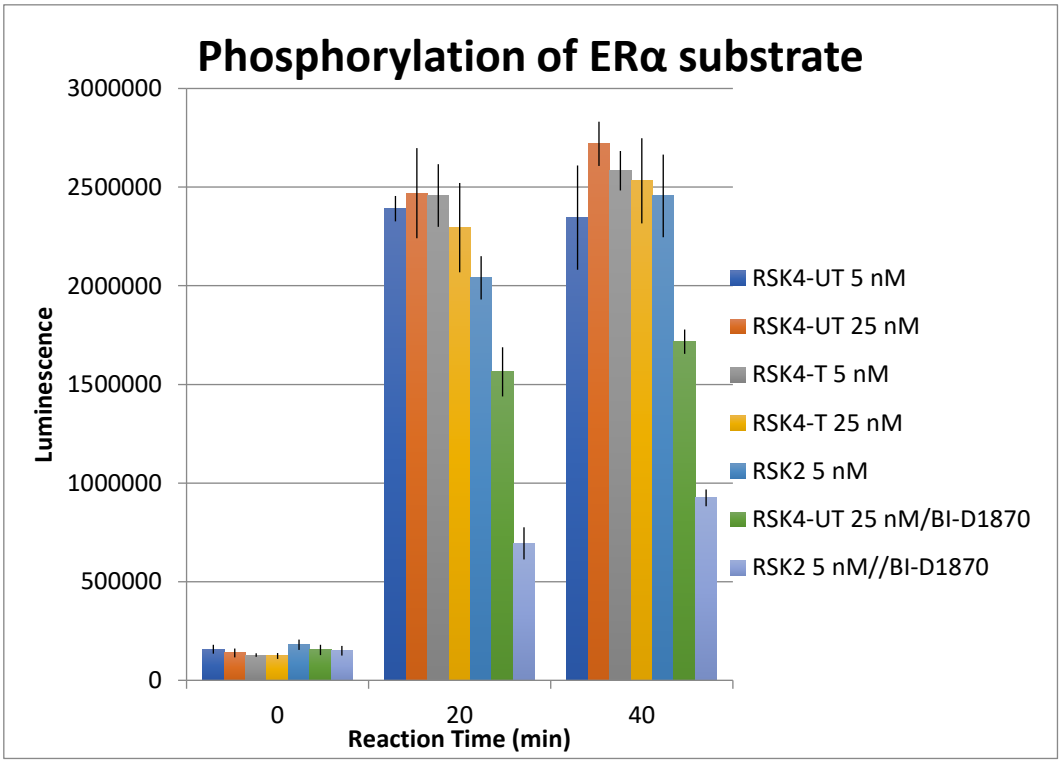

Figure 36 – Preliminary *in vitro* kinase assay. Two different fractions of RSK4 (treated, T, and untreated, UT with U0126) in two different concentrations (5 and 25 nM) were used. RSK4 was pre-incubated with BI-D1870 (3 μM) for 2 h. ATP (10 μM) reaction time were 20 and 40 min, including negative control with EDTA. RSK2 (5 nM) was used as positive control.

To assess if RSK4 was obtained in a partially versus fully actived state, the phosphorylation of ERα was assessed at increasing concentrations of ERK2, while maintaining RSK4 and ATP concentrations fixed at 1 nM and 10 μM, respectively, and reaction time at 20 min. If RSK4 is not fully phosphorylated, an increase in the luminescence should be observed with increasing concentrations of ERK2 as a consequence of more active RSK4 available to phosphorylate ERα. The experiment was also carried out in the absence of ERK2, to set up the minimum phosphorylation imposed by active RSK4. All conditions were assayed in the presence and absence of BI-D1870. However, as it can be seen in **Figure 37**, the phosphorylation levels of ERα did not increase with increasing ERK2 concentration, suggesting that RSK4 is indeed already fully active.

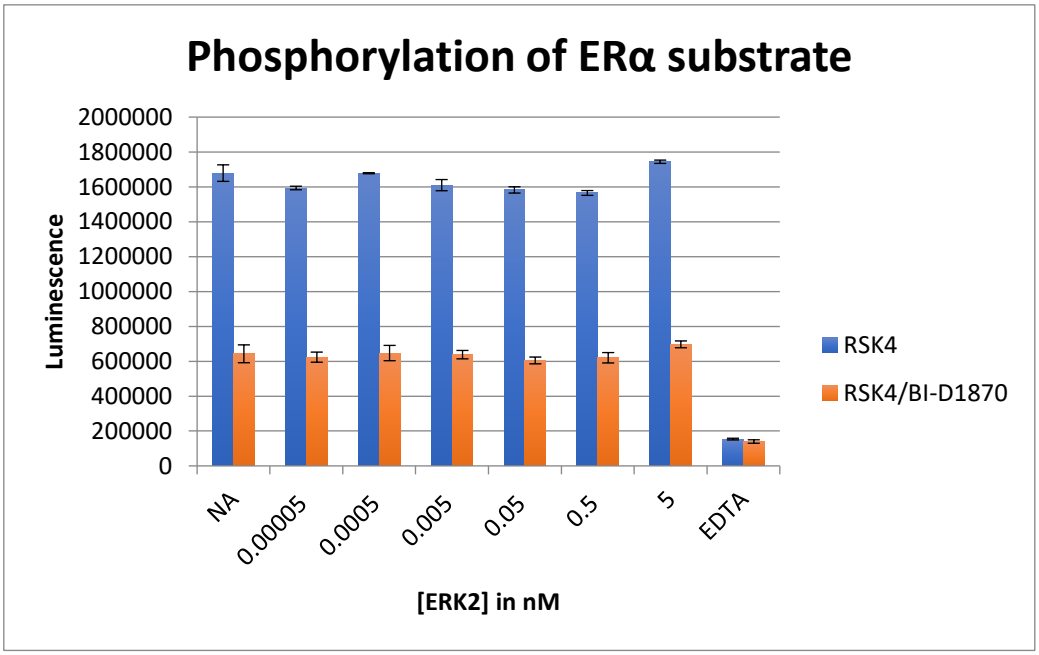

Figure 37 – Preliminary *in vitro* kinase assay. RSK4 (1 nM) and ERK2 (0.00005 to 5 nM, in 10-fold increments) were pre-incubated with BI-D1870 (3 μM) for 2 h. ATP (10 μM) reaction time was 20 min, including negative control with EDTA.

Nevertheless, it could also be that a difference in the readout could not be detected because of the conditions used. Therefore, two titration experiments were carried out to evaluate the influence of both ATP concentration and reaction time in the RSK4 activity assay. In the former, increasing concentrations of ATP (1 – 2000 μM) were evaluated at

a fixed RSK4 concentration of 1 nM and 20 min reaction time, both in the presence and absence of BI-D1870. As depicted in **Figure 38**, ATP concentration does not have any effect on substrate phosphorylation either. However, it does affect inhibition by BI-D1870. Thus, the higher the concentration of ATP, the less inhibition of phosphorylation is achieved, confirming the expected ATP-competitive behaviour of the inhibitor.

Likewise, when a time-course RSK4 activity assay (5–30 min) was carried out, maintaining RSK4 at 0.5 nM and ATP at 1 and 10 µM concentrations, no substantial differences were obtained (**Figure 39**).

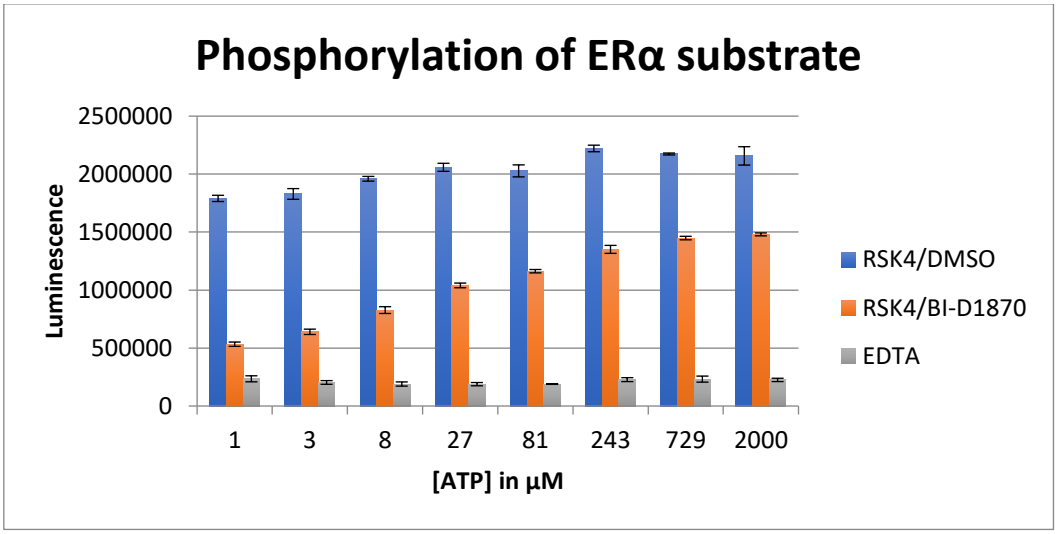

Figure 38 – Preliminary *in vitro* kinase assay. RSK4 (1 nM) was pre-incubated with BI-D1870 (3 µM) for 2 h. ATP (1 µM to 2000 µM) reaction time was 20 min, including negative control with EDTA.

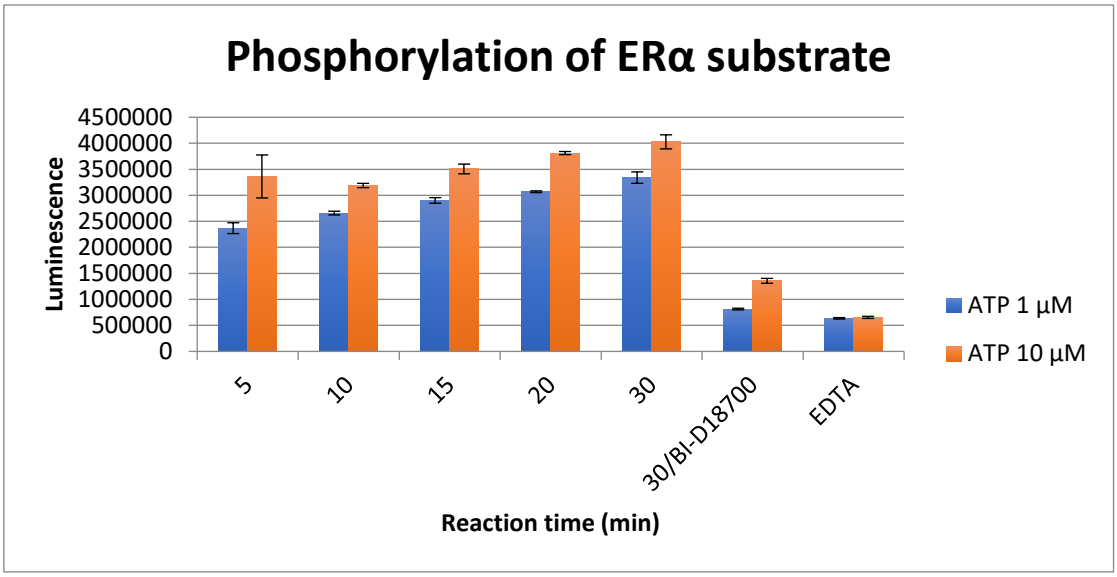

Figure 39 – Preliminary *in vitro* kinase assay. RSK4 (0.5 nM) was pre-incubated with BI-D1870 (3 µM) for 2 h. ATP (1 or 10 µM) was added and reaction was stopped with 5, 10, 15, 20 or 30 min, including negative control with EDTA.

In a last attempt to confirm that RSK4 is fully activated, the reaction time titration was repeated lowering the concentration of RSK4 even more (0.1 and 0.01 nM) and evaluating the outcome in the absence and presence of ERK2 at 1 nM concentration (10 and 100 times higher than that of RSK4). Additionally, the effect of treatment with BI-D1870 and GDC-0994, a known ERK2 inhibitor, at 3 µM concentration was evaluated. Unfortunately, the results displayed in **Figure 40** verify that recombinant RSK4 was obtained in a completely active state since no difference could be observed in the ERα phosphorylation levels in the presence and absence of the RSK4 upstream kinase ERK2, regardless of RSK4 concentration and reaction time. Furthermore, the ERK2 inhibitor showed no effect on this outcome either, which reinforces previous observations.

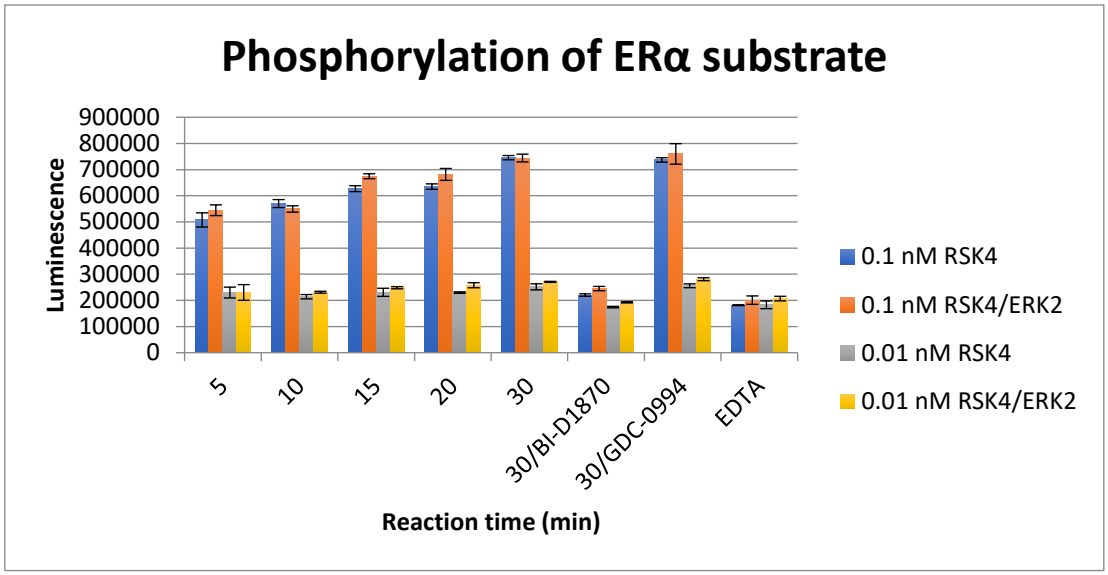

Figure 40 – Preliminary *in vitro* kinase assay. RSK4 (0.1 or 0.01 nM) and ERK2 (1 nM) were pre-incubated with BI-D1870 (3 μM) or GDC-0994 (3 μM) for 2 h. ATP (1 μM) was added and reaction was stopped with 5, 10, 15, 20 or 30 min, including negative control with EDTA.

In summary, these assays suggest that recombinant RSK4 is indeed fully activated, even after treatment during protein expression with the MEK inhibitor U0126. Unfortunately, this fact hampers the study of our floxacin derivatives since the initial findings revealed these compounds to be inhibitors of RSK4 activation, but not of its activity.

To confirm this theory, trovafloxacin (100 μM) was tested using previous described conditions (RSK4 at 0.5 nM, ERK2 at 5 nM, ATP at 250 μM or 5 μM, and reaction time at 15 min). As expected, there was no decrease of RSK4 phosphorylation in comparison to DMSO (data not shown).

There are feasible protocols in place to dephosphorylate kinases, but due to time constrains, this could not be done during my placement. However, once the inactive RSK4 has been obtained in further studies, the assay conditions would be optimised, and the library of compounds evaluated in terms of their ability to inhibit RSK4 activation.

2.2.2. Cell-based assay

To be able to study the effect of our trovafloxacin derivatives on the phosphorylation state of RSK4 in live cells, a cell line that stably overexpresses RSK4 is necessary.

Recombinant proteins can be overexpressed in several mammalian cell lines, the most common being Chinese hamster ovary (CHO) and human embryonic kidney 293 (HEK293) cells. For this, an expression vector containing the gene of interest must be transfected into the cell's nucleus. Transgene integration can be achieved through different expression vector methods, with lentivirus vectors particularly interesting due to their ability to integrate into the cell genome in high yields, allowing long-term stable expression.[99,100]

However, generating stable cell lines can take between four and six months of laboratory work, including laborious single cell cloning.[99] One alternative is to integrate the gene of interest with a co-expressed marker, such as the Green Fluorescent Protein (GFP).[101] In this type of system, both gene of interest and marker are translated from the same vector and therefore protein expression levels are coupled.[102] Thus, cells that stably express GFP (and consequently the gene of interest) can then be selected by Fluorescence-Activated Cell Sorting (FACS), and expanded to finally provide the necessary cell line overexpressing the target protein (**Figure 41**).

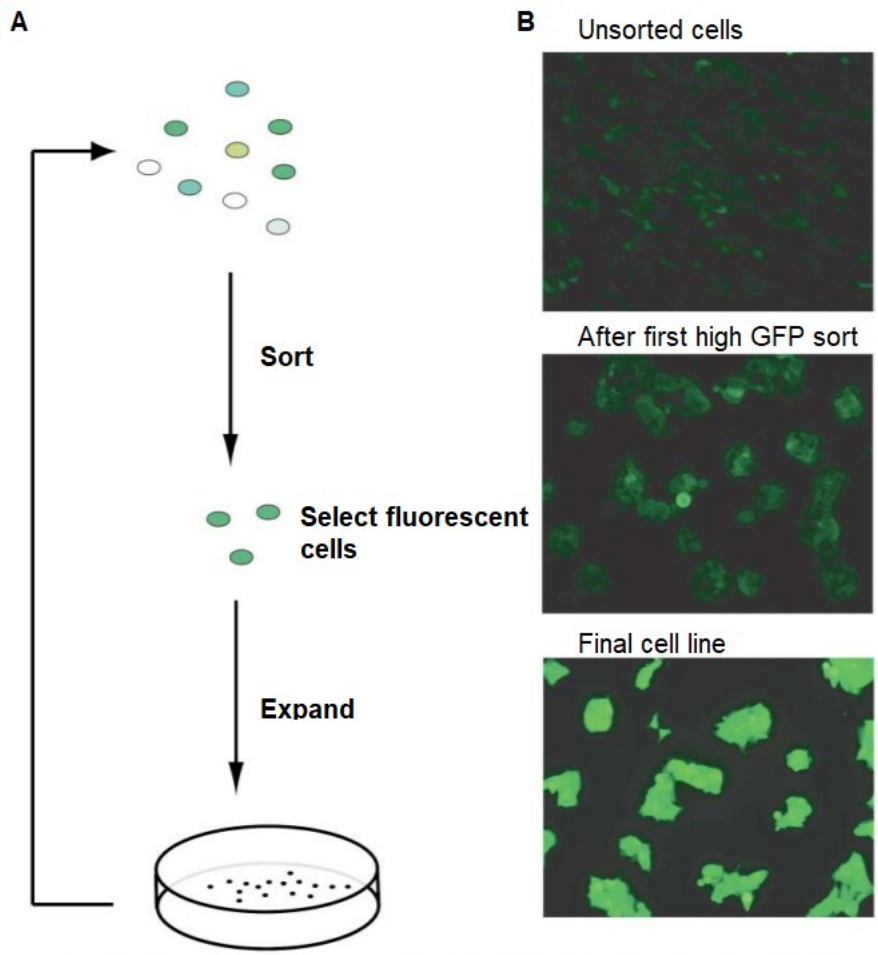

Figure 41 – GFP-selection in mammalian cell lines. A. General scheme of cell line enrichment. B. Progression of enrichment process monitored by fluorescence microscopy. Adapted from Mancia et al.[102]

Once the cell line is overexpressing the protein of interest, there are different ways to evaluate kinase activity with cell-based assays, ranging from target specific to phenotypic readouts.[103] The former usually evaluates specific phosphorylation sites, or even a secondary response to phosphorylation, such as induced protein-protein interaction. One possible limitation of this type of assay is the assumption that endogenous and exogenous targets will behave similarly. Phenotype assays on the other hand will consider cell proliferation and differentiation for example. However, a variety of cellular mechanisms may interfere with the chosen readout.

Herein, RSK4 was engineered into HEK293 cells and site-specific phosphorylation was analysed by immunoblotting. This allowed comparison with the biochemical assay

(previously desrcibed), providing information about the behaviour of phosphorylation and activation of RSK4 when purified and when engineered into a cell line.

2.2.2.1. Generating a stable cell-line overexpressing RSK4

A lentivirus encoding RSK4 and GFP (already available at the Lannigan laboratory) was used to transduce HEK293 cells. After transduction, cells were sorted using FACS by means of the fluorescent GFP protein attached to RSK4. Transfected cells after FACS sorting and expansion are shown below (**Figure 42**).

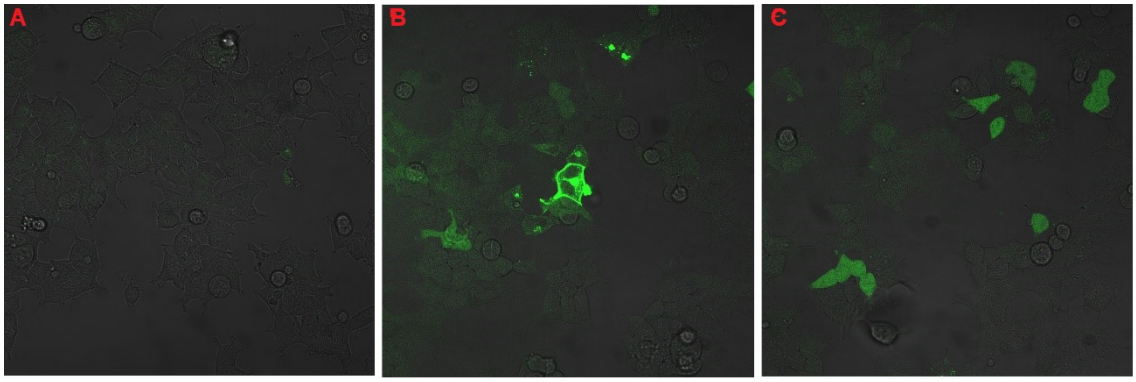

Figure 42 – HEK293 cells expressing RSK4 and GFP marker (green). A. Negative control; B, C. RSK4-GFP in green.

2.2.2.2. Cell-based assay - development

With RSK4 being stably expressed in HEK293 cells, a cell-based assay could be developed to evaluate post-translational phosphorylation levels. Since floxacin analogues are meant to be inhibitors of RSK4 activation, this is, of its phosphorylation by ERK2, the readout of this experiment will be RSK4 phosphorylation. To assess this event, an external stimulus such as a growth factor, is necessary to trigger the activation of the signalling pathway. Thus, in the absence of inhibitors, RSK4 will be fully phosphorylated, while in the presence of compounds that disrupt this process activation levels will be decreased.

Specifically, U0126 will be used as negative control. Considering that it inhibits ERK2 phosphorylation, thus preventing RSK4 phosphorylation, its use in the experiment will establish the minimum phosphorylation levels that will be obtained. As shown in **Figure 43**, using a phosphorylation site-specific antibody for the RSK family, two bands can be seen. The lower band correspond to endogenous RSK1–4 (all four RSKs have similar sizes thus making it difficult to differentiate them) and the second band correspond to the GFP-engineered RSK4 at around 119 kDa (92 kDa of RSK4 plus 27 kDa corresponding the GFP tag). When stimulated with EGF, expression of endogenous RSKs and exogenous RSK4 are increased when cells are treated with DMSO (positive control). On the other hand, when cells are treated with 10 μM U0126, there is no detection of RSK expression (negative control).

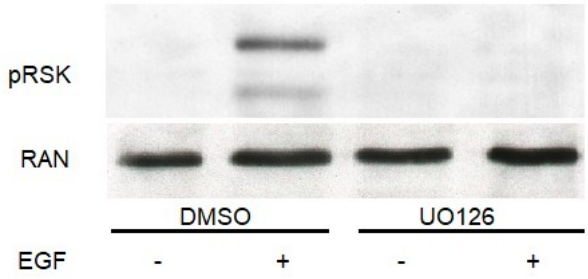

Figure 43 – Western blot of cell lysates from engineered HEK293 cells. Detection of RAN was used as loading control

Following a general assay procedure developed by Dummler et al.,[28] cells were incubated for 2 h with 50 μM inhibitors, 10 μM U0126 or vehicle (DMSO). 20 mins prior to the end of incubation period, EGF at a final concentration of 20 nM was added to the cells and incubated for the remaining time, followed by lysis. The lysates were then subjected to immunoblotting using anti-phosphorylation antibodies to detect phosphorylated RSK4 (endogenous and exogenous) and normalised against the total amount of GFP detected using a GFP specific antibody

The most soluble analogues were tested and are shown in **Figure 44**. A trend can be seen: all but one bear a polar group on the R_3 side chain. **90** does not have a polar group in the side chain; however, it is one of the two analogues with the modified core which might explain the better solubility.

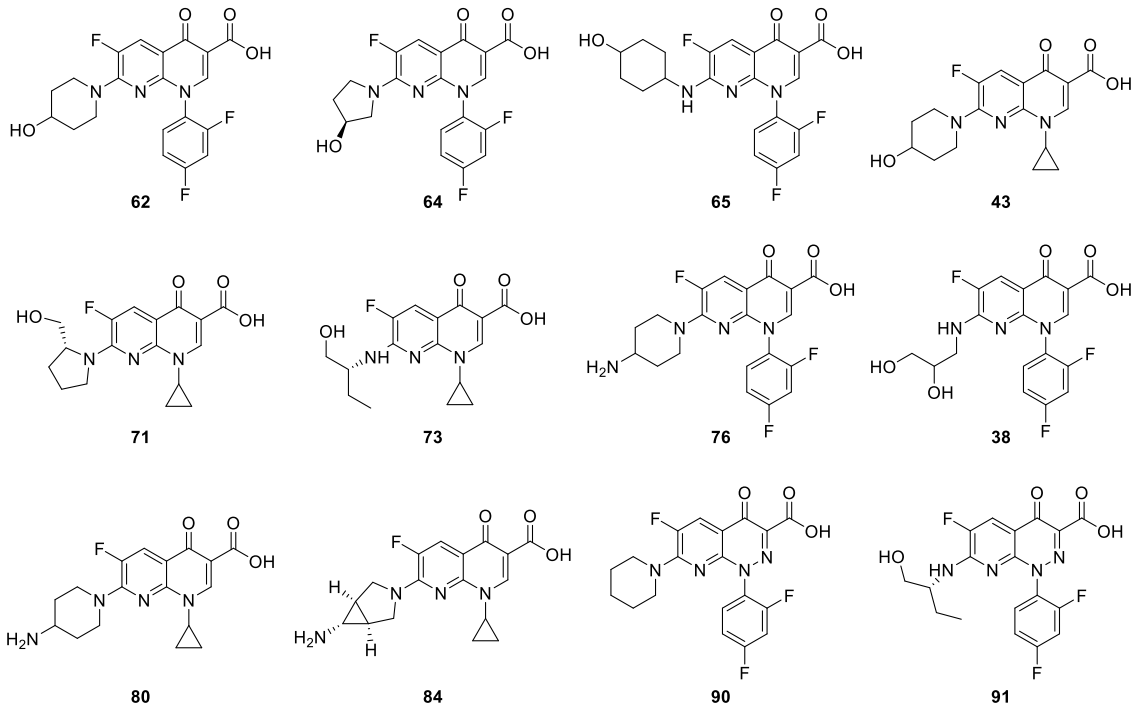

Figure 44 – Analogues tested in the cell-based assay.

Results obtained from the assay are shown in **Figure 45** and in **Figure 46**. Graphs were obtained by quantification of the bands of exogenous RSK4 (represented by columns) and endogenous RSK (represented by lines) of the Western blots using ImageJ.

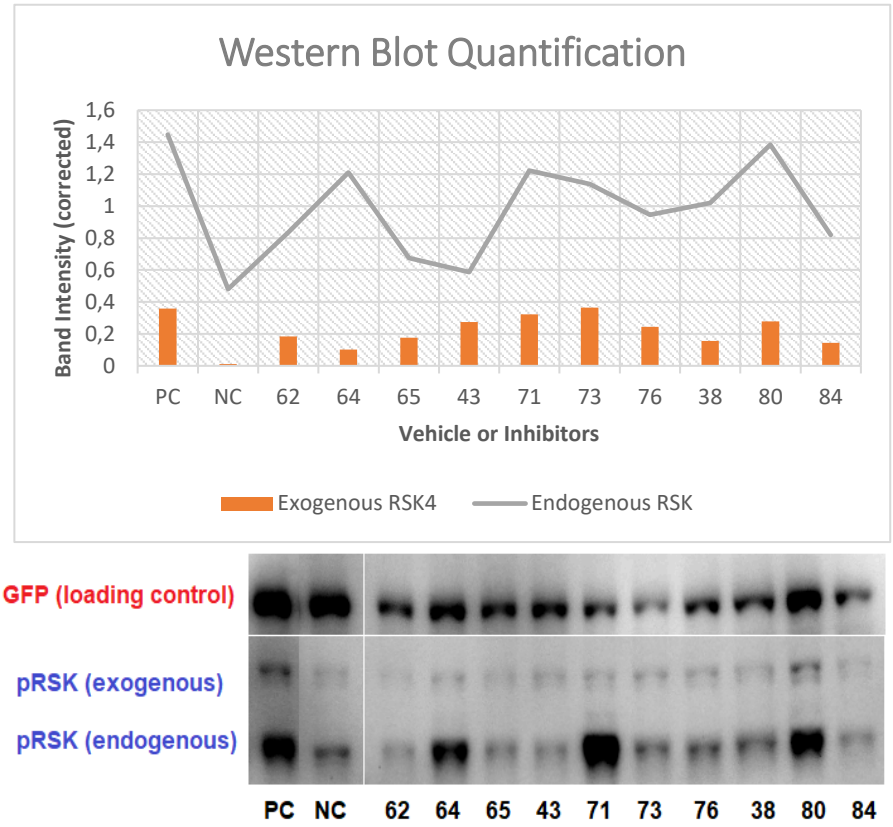

Figure 45 – Results of cell-based assay for some analogues. PC= positive control (DMSO); NC= negative control (U0126).

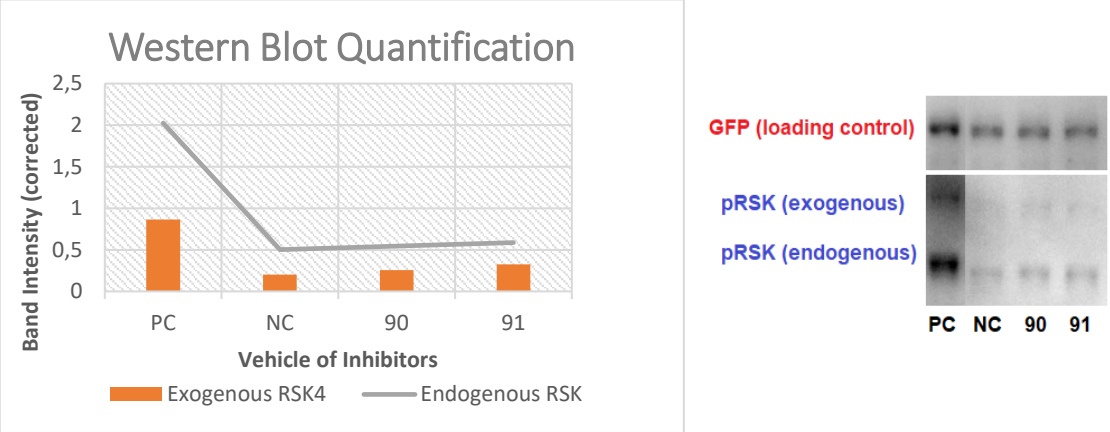

Figure 46 – Results of cell-based assay for analogues **90** and **91**. PC= positive control (DMSO); NC= negative control (U0126).

As it can be seen in both figures, endogenous RSK had a higher expression than exogenous RSK4. This can be attributed to the use of an antibody that is not specific to detect phosphorylation of a single isoform (there are currently no specific antibodies to detect RSK4 phosphorylation). Therefore, the endogenous band is probably the sum of the phosphorylation detected in all isoforms hence the higher intensity.

On the other hand, the higher band detected by the same antibody is specific for RSK4 since this isoform is the only one containing the GFP tag. The analysis of these bands in combination with their quantification should provide a first insight into the inhibitory activity of the tested analogues.

Indeed, analogues **38**, **62**, **64**, **65**, **84**, **90**, and **91** showed at least 50% inhibition if compared to the controls used in the assay. Of these, only one, **84**, has a cyclopropyl as R_2. All the remaining bear a 2,4-difluorophenyl at this position, showing that this group might be important to the inhibitory activity. Moreover, five of the seven analogues bear a hydroxyl group on the R_3 side chain, group that might also be crucial to activity, besides improving solubility as already mentioned.

These are initial observations that can be further investigated with more in-depth analysis, such as a dose-response assay. Furthermore, complementing assays, such as cell viability, can also provide necessary information into the behave of the compounds in the cell-based assay.

In addition, a summary of some physico-chemical properties of these analogues is listed below (Table x). Octanol-water partition coefficient logP and Topological Polar Surface Area (TPSA) are properties that can easily be calculated with online tools (in this case, using Molinspiration property calculation service, http://www.molinspiration.com/cgi-bin/properties). These can provide useful when planning the next modifications and analogues. For instance, analogues **90** and **91** have an improved logP, showing that core modifications can indeed improve solubility, among other drug-like properties and predictions.[104–106]

Table 6 – Summary of physico-chemical properties of most active analogues.

Entry	M.W.	logP	TPSA
38	409.32	-0.82	124.68
62	419.36	-0.27	95.66
64	405.33	0.19	95.66
65	433.39	0.74	104.45
84	344.35	0.42	101.46
90	404.35	2.37	88.33
91	408.34	1.45	117.34

2.2.2.3. Analysis by bottom-up/shotgun proteomics and tandem mass spectrometry

Next, it was necessary to confirm whether the anti-phosphorylation RSK antibody was indeed targeting exogenous RSK4. The best option would be to run an immunoprecipitation assay; whereby the antibody-antigen complex would be captured, purified, and analysed by tandem mass spectrometry (LC-MS/MS). However, due to time constraints, a simpler process was adapted, whereby, guided by a Western blot, the RSK4 band was excised from an SDS-PAGE gel and analysed by LC-MS/MS. Whilst this will not categorically say if the antibody reacts with RSK4, we can look for changes in phosphorylation by Western blot and mass spectrometry in tandem to further support that the antibody is indeed targeting RSK4.

The analysis of peptides released from proteins through proteolysis is called bottom-up proteomics and when this is performed in a mixture of proteins, it is called shotgun proteomics. These peptides can then be fractioned and subject to tandem mass spectrometry and identified by comparison with a protein database.[107]

Having this is mind, a short shotgun experiment was planned. Engineered HEK293 cells were treated either with DMSO or U0126 (following the same procedure for the cell-based assay) and purified by gel electrophoresis. Guided by a western blot with the GFP antibody (**Figure 47**), small pieces (1 mm^3) of the gel, where exogenous RSK4 was believed to be, were cut, reduced, alkylated and digested with trypsin (in-gel digestion)[108]. The peptides were then subjected to reversed phase HPLC (Ultimate 3000 UHPLC, Thermo Scientific) directly coupled to a high-resolution mass spectrometer (Velos Pro, Thermo Scientific) and analysed by top 10 CID with dynamic exclusion enabled.

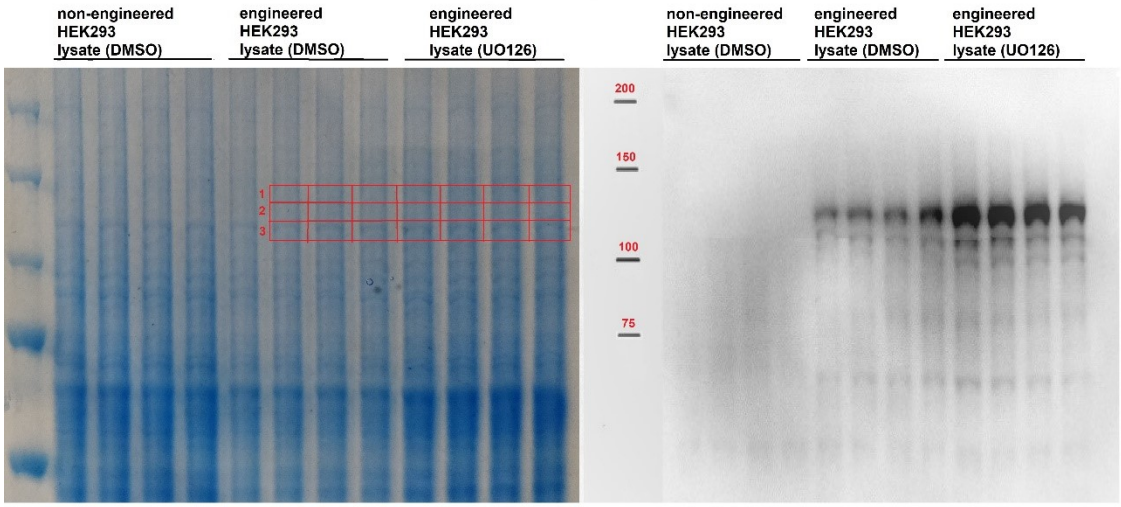

Figure 47 – SDS-PAGE and Western analysis (anti-GFP antibody) of HEK293 cell lysates (non-engineered and engineered). Four wells of each sample (20 µg) were ran and, after in-gel digestion, pooled together (total 80 µg). The bands corresponding to exogenous RSK4 were divided into three sessions (high, middle, and low) and analysed separately.

The mass spectra were searched against a well annotated and manually curated database of human proteins (Swissprot, accessed 08\2018) using Mascot Server (Matrix Science). Cysteines were assumed to be carbamidomethylated and oxidation of methionine and phosphorylation of S/T were included as variable modifications. Over 600 proteins were identified, including RSK4 (gene RPS6KA6); no other RSK proteins were identified from the region of the gel. Furthermore, phosphorylated peptides from RSK4 were identified, the fragmentation spectra (MS2) of these peptides were manually

inspected (see example spectra **Figure 48**). **Table 7** shows a summary of the peptides found to be phosphorylated and the respective phosphorylation sites of RSK4.

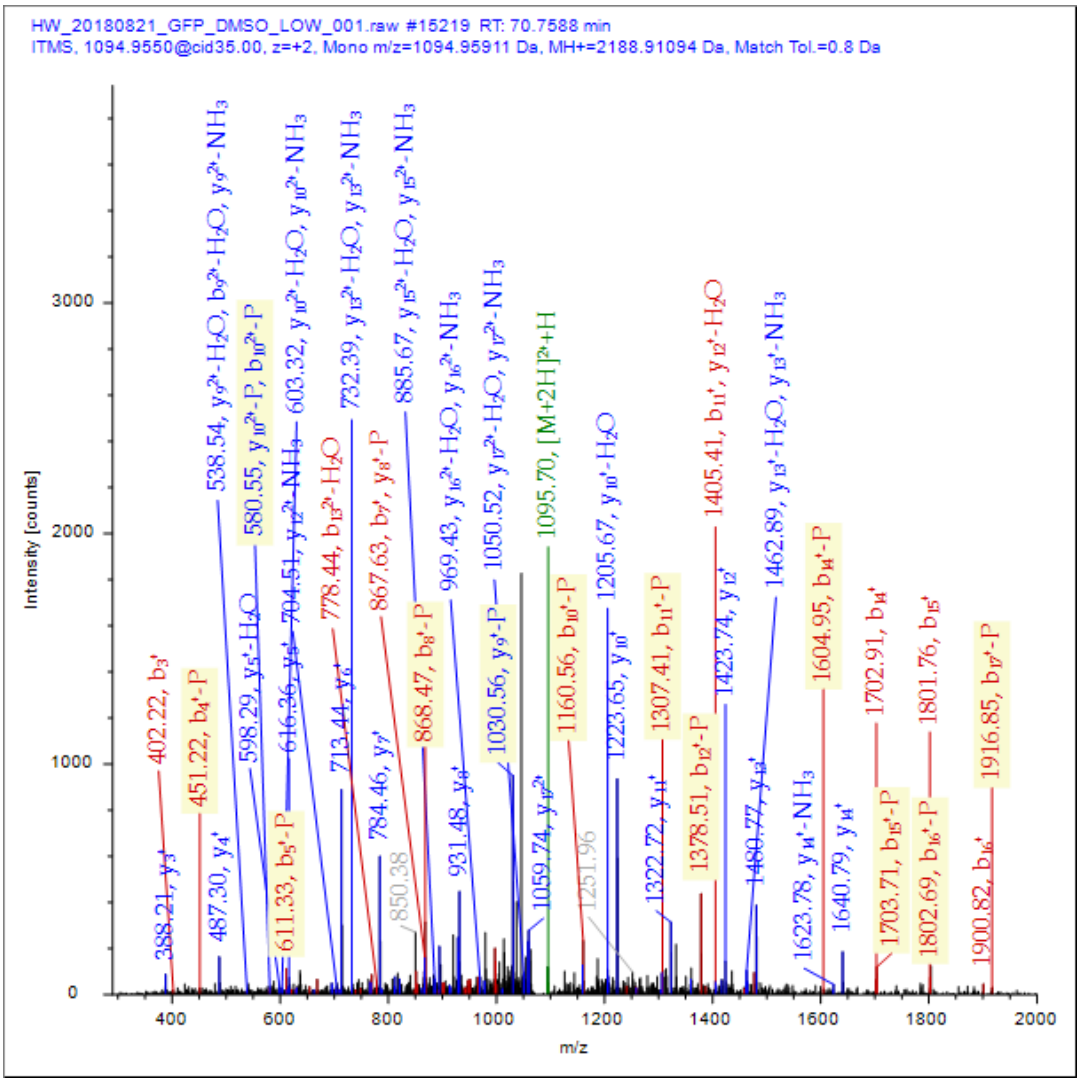

Figure 48 – Example of fragmentation spectra (MS2).

Table 7 - Phosphorylated peptides found in engineered HEK293 cells. Values are chromatographed peak areas.

Phosphorylation sites of RSK4	Anntated Sequence	DMSO	U0126
Ser232	AYsFcGTVEYmAPEVVNR	38878,56934	-
Ser389	GFsFVATSIAEEYK	51800,86133	36130,43652
Unknown residue	LTDFGLSKEsVDQEKK	29874,57227	-
Total Phosphorylation	-	120554,0029	36130,43652

Serine residues 232 and 389 were found to be phosphorylated when cells were treated with DMSO, but only Ser389 was found to be phosphorylated in the presence of U0126. **Figure 49** shows the relative intensity of phosphorylation across all phosphorylated residues and total phosphorylation found. Phosphorylation of Ser389 seems to be unchanged in both treatments. Interestingly, one phosphorylated residue was found with an annotated sequence that is different from the known phosphorylation sites of RSK4. Moreover, RSK4 phosphorylation sitesThr368, Ser372, Thr581, and Ser742 were not found after fragmentation.

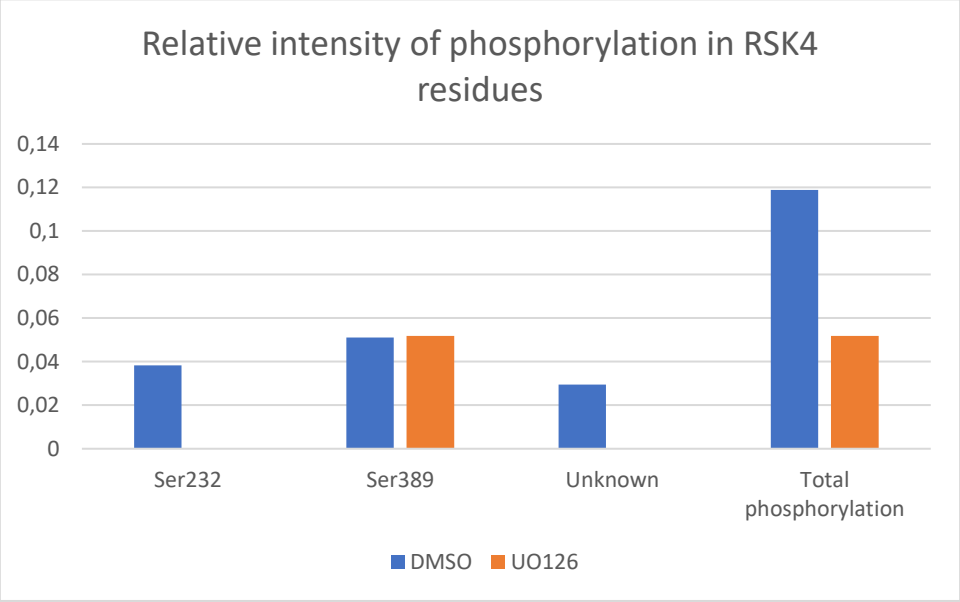

Figure 49 – Relative intensity of RSK4 phosphorylation. Values were found by dividing individual chromatographed peak areas by the total peak area found for RSK4 peptides.

This short experiment suggests that exogenous RSK4 was targeted by the GFP antibody and that a difference in phosphorylation with the chosen controls could be seen, validating the cell-based assay. It is important to note however that the presented data is very limited due to time constraints. More experiments in triplicates need to be done to fully prove this theory.

2.3. *In vivo* studies

As previously stated, trovafloxacin was synthesised and sent to our collaborators at Hammersmith Hospital, Prof. Seckl and Dr. Pardo, to be further studied in an animal model.

For this, a cell line-derived xenograft (CDX) mouse model was created. The A549 hypotriploid epithelial cell line is a well-characterised and studied cellular model for lung cancer. To create the metastatic model, luciferase-encoding A549 cells were injected into nude mice, allowing tumour progression to be tracked via bioluminescence (luciferase fluorescence after injection of luciferin). Once tumours became palpable, a two-week daily treatment with trovafloxacin was started, in combination or not with cisplatin (once a week), and whole-animal imaging was taken on the first and last day of treatment. As it can be seen in **Figure 50**, treatment with trovafloxacin alone was more effective in reducing tumour size than the most common current line of treatment for lung cancer patients, cisplatin. Notably, the best results were obtained when both cisplatin and trovafloxacin were administered in combination. Similar results were found when a RSK4 CRISPR xenograft model (knockout for RSK4) was used and the mice were treated with cisplatin, but not with trovafloxacin. This result points out to an on-target effect of trovafloxacin in lung cancer xenograft models.

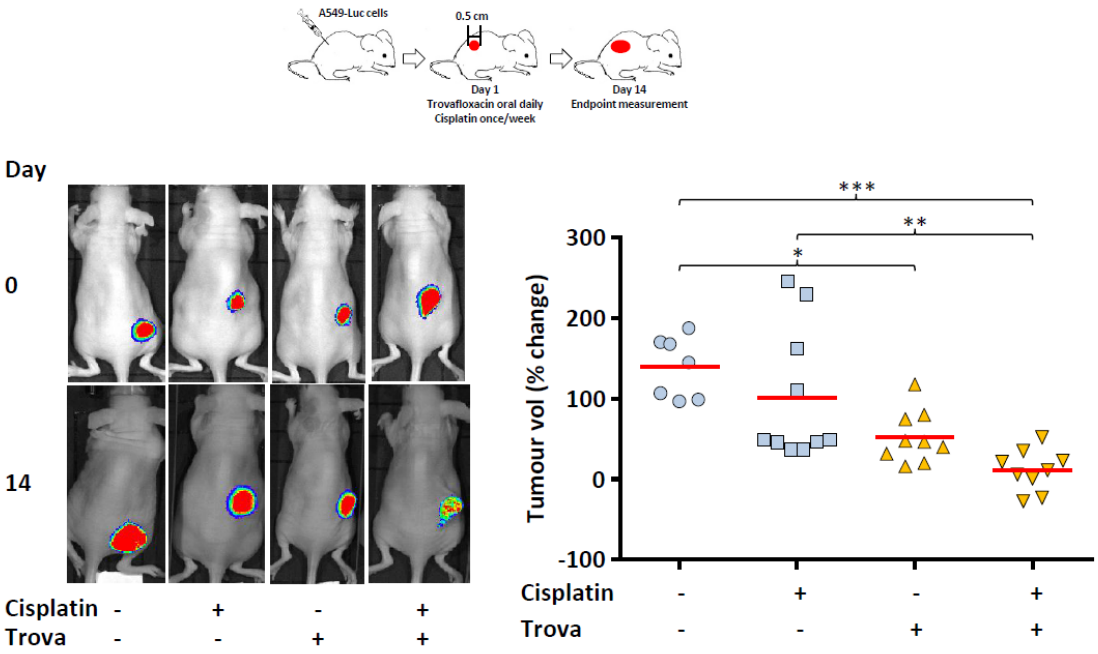

Figure 50 – A549 xenograft mice model experiment. Left panel: representative images from each condition showing luciferase signal at day 0 and 14. Right panel: % change in tumour volume at day 14. Red bar represents the median. From Chrysostomou et al. (submitted manuscript).

3. Conclusions and Future Work

Kinase RSK4 is a tumour promoter in the lungs and its inhibition decreases cell survival, mobility, and invasion as well as sensitising cancer cells to common chemotherapeutic agents. Considering that fluoroquinolones trovafloxacin and moxifloxacin are thought to be inhibitors of RSK4 activation, 47 floxacin analogues were synthesised aiming to improve fluoroquinolones inhibition profile. These analogues showed an intrinsic low solubility in organic solvents, such as DMSO, fact which prevented the use of some of these analogues in the biological assays. In an attempt to improve solubility, a different naphthyridine core were included in the compound library. These showed better solubility indeed and, in the future, this could be further explored as well as other similar modifications.

To evaluate these analogues, two target-based assays were envisaged. First, a biochemical assay, using recombinant ERK2 and RSK4, was planned. However, due to the constitutive phosphorylation of RSK4, the activation assay could not be advanced. In future work, RSK4 will be dephosphorylated and different conditions could be found for the desired activation assay.

A cell-based assay was also planned. Phosphorylation of overexpressed, exogenous RSK4 was evaluated using immunoblotting. Initial results show that a 2,4-difluorophenyl group at N1 and a hydroxyl group in the R7 side chain seem to be important for the inhibition of RSK4 phosphorylation. In addition, the assay was validated using bottom-up/shotgun proteomics and tandem mass spectrometry. In the future, this assay can be further explored, for example with a cell viability study. Furthermore, analogues showing interesting inhibition profiles could be further tested in dose-response assays.

Additionally, in collaboration with Prof. Seckl and Dr. Pardo's group, synthesised trovafloxacin was evaluated *in vivo*, using xenograft models and RSK4 was indeed confirmed as a target in lung tumours.

In combination, the confirmation of RSK4 being a target and the two assays developed herein can provide a first SAR necessary to initiate a drug discovery programme in lung cancer.

4. Experimental

4.1. Chemistry general procedures

All reactions were performed under an atmosphere of dry nitrogen. Room temperature (r.t.) refers to ambient temperature. Temperatures of 0 °C were achieved using an ice-water bath, whilst lower temperatures were achieved using a 2-propanol/dry ice bath. Reagents and solvents were supplied from commercial sources and used as supplied. Where anhydrous conditions were required, triethylamine and pyridine were distilled over calcium hydride, methanol was distilled over magnesium, and other anhydrous chemicals were obtained commercially. Column chromatography was carried out using Fluorochem 60 silica gel (230–400 mesh, 40-63 μm). Thin layer chromatography (TLC) was performed on aluminium plates using Merck Kiesegel 60 F254 (230–400 mesh). Fluorescent treated silica was visualised under UV (254 nm), or by staining with potassium permanganate or ninhydrin solutions. Solvents were removed by rotary evaporator at 40˚C or below and the compounds further dried under high vacuum. ^{1}H, ^{13}C, and ^{19}F NMR (nuclear magnetic resonance) were recorded on a Bruker Advance 400 spectrophotometer at 400, 100, and 377 MHz respectively, or ^{13}C NMR were recorded on a Bruker Advance 500 spectrophotometer at 125 MHz. Chemical shifts are referenced to the residual solvent peak. Proton spectra chemical shift (δH) are quoted in parts per million (ppm) to the nearest 0.01 ppm. Coupling constants (*J*) are reported in Hertz (Hz) to the nearest 0.1 Hz. Data are reported as follows: chemical shift, multiplicity (s, singlet; d, doublet; t, triplet; m, multiplet; or as a combination of these), coupling constant(s), integration and assignment. Carbon spectra were recorded with broadband proton spin decoupling and chemical shifts (δC) are quoted in ppm to the nearest 0.1 ppm. Coupling constants (*J*) to 19F are reported in Hz to the nearest 1 Hz. Fluorine spectra chemical shifts (δF) are quoted in parts per million (ppm) to the nearest 0.1 ppm. Melting points were obtained on a Reichert-Thermovar melting point apparatus and are

uncorrected. Neat infrared spectra were recorded on a Perkin Elmer Frontier FT-IR Spectrometer. Reported absorptions are given in wavenumbers (cm^{-1}). High resolution mass spectra were recorded by the Imperial College London Department of Chemistry Mass Spectroscopy Service using a Micromass Autospec Premier and Micromass LCT Premier spectrometer. Mass values are quoted within the error limits of ±5 ppm mass units. ESI refers to electrospray mass ionisation and EI to electron impact. Elemental analyses were measured by Stephen Boyer at London Metropolitan University. All values are given as percentage.

General Procedure A: Coupling between naphthyridine core and amine

To a solution of the naphthyridine core (1 eq) in pyridine, amine (2 eq) was added and the mixture was allowed to stir at r.t. for 4 h. Pyridine was then removed under reduced pressure, and the residue was partitioned between DCM and H_2O. The organic layer was dried with $MgSO_4$ and evaporated under reduced pressure to give a solid, which was further suspended in water and stirred at r.t. for 24 h. The solid was filtered and dried.

General Procedure B: Deprotection with aqueous HCl

A suspension of the protected, 7-substitued naphthyridine (1 eq) in 6 M HCl was heated to reflux for 24 h. The mixture was evaporated to dryness under reduced pressure. The residue was then suspended in MeOH and allowed to stir for 24 h at r.t. The solid was then filtered and dried.

General Procedure C: Deprotection with HCl

A suspension of the protected, 7-substitued naphthyridine (1 eq) in 2 M HCl in diethyl ether was allowed to stir at r.t. for 72 h. The mixture was evaporated to dryness under reduced pressure. The residue was then suspended in MeOH and allowed to stir for 24h at r.t. The solid was then filtered and dried.

General Procedure D: Deprotection with CH_3SO_3H

To a suspension of the protected, 7-substitued naphthyridine (1 eq) in THF/H_2O (9:1), methanesulfonic acid 97% (10 eq.) was added and the mixture was allowed to stir under reflux for 24 h. The mixture was evaporated to dryness under reduced pressure. The residue was then suspended in ethanol and allowed to stir for 24 h at r.t. The solid was then filtered and dried.

4.2. Chemistry synthesis

Compound 1: Ethyl 1-2,4-difluorophenyl-6-fluoro-7-chloro-1,4-dihydro-4-oxo-1,8-naphthyridine-3-carboxylate

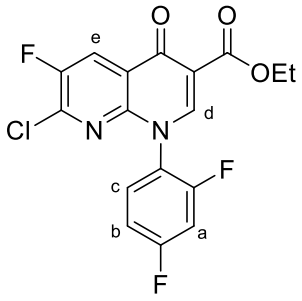

K_2CO_3 (1.02 g, 7.38 mmol) was added to a solution of **5** (2.95 g, 7.05 mmol) in acetonitrile (50 mL). The solution was heated to reflux overnight. The solvent was then evaporated to dryness and the residue was dissolved in DCM, washed with H_2O twice, dried over $MgSO_4$, and purified by column chromatography (99:1 DCM/MeOH), affording 2.53 g (94%) of **1**, as a white solid.

R_f 0.84 (9:1 DCM/MeOH).

M.p. 181–184 ºC.

^{1}H NMR (400 MHz, $CDCl_3$) δ 1.42 (t, *J* = 7.2, 3H, $OCH_2C\underline{H}_3$), 4.42 (q, *J* = 7.2, 2H, $OC\underline{H}_2CH_3$), 7.09–7.15 (m, 2H, **b** and **c**), 7.42–7.47 (m, 1H, **a**), 8.49 (d, *J* = 8.2, 1H, **e**), 8.56 (s, 1H, **d**).

^{13}C NMR (100 MHz, $CDCl_3$) δ 14.3, 61.5, 105.6 (d, *J* = 25), 112.6 (d, *J* = 26), 113.4, 123.2 (d, *J* = 10), 129.9 (d, *J* = 42), 142.8, 144.7, 149.3, 151.5, 154.1, 156.8, 159.2, 162.2, 164.2, 173.4.

IR 3081, 1693**.**

HRMS (ES-ToF) *m/z* found 383.0426, $C_{17}H_{11}ClF_3N_2O_3$ requires 383.0410.

Compound 2: Ethyl 7-chloro-1-cyclopropyl-6-fluoro-4-oxo-1,4-dihydro-1,8-naphthyridine-3-carboxylate

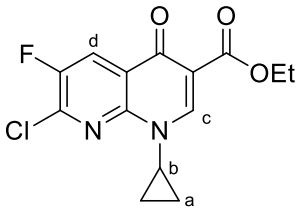

K_2CO_3 (0.56 g, 4.05 mmol) was added to a solution of **7** (1.35 g, 3.89 mmol) in acetonitrile (30 mL) and the solution was heated to reflux overnight. The solvent was then evaporated to dryness and the residue was dissolved in DCM, washed with H_2O twice, dried over $MgSO_4$, and purified by column chromatography (99:1 DCM/MeOH), affording 0.73 g (60%) of **14**, as a white solid.

***R**f* 0.79 (94:6 CM/MeOH).

M.p. 174.1–176.3 ºC.

^{1}H NMR (400 MHz, $CDCl_3$) δ 1.02–1.11 (m, 2H, **a**), 1.29–1.36 (m, 2H, **a**), 1.42 (t, *J* = 7.1, 3H, $OCH_2C\underline{H}_3$), 3.66 (m, 1H, **b**), 4.41 (q, *J* = 7.1, 2H, $OC\underline{H}_2CH_3$), 8.44 (d, *J*=7.4, 1H, **d**), 8.66 (s, 1H, **c**).

^{13}C NMR (100 MHz, $CDCl_3$) δ 7.7, 14.4, 34.4, 61.3, 112.2, 123.1 (d, *J* = 21), 123.9, 145.9, 148.9, 151.3, 153.9, 164.8, 173.2.

Compound 4: Ethyl 2,6-dichloro-5-fluoronicotinylacetate

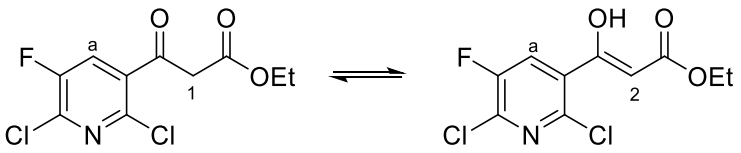

2,6-Dichloro-5-fluoronicotinic acid (2.0 g, 9.56 mmol) was dissolved in $SOCl_2$ (10 mL) and the mixture was heated at 80 °C for 2 h. The $SOCl_2$ was then removed by evaporation under reduced pressure yielding 2,6-dichloro-5-fluoronicotinyl chloride (**3**) as a yellowish oil. Monoethyl malonate (2.30 mL, 19.48 mmol) and biquinoline (1.0 mg) were dissolved in 100 mL of dry THF and cooled to -30 °C. A solution of 2.5 M *n*-butyllithium in hexane (15.6 mL) was added until a light pink colour remained at -5 °C. The suspension was then cooled to -50 °C. **3** was then dissolved in 10 mL of dry THF and added to the suspension dropwise. After the addition, the dry ice bath was removed and the reaction allowed to stir at r.t. for 1 h. The reaction was acidified with 1 N HCl to approximately pH 1 and was extracted with ether. The ether fraction was washed with saturated aqueous sodium bicarbonate solution and then water. The organic layer was dried ($MgSO_4$) and evaporated to dryness yielding a residue, which was then recrystallized in pentane to give 2.66 g (88%) of **4** (and its enol form) as a white solid.

***R**f* 0.59 (DCM). **M.p.** 60–62 ºC.

^{1}H NMR (400 MHz, $CDCl_3$) δ 1.27 (t, *J* = 7.1, 3H, $OCH_2C\underline{H}_3$), 1.36 (t, *J* = 7.1, 3H, $OCH_2C\underline{H}_3$), 4.11 (s, 2H, **1**), 4.21 (q, *J* = 7.1, 2H, $OC\underline{H}_2CH_3$), 4.30 (q, *J* = 7.1, 2H, $OC\underline{H}_2CH_3$), 5.85 (s, 1H, **2**), 7.84 (d, *J* = 2.2, 1H, **a**), 7.86 (d, *J* = 1.7, 1H, **a**), 12.58 (s, 1H, OH). **^{13}C NMR** (100 MHz, $CDCl_3$) δ 14.0, 14.1, 48.4, 61.1, 61.9, 94.9, 126.9 (d, *J* = 22), 127.6 (d, *J* = 21), 130.3, 133.8 152.6, 155.2, 165.1, 172.4, 191.1.

Compound 5: Ethyl 3-2,4-difluoroanilino-2-(2,6-dichloro-5-fluoronicotinyl)acrylate

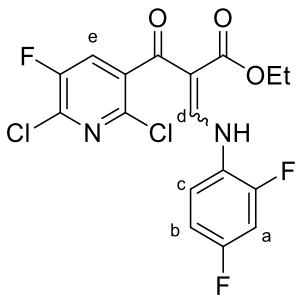

4 (1.32 g, 4.74 mmol) was dissolved in triethyl orthoformate (2.0 mL, 12.02 mmol) and Ac_2O (10 mL, 42.31 mmol), and the solution was heated at 130 °C for 1 h. The solution was evaporated under reduced pressure to a mobile oil, which was dissolved in DCM (10 mL), and 2,4-difluoroaniline (1.0 mL, 9.82 mmol) was added. After stirring at r.t. for 0.5 h, the solution was evaporated to dryness and the product was purified by column chromatography (9:1 DCM/pentane,), affording 1.54 g (78%) of **5** as a yellow solid.

***R**_f* 0.45 (DCM).

M.p. 119–121 ºC.

^{1}H NMR (400 MHz, DMSO-d_6) δ 1.01 (t, *J* = 7.0 H, 3H, $OCH_2C\underline{H}_3$), 3.99 (q, *J* = 7.0, 2H, $OC\underline{H}_2CH_3$), 7.18–7.27 (m, 1H, **b** or **c**), 7.48–7.57 (m, 1H, **b** or **c**), 7.82–7.96 (m, 1H, **a**), 8.17 (d, *J* = 7.8, 1H, **d**), 8.19 (d, *J* = 7.9, 1H, **d**), 8.58 (d, *J* = 14.2, 1H, **e**), 8.67 (d, *J* = 13.6, 1H, **e**).

^{13}C NMR (100 MHz, DMSO-d_6) δ 13.8, 14.2, 60.4, 60.5, 102.7, 105.2 (d, *J* = 87.8), 113.0 (d, *J* = 22), 122.2 (d, *J* = 11), 126.4 (d, *J* = 22), 139.4, 152.9, 155.1, 156.0, 158.9, 165.4, 188.9.

Compound 6: Ethyl 3-(cyclopropylamino)-2-[(2,6-dichloro-5-fluoropyridin-3-yl)carbonyl]prop-2-enoate

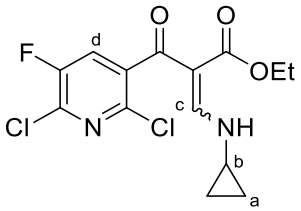

4 (1.32 g, 4.74 mmol) was dissolved in triethyl orthoformate (2.0 mL, 12.02 mmol) and Ac_2O (10 mL, 42.31 mmol), and the solution was heated at 130 °C for 1 h. The solution was evaporated under reduced pressure to a mobile oil, which was then dissolved in DCM (10 mL), and cyclopropylamine (1.0 mL, 9.82 mmol) was added. After stirring at r.t. for 0.5 h, the solution was evaporated to dryness and the product was purified by column chromatography (9:1 DCM/pentane), affording 1.54 g (76%) of **6** as a yellow solid.

***R**_f* 0.56 (DCM).

^{1}H NMR (400 MHz, $CDCl_3$) δ 0.84–1.02 (m, 4H, **a**), 1.07 (t, *J* = 7.1, 3H, $OCH_2C\underline{H}_3$), 3.98 (m, 1H, **b**), 4.05 (q, *J* = 7.1, 2H, $OC\underline{H}_2CH_3$), 7.34 (d, *J*=7.2, 1H, **d**), 7.41 (d, *J* = 7.2, 1H, **d**), 8.30 (d, *J* = 13.9, 1H, **c**), 8.38 (d, *J* = 14.5, 1H, **c**).

^{13}C NMR (100 MHz, $CDCl_3$) δ 6.7, 13.5, 14.0, 30.9 60.0, 60.2, 100.5, 124.4 (d, *J* = 23), 136.3 (d, *J* = 20), 139.0, 139.7, 152.7, 155.3, 161.2, 161.7, 165.9, 188.5.

Compound 7: (1α,5α,6α)-3-Benzyl-6-nitro-2,4-dioxo-3-azabicyclo[3.1.0]hexane

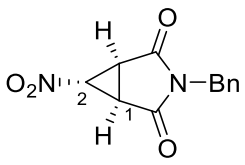

N-benzylmaleimide (1.0 g, 5.34 mmol) and K_2CO_3 (0.74g, 5.35 mmol) were dissolved in acetonitrile (10 mL), and bromonitromethane (0.40 mL, 5.74 mmol) in acetonitrile (1 mL), was added over 4 h dropwise, at r. t. Upon completion of the addition, bromonitromethane (0.1 mL, 1.43 mmol) was added every four hours, until a total of 2eq. had been added. After 48 h, the solvent was evaporated and the crude nitrocyclopropane was purified by column chromatography (8:2 pentane/EtOAc), affording **7** (0.37 g, 28%) as a white solid.

***R**f* 0.53 (8:2 pentane/EtOAc).

M.p. 98–100 ºC.

^{1}H NMR (400 MHz, $CDCl_3$) δ 3.36 (d, *J* = 1.7, 2H, **1**), 4.49 (t, *J* = 1.7, 1H, **2**), 4.55 (s, 2H, Bn CH_2), 7.30–7.37 (m, 5H, Bn aromatic CH).

^{13}C NMR (100 MHz, $CDCl_3$) δ 27.6, 42.7, 62.4, 128.5, 128.7, 128.9, 134.8, 168.4.

Compound 8: (1α,5α,6α)-3-Benzyl-6-nitro-3-azabicyclo[3.1.0]hexane

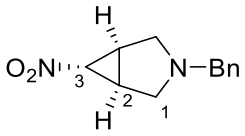

BH_3·THF complex (12.2 mL, 12.2 mmol) was added to a solution of **7** (0.75 g, 3.05 mmol) in dry THF (20 ml). The mixture was refluxed for 3 h, cooled to 5 ºC, and 6 mL of methanol was carefully added. The mixture was then refluxed for 0.5 h. The solvent was evaporated and the residual oil was dissolved in DCM and washed with H_2O twice. The organic layer was dried over anhydrous $MgSO_4$ and evaporated to provide 0.47 g (70%) of **8** as an oil.

R_f 0.81 (8:2 pentane/EtOAc).

^{1}H NMR (400 MHz, $CDCl_3$) δ 1.80–1.83 (m, 2H, **2**), 2.33 (t, *J* = 7.0, 2H, **3**), 2.55 (m, 2H, **1**), 2.92 (m, 2H, **1**), 3.60 (s, 2H, Bn CH_2), 7.23–7.32 (m, 5H, Bn aromatic CH).

^{13}C NMR (100 MHz, $CDCl_3$) δ 29.7, 53.4, 58.2, 61.1, 127.2, 128.3, 128.4, 138.4.

Compound 10: (1α,5α,6α)-3-Benzyl-6-*tert*-butyloxycarbonylamino-3-azabicyclo[3.1.0]hexane

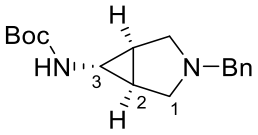

Pt/C 10% wet (0.34 g, 50% w/w) was added to a solution of **8** (0.68 g, 3.11 mmol) in MeOH (10 mL) and the mixture was hydrogenated in a Parr Shaker at 3.5 atm overnight. The catalyst was then filtered and the filtrate concentrated under vacuum giving the crude (1α,5α,6α)-3-benzyl-6-amino-3-azabicyclo[3.1.0]hexane **9** in quantitative yield. To the crude product in THF (20 mL), di-*t*-butyl-dicarbonate (0.79 g, 3.62 mmol) and Et_3N (0.8 mL, 5.77 mmol) were added. The mixture was allowed to stir for 5 h at r.t. The solvent was then evaporated and the crude product was purified by column chromatography (8:2 pentane/EtOAc), giving 0.63 g (79%) of **10** as a white solid.

R_f 0.28 (8:2 pentane/EtOAc).

^{1}H NMR (400 MHz, $CDCl_3$) δ 1.45 (s, 9H, Boc $(CH_3)_3$), 1.60 (br s, 2H, **2**), 2.35 (br s, 1H, **3**), 2.57–2.64 (m, 2H, **1**), 2.92–2.96 (m, 2H, **1**), 3.59 (s, 2H, Bn CH_2), 4.59 (br s, 1H, NH), 7.22–7.30 (m, 5H, Bn aromatic CH).

^{13}C NMR (100 MHz, $CDCl_3$) δ 24.5, 28.4, 30.5, 54.1, 58.9, 79.4, 126.7, 128.1, 128.4, 139.4, 156.4.

Compound 11: (1α,5α,6α)-3-Benzyl-6-*tert*-butyloxycarbonylamino-3-azabicyclo[3.1.0]hexane

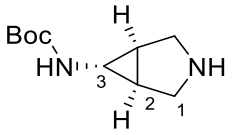

$Pd(OH)_2$ 20% wet (0.05 g, 50% by weight) was added to a solution of **10** (0.10 g, 0.35 mmol) in MeOH (5 mL). The mixture was hydrogenated in a Parr Shaker at 3.5 atm for 6 h. The catalyst was filtered and the solvent was evaporated to provide **11** (0.062 g, 90%) as a colourless oil.

***R*$_f$** 0.25 (92:8 DCM/MeOH).

^{1}H NMR (400 MHz, $CDCl_3$) δ 1.45 (s, 9H, Boc $(CH_3)_3$), 1.75 (m, 2H, **2**), 2.35 (t, *J* = 7.0, 2H, **3**), 2.56 (m, 2H, **1**), 2.92 (m, 2H, **1**), 4.63 (br s, 1H).

^{13}C NMR (100 MHz, $CDCl_3$) δ 28.4, 30.2, 48.6, 56.5, 79.4, 156.8.

IR 1696, 3359.

HRMS (ES-ToF)) *m/z* found 199.1398 $[M+H]^+$, $C_{10}H_{19}N_2O_2$ requires 199.1447.

Compound 12: Ethyl (1α,5α,6α)-7-(6-*tert*-butyloxycarbonylamino-3-azabicyclo[3.1.0]hexan-3-yl)-1-(2,4-difluorophenyl)-6-fluoro-1,4-dihydro-4-oxo-1,8-naphthyridine-3-carboxylate

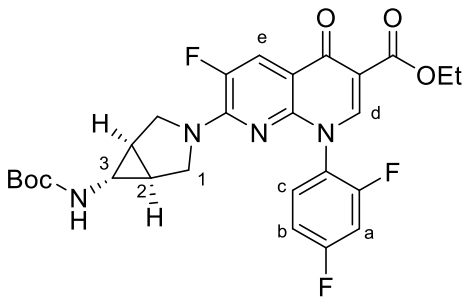

Ethanol (15 mL), **1** (0.40 g, 1.05 mmol), **11** (0.16 g, 0.08 mmol) and Et_3N (0.15 mL, 1.08 mmol) were heated to reflux for 5 h. The solvent was then evaporated to dryness and the crude product was purified by column chromatography (99:1 DCM/MeOH), affording **12** (0.403 g, 89%) as a white solid.

***R*$_f$** 0.63 (92:8 DCM/MeOH).

^{1}H NMR (400 MHz, $CDCl_3$) δ 1.40 (t, *J* = 7.2, 3H, $OCH_2C\underline{H}_3$), 1.44 (s, 9H, Boc $(CH_3)_3$), 1.75 (m, 2H, **2**), 2.30 (t, *J* = 7.0, 2H, **3**), 2.47 (m, 2H, **1**), 2.86 (m, 2H, **1**), 4.39 (q, *J* = 7.2, 2H, $OC\underline{H}_2CH_3$), 4.73 (br s, 1H, NH), 7.02–7.09 (m, 2H, **b** and **c**), 7.34–7.40 (m, 1H, **a**), 8.08 (d, *J* = 12.7, 1H, **e**), 8.36 (s, 1H, **d**).

^{13}C NMR (100 MHz, $CDCl_3$) δ 14.4, 24.7, 29.7, 33.6 50.2, 61.0, 79.9, 105.0 (d, *J* = 24), 111.9, 112.9 (d, *J* = 24), 114.2, 120.0, 124.6 (d, *J* = 10), 130.0 (d, *J* = 12), 144.7, 145.3, 147.2, 147.3, 148.4 156.1, 156.8, 165.3, 173.8.

Compound 13: (1α,5α,6α)-7-(6-Amino-3-azabicyclo[3.1.0]hex-3-yl)-1-(2,4-difluorophenyl)-6-fluoro-1,4-dihydro-4-oxo-1,8-naphthyridine-3-carboxylic acid, methanesulfonate

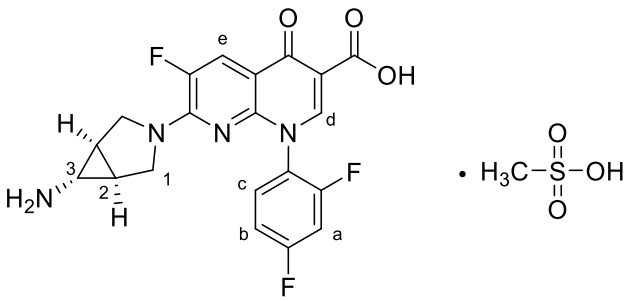

A solution of **12** (0.30 g, 0.55 mmol) in 9:1 THF/H_2O (10 mL) was treated with 97% methanesulfonic acid (0.11 mL, 1.7 mmol) and heated to reflux for 40 h. The reaction mixture was then cooled to r.t. and DCM (5 mL) and H_2O (10 mL) were added to the solution, and the two resultant layers were separated. The aqueous layer was then lyophilised, and the resultant crude salt was further refluxed in 2-propanol for 18 h. The reaction mixture was cooled to room temperature and allowed to stir for further 2 h. The crystalline product was then filtered, yielding **13** as an off-white solid (0.22 g, 77%).

^{1}H NMR (400 MHz, $CDCl_3$) δ 1.57–1.63 (m, 2H, **2**), 2.33 (s, 3H, $SO_3C\underline{H}_3$), 2.44 (br s, 1H, **3**), 2.50 (m, 1H, **3**), 2.52–2.60 (m, 2H, **1**), 2.93–2.99 (m, 2H, **1**), 7.34–7.39 (m, 1H, **b** or **c**), 7.59–7.64 (m, 1H, **b** or **c**), 7.78–7.83 (m, 1H, **a**), 8.07 (d, *J* = 12.5, 1H, **e**), 8.83 (s, 1H, **d**). **^{13}C NMR** (100 MHz, DMSO-d_6) δ 25.9, 30.7, 49.3, 61.5, 104.3 (d, *J* = 25), 108.4, 110.4, 111.8 (d, *J* = 24), 117.3 (d, *J* = 21), 130.3 (d, *J* = 11), 144.2, 145.5, 146.8, 147.4, 148.3, 155.5, 160.9, 164.8, 176.50. **IR** 1727, 2936. **HRMS** (ESI) *m/z* found 417.1168 $[M+H]^+$, $C_{20}H_{16}F_3N_4O_3$ requires 417.1175.. **Elemental analysis** calcd. for $C_{20}H_{15}F_3N_4O_3 \cdot CH_4SO_3$: C, 49.22; H, 3.74; N, 10.93, found: C, 49.15; H, 3.69; N, 10.86.

Compound 14: Ethyl 7-[4-(*tert*-butyloxycarbonyl)piperazin-1-yl]-1-(2,4-difluorophenyl)-6-fluoro-4-oxo-1,4-dihydro-1,8-naphthyridine-3-carboxylate

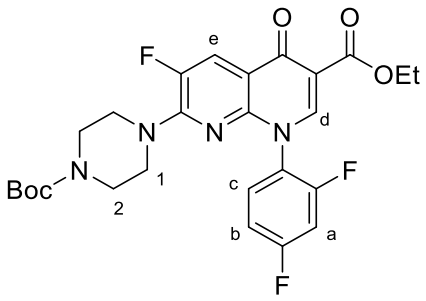

Prepared as described in General Procedure A, using **1** and 1-boc-piperazine, yielding **14** as a white solid (0.035 g, 34%).

***R*$_f$** 0.65 (92:8 DCM/MeOH).

^{1}H NMR (400 MHz, $CDCl_3$) δ 1.41 (t, *J* = 7.1, 3H, $OCH_2C\underline{H}_3$), 1.47 (s, 9H, Boc $(CH_3)_3$), 3.42–3.44 (m, 4H, **1** or **2**), 3.48–3.51 (m, 4H, **1** or **2**), 4.40 (q, *J* = 7.1, 2H, $OC\underline{H}_2CH_3$), 7.04–7.11 (m, 2H, **b** and **c**), 7.37–7.43 (m, 1H, **a**), 8.17 (d, *J* = 13.2, 1H, **e**), 8.42 (s, 1H, **d**).

^{13}C NMR (100 MHz, $CDCl_3$) δ 14.4, 28.4, 46.6, 50.2, 61.2, 80.2, 104.3 (d, *J* = 25), 108.4, 110.4, 111.8 (d, *J* = 24), 117.3 (d, *J* = 21), 130.3 (d, *J* = 11), 144.2, 145.5, 146.8, 147.4, 148.3, 154.2, 156.5, 162.9, 164.8, 174.5.

IR 1731, 2931.

Compound 15: Ethyl 1-(2,4-difluorophenyl)-6-fluoro-7-(4-methylpiperazin-1-yl)-4-oxo-1,4-dihydro-1,8-naphthyridine-3-carboxylate

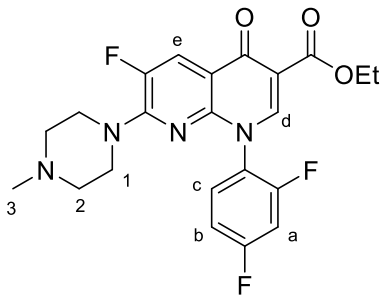

Prepared as described in General Procedure A, using **1** and 1-methylpiperazine, affording 0.035 g (40%) of **15** as a white solid.

***R*$_f$** 0.49 (92:8 DCM/MeOH).

^{1}H NMR (400 MHz, $CDCl_3$) δ 1.41 (t, *J* = 7.2, 3H, $OCH_2C\underline{H}_3$), 2.29 (s, 3H, **3**), 2.40 (t, *J*=4.8, 4H, **1** or **2**), 3.56 (t, *J* = 4.8, 4H, **1** or **2**), 4.40 (q, *J* = 7.2, 2H, $OC\underline{H}_2CH_3$), 7.03–7.10 (m, 2H, **b** and **c**), 7.37–7.43 (m, 1H, **a**), 8.14 (d, *J* = 13.4, 1H, **e**), 8.41 (s, 1H, **d**).

^{13}C NMR (100 MHz, $CDCl_3$) δ 14.4, 46.2, 47.6, 54.2, 61.0, 104.3 (d, *J* = 25), 108.4, 110.4, 111.8 (d, *J* = 24), 117.3 (d, *J* = 21), 130.3 (d, *J* = 11), 144.2, 145.5, 147.4, 148.3, 154.2, 156.5, 162.9, 164.8, 174.5.

IR 1709, 2978.

Compound 16: Ethyl 1-(2,4-difluorophenyl)-6-fluoro-7-(piperidin-1-yl)-4-oxo-1,4-dihydro-1,8-naphthyridine-3-carboxylate

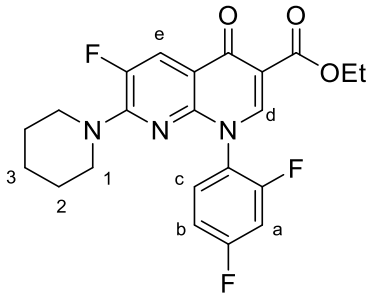

Prepared as described in General Procedure A, using **1** and piperidine, affording 0.122g (73%) of **16** as a white solid.

R_f 0.68 (92:8 DCM/MeOH).

^{1}H NMR (400 MHz, $CDCl_3$) δ 1.40 (t, *J* = 7.1, 3H, $OCH_2C\underline{H}_3$), 1.50–1.56 (m, 4H, **2**), 1.61–1.66–1.70 (m, 2H, **3**), 3.48 (t, *J* = 5.2, 4H, **1**), 4.38 (q, *J* = 7.1, 2H, $OC\underline{H}_2CH_3$), 7.01–7.09 (m, 2H, **b** and **c**), 7.38–7.43 (m, 1H, **a**), 8.09 (d, *J* = 13.5, 1H, **e**), 8.39 (s, 1H, **d**).

^{13}C NMR (100 MHz, $CDCl_3$) δ 14.4, 24.6, 25.8, 48.1, 48.2, 61.0, 104.3 (d, *J* = 25), 105.1, 111.8 (d, *J* = 24), 115.0, 120.8 (d, *J* = 21), 124.7, 130.1 (d, *J* = 11), 145.1, 148.5, 149.7, 156.7, 161.6, 165.2, 173.8.

IR 1687, 2932.

Compound 17: Ethyl 7-(cyclohexylamino)-1-(2,4-difluorophenyl)-6-fluoro-4-oxo-1,4-dihydro-1,8-naphthyridine-3-carboxylate

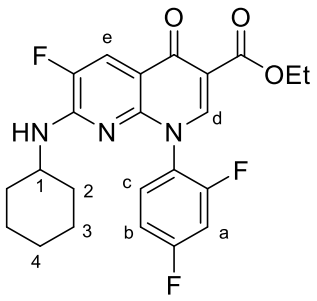

Prepared as described in General Procedure A, using **1** and cyclohexylamine, affording 0.027 g (23%) of **17** as a white solid.

***R*$_f$** 0.65 (92:8 DCM/MeOH).

^{1}H NMR (400 MHz, $CDCl_3$) δ 1.12–1.19 (m, 4H, **3**), 1.27–1.32 (m, 2H, **4**), 1.41 (t, *J* = 7.2, 3H, $OCH_2C\underline{H}_3$), 1.80–1.90 (m, 4H, **2**), 3.36 (br s, 1H, **1**), 4.40 (q, *J* = 7.2, 2H, $OC\underline{H}_2CH_3$), 7.01–7.10 (m, 2H, **b** and **c**), 7.37–7.43 (m, 1H, **a**), 8.07 (d, *J* = 10.5, 1H, **e**), 8.40 (s, 1H, **d**).

^{13}C NMR (100 MHz, $CDCl_3$) δ 14.4, 25.4, 25.8, 32.6, 48.2, 61.0, 104.4 (d, *J* = 25), 105.1, 111.9 (d, *J* = 24), 115.1, 121.0 (d, *J* = 21), 124.9, 130.1 (d, *J* = 12), 145.4, 148.4, 149.7, 151.2, 156.7, 161.2, 165.0, 173.6.

IR 1722, 2973.

Compound 18: Ethyl 1-(2,4-difluorophenyl)-6-fluoro-7-(methylamino)-4-oxo-1,4-dihydro-1,8-naphthyridine-3-carboxylate

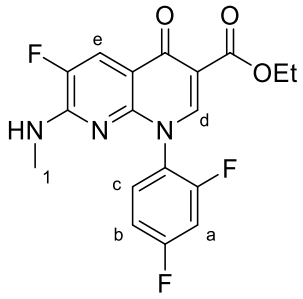

Prepared as described in General Procedure A, using **1** and methylamine, affording 0.043 g (43%) of **18** as a white solid.

R_f 0.54 (92:8 DCM/MeOH).

^{1}H NMR (400 MHz, $CDCl_3$) δ 1.41 (t, *J* = 7.1, 3H, $OCH_2C\underline{H}_3$), 2.79 (d, *J* = 4.8, 3H, **1**), 4.40 (q, *J* = 7.1, 2H, $OC\underline{H}_2CH_3$), 5.25 (br s, 1H, NH), 7.03–7.10 (m, 2H, **b** and **c**), 7.39–7.45 (m, 1H, **a**), 8.08 (d, *J* = 10.1, 1H, **e**), 8.39 (s, 1H, **d**).

^{13}C NMR (100 MHz, $CDCl_3$) δ 14.4, 28.9, 61.1, 104.7 (d, *J* = 24), 105.1, 111.9 (d, *J* = 24), 113.0, 114.3, 117.3 (d, *J* = 21), 130.3 (d, *J* = 11), 146.5, 148.4, 150.0, 156.9, 161.6, 165.5, 173.9.

IR 1688, 2977.

Compound 19: Ethyl 1-(2,4-difluorophenyl)-6-fluoro-4-oxo-7-(propan-2-ylamino)-1,4-dihydro-1,8-naphthyridine-3-carboxylate

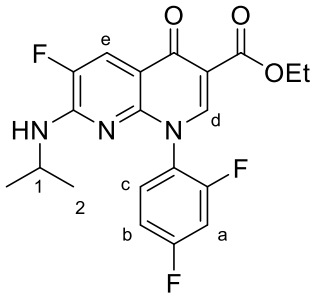

Prepared as described in General Procedure A, using **1** and 2-propylamine, affording 0.106 g (59%) of **19** as a white solid.

***R*$_f$** 0.58 (92:8 DCM/MeOH).

^{1}H NMR (400 MHz, $CDCl_3$) δ 1.11 (*pseudo*dd, *J* = 6.4, 16, 6H, **2**), 1.41 (t, *J* = 7.1, 3H, $OCH_2C\underline{H}_3$), 3.73 (sext, *J* = 6.4, 1H, **1**), 4.40 (q, *J* = 7.1, 2H, $OC\underline{H}_2CH_3$), 5.06 (br s, 1H, NH), 7.02–7.10 (m, 2H, **b** and **c**), 7.38–7.43 (m, 1H, **a**), 8.07 (d, *J* = 10.1, 1H, **e**), 8.39 (s, 1H, **d**).

^{13}C NMR (100 MHz, $CDCl_3$) δ 14.4, 22.0, 42.5, 61.1, 104.5 (d, *J* = 23), 105.2, 112.0 (d, *J* = 24), 113.1, 116.6, 117.1 (d, *J* = 21), 127.5 (d, *J* = 11), 144.0, 149.7, 151.0, 152.6, 157.9, 162.5, 165.2, 172.5.

IR 1708, 2932.

Compound 20: Ethyl 1-(2,4-difluorophenyl)-6-fluoro-4-oxo-7-(propylamino)-1,4-dihydro-1,8-naphthyridine-3-carboxylate

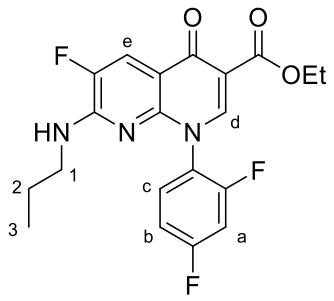

Prepared as described in General Procedure A, using **1** and *n*-propylamine, affording 0.078 g (49%) of **20** as a white solid.

***R*$_f$** 0.66 (92:8 DCM/MeOH).

^{1}H NMR (400 MHz, $CDCl_3$) δ 0.82 (t, *J* = 7.4, 3H, **3**), 1.42 (t, *J* = 7.1, 3H, $OCH_2C\underline{H}_3$), 1.48–1.54 (m, 2H, **2**), 3.41 (t, *J* = 7.1 Hz, 2H, **1**), 4.41 (q, *J* = 7.1, 2H, $OC\underline{H}_2CH_3$), 5.35 (br s, 1H, NH), 7.01–7.14 (m, 2H, **b** and **c**), 7.42 (td, *J* = 8.7, 5.8, 1H, **a**), 8.09 (d, *J* =10.6, 1H, **e**), 8.40 (s, 1H, **d**).

^{13}C NMR (100 MHz, $CDCl_3$) δ 11.2, 14.4, 22.2, 42.8, 61.1, 104.7 (d, *J* = 24), 105.1, 111.9 (d, *J* = 24), 113.0, 114.3, 117.2 (d, *J* = 21), 130.1 (d, *J* = 11), 146.9, 148.5, 149.7, 156.7, 161.6, 165.2, 173.8.

IR 1718, 2937.

Compound 21: Ethyl 7-(cyclopropylamino)-1-(2,4-difluorophenyl)-6-fluoro-4-oxo-1,4-dihydro-1,8-naphthyridine-3-carboxylate

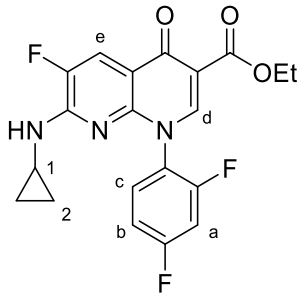

Prepared as described in General Procedure A, using **1** and cyclopropylamine, affording 0.128 g (81%) of **21** as a white solid.

R_f 0.62 (92:8 DCM/MeOH).

^{1}H NMR (400 MHz, $CDCl_3$) δ 0.57 (m, 4H, **2**), 1.42 (t, *J* = 7.1, 3H, $OCH_2C\underline{H}_3$), 2.45 (m, 1H, **1**), 4.41 (q, *J* = 7.1, 2H, $OC\underline{H}_2CH_3$), 5.49 (br s, 1H, NH), 7.01–7.15 (m, 2H, **b** and **c**), 7.45 (td, *J* = 8.6, 5.8, 1H, **a**), 8.10 (d, *J* = 10.3, 1H, **e**), 8.44 (s, 1H, **a**).

^{13}C NMR (100 MHz, $CDCl_3$) δ 6.9, 14.4, 23.5, 42.8, 61.1, 104.6 (d, *J* = 24), 105.0, 111.7 (d, *J* = 24), 113.0, 114.6, 117.4 (d, *J* = 21), 130.1 (d, *J* = 11), 145.9, 147.1, 156.7, 161.6, 165.2, 174.0.

IR 1720, 2969.

Compound 22: Ethyl 1-(2,4-difluorophenyl)-6-fluoro-4-oxo-7-(pyrrolidin-1-yl)-1,4-dihydro-1,8-naphthyridine-3-carboxylate

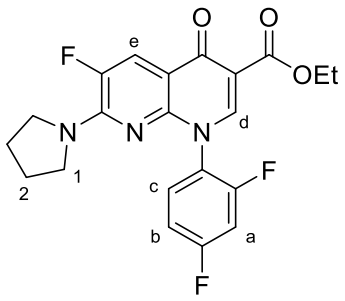

Prepared as described in General Procedure A, using **1** and pyrrolidine, affording 0.104g (62%) of **22** as a white solid.

***R*$_f$** 0.76 (92:8 DCM/MeOH).

^{1}H NMR (400 MHz, $CDCl_3$) δ 1.42 (t, *J* = 7.1, 3H, $OCH_2C\underline{H}_3$), 1.90–1.93 (m, 4H, **2**), 3.50 (br s, 4H, **1**), 4.40 (q, *J* = 7.1, 2H, $OC\underline{H}_2CH_3$), 7.00–7.10 (m, 2H, **b** and **c**), 7.36–7.44 (m, 1H, **a**), 8.07 (d, *J* = 12.8, 1H, **e**), 8.37 (s, 1H, **a**).

^{13}C NMR (100 MHz, $CDCl_3$) δ 14.4, 48.3, 48.4, 61.1, 104.9 (d, *J* = 23), 105.1, 111.9 (d, *J* = 24), 112.8, 113.6, 119.3 (d, *J* = 21), 130.0 (d, *J* = 12), 144.9, 145.6, 146.9, 161.6, 165.4, 174.0.

IR 1728, 2931.

Compound 23: Ethyl 1-2,4-difluorophenyl-6-fluoro-7-{[(2*R*)-1-hydroxybutan-2-yl]amino}-1,4-dihydro-4-oxo-1,8-naphthyridine-3-carboxylate

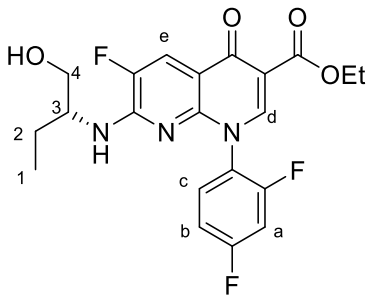

Prepared as described in General Procedure A, using **1** and (*R*)-2-aminobutan-1-ol, affording 0.104 g (62%) of **23** as a white solid.

***R*$_f$** 0.42 (92:8 DCM/MeOH).

^{1}H NMR (400 MHz, $CDCl_3$) δ 0.82 (t, *J* = 7.4, 3H, **1**), 1.40 (t, *J* = 7.2, 3H, $OCH_2C\underline{H}_3$), 1.50–1.54 (m, 2H, **2**), 1.98–2.04 (m, 1H, **3**), 3.57–3.60 (m, 2H, **4**), 4.39 (q, *J* = 7.2, 2H, $OC\underline{H}_2CH_3$), 5.51 (br s, 1H, NH), 7.04–7.11 (m, 2H, **b** and **c**), 7.38–7.43 (m, 1H, **a**), 8.07 (d, *J* = 10.4, 1H, **e**), 8.37 (s, 1H, **d**).

^{13}C NMR (100 MHz, $CDCl_3$) δ 14.4, 23.9, 27.5, 48.4, 49.5, 61.1, 104.9 (d, *J* = 24), 105.2 (d, *J* = 24), 112.2, 114.1, 119.3 (d, *J* = 21), 130.0 (d, *J* = 12), 144.9, 145.6, 146.6, 161.6, 164.0, 174.0.

IR 1712, 2856.

Compound 24: Ethyl 7-[4-(*tert*-butyloxycarbonyl)piperazin-1-yl]-1-cyclopropyl-6-fluoro-4-oxo-1,4-dihydro-1,8-naphthyridine-3-carboxylate

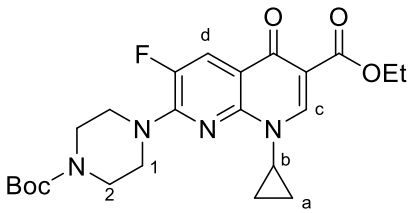

Prepared as described in General Procedure A, using **2** and 1-boc-piperazine, affording 0.094 g (63%) of **24** as a white solid.

R_f 0.77 (92:8 DCM/MeOH).

^{1}H NMR (400 MHz, $CDCl_3$) δ 1.00–1.09 (m, 2H, **a**), 1.16–1.31 (m, 2H, **a**), 1.42 (t, *J* = 7.2, 3H, $OCH_2C\underline{H}_3$), 1.51 (s, 9H, Boc $(CH_3)_3$), 3.52 (m, 1H, **b**), 3.58–3.67 (m, 4H, **1**), 3.78–3.85 (m, 4H, **2**), 4.40 (q, *J* = 7.2, 2H, $OC\underline{H}_2CH_3$), 8.15 (d, *J* = 13.2, 1H, **d**), 8.53 (s, 1H, **c**).

^{13}C NMR (100 MHz, $CDCl_3$) δ 7.4, 14.4, 28.4, 33.9, 46.9, 60.9, 80.3, 111.6, 116.6, 121.4, 121.7 (d, *J* = 20), 145.9, 147.5, 148.6, 149.6, 149.7, 154.7, 165.7, 173.5.

IR 1702, 2978.

Compound 25: Ethyl 1-cyclopropyl-6-fluoro-7-(4-methylpiperazin-1-yl)-4-oxo-1,4-dihydro-1,8-naphthyridine-3-carboxylate

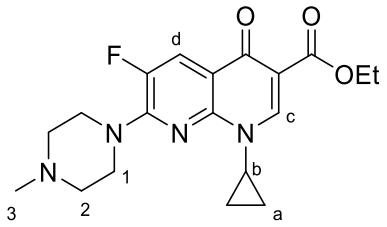

Prepared as described in General Procedure A, using **2** and 1-methylpiperazine, affording 0.079 g *(*60%) of **25** as a white solid.

***R*$_f$** 0.58 (92:8 DCM/MeOH).

^{1}H NMR (400 MHz, $CDCl_3$) δ 1.00–1.09 (m, 2H, **a**), 1.15–1.32 (m, 2H, **a**), 1.43 (t, *J* = 7.1, 3H, $OCH_2C\underline{H}_3$), 2.38 (s, 3H, **3**), 2.58 (t, *J* = 4.9, 4H, **1**), 3.53 (m, 1H, **b**) 3.84–3.91 (m, 4H, **2**), 4.41 (q, *J* = 7.1, 2H, $OC\underline{H}_2CH_3$), 8.13 (d, *J* = 13.6, 1H, **d**), 8.53 (s, 1H, **c**).

^{13}C NMR (100 MHz, $CDCl_3$) δ 7.4, 14.4, 33.9, 46.1, 54.9, 60.9, 111.4, 120.8, 121.0 (d, *J*= 20), 146.0, 147.2, 148.6, 149.7, 154.7, 165.9, 173.5.

IR 1671, 2983.

Compound 26: Ethyl 1-cyclopropyl-6-fluoro-4-oxo-7-(piperidin-1-yl)-1,4-dihydro-1,8-naphthyridine-3-carboxylate

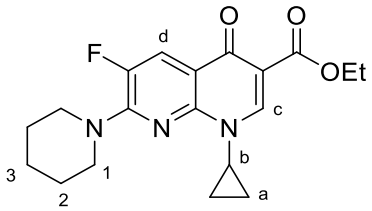

Prepared as described in General Procedure A, using **2** and piperidine. 0.061 g (77%) of **26** as a white solid.

***R*$_f$** 0.68 (92:8 DCM/MeOH).

^{1}H NMR (400 MHz, $CDCl_3$) δ 1.01–1.08 (m, 2H, **a**), 1.17–1.25 (m, 2H, **a**), 1.43 (t, *J* = 7.1, 3H, $OCH_2C\underline{H}_3$), 1.65–1.81 (m, 6H, **3** and **2**), 3.52 (m, 1H, **b**), 3.81 (t, *J* = 4.9, 4H, **1**), 4.40 (q, *J* = 7.1, 2H, $OC\underline{H}_2CH_3$), 8.09 (d, *J* = 13.7, 1H, **d**), 8.51 (s, 1H, **c**).

^{13}C NMR (100 MHz, $CDCl_3$) δ 7.4, 14.4, 24.8, 26.0, 33.8, 48.4, 61.0, 111.4, 120.8, 121.0 (d, *J* = 20), 146.0, 147.2, 148.6, 149.7, 154.7, 165.9, 173.5.

IR 1692, 2977.

Compound 27: Ethyl 1-cyclopropyl-6-fluoro-7-(methylamino)-4-oxo-1,4-dihydro-1,8-naphthyridine-3-carboxylate

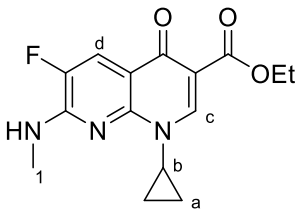

Prepared as described in General Procedure A, using **2** and methylamine, affording 0.050 g (52%) of **27** as a white solid.

***R*$_f$** 0.54 (92:8 DCM/MeOH).

^{1}H NMR (400 MHz, $CDCl_3$) δ 1.01–1.11 (m, 2H, **a**), 1.24 (dt, *J* = 7.3, 1.7, 2H, **a**), 1.43 (t, *J* = 7.1, 3H, $OCH_2C\underline{H}_3$), 3.19 (d, *J* = 4.8, 3H, **1**), 3.60 (m, 1H, **b**), 4.41 (q, *J* = 7.1, 2H, $OC\underline{H}_2CH_3$), 5.35 (br s, 1H, NH), 8.07 (d, *J* = 10.7, 1H, **d**), 8.51 (s, 1H, **c**).

^{13}C NMR (100 MHz, $CDCl_3$) 7.5, 14.4, 27.8, 34.0, 60.9, 111.6, 114.6, 117.1 (d, *J* = 20), 144.6, 146.8, 148.3 150.5, 154.7, 165.9, 173.7.

IR 1710, 2978.

Compound 28: Ethyl 1-cyclopropyl-6-fluoro-7-(4-hydroxypiperidin-1-yl)-4-oxo-1,4-dihydro-1,8-naphthyridine-3-carboxylate

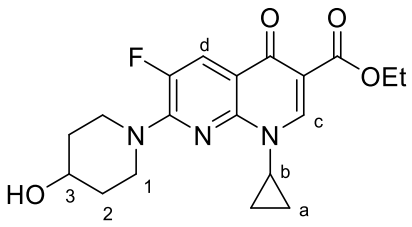

Prepared as described in General Procedure A, using **2** and 4-hydroxypiperidine, affording 0.090 g (74%) of **28** as a white solid.

***R*$_f$** 0.40 (92:8 DCM/MeOH).

^{1}H NMR (400 MHz, $CDCl_3$) δ 1.04 (tdd, *J*= 7.3, 4.1, 0.9, 2H, **a**), 1.23 (tdd, *J*= 7.3, 4.1, 0.9, 2H, **a**), 1.42 (t, *J*= 7.2, 3H, $OCH_2C\underline{H}_3$), 1.97–2.10 (m, 2H, **1**), 3.43–3.57 (m, 3H, **1** and **3**), 4.05 (m, 1H, **b**), 4.26 (ddd, *J* = 13.6, 6.6, 4.1 Hz, 4H, **2**), 4.40 (q, *J* = 7.2, 2H, $OC\underline{H}_2CH_3$), 8.12 (d, *J* = 13.4, 1H, **d**), 8.52 (s, 1H, **c**).

^{13}C NMR (100 MHz, $CDCl_3$) δ 8.3, 14.4, 34.1, 35.3, 45.7, 61.0, 66.4, 109.0, 113.8, 120.2 (d, *J* = 20), 148.2, 148.9, 149.9, 150.9, 165.5, 173.9.

IR 1718, 2924.

Compound 29: 1-(2,4-Difluorophenyl)-6-fluoro-4-oxo-7-(piperazin-1-yl)-1,4-dihydro-1,8-naphthyridine-3-carboxylic acid, hydrochloride

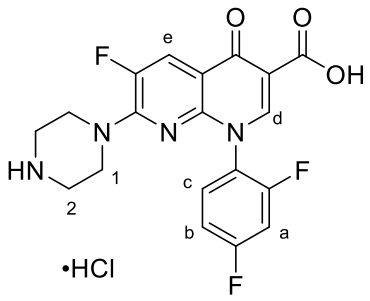

Prepared as described in General Procedure B using **14**, affording 0.019 g (56%) of **29** as a white solid.

^{1}H NMR (400 MHz, DMSO-d_6) δ 3.12 (br s, 4H, **1**), 3.72 (t, *J* = 5.1, 4H, **2**), 7.36 (td, *J* =8.7, 2.7,1H, **b** or **c**), 7.61 (ddd, *J*= 11.1, 9.1, 2.8, 1H, **b** or **c**), 7.83 (td, *J* = 8.7, 5.8, 1H, **a**), 8.27 (d, *J* = 13.0, 1H, **e**), 8.92 (s, 1H, **d**), 9.12 (br s, 2H), 14.84 (br s, 1H, OH).

^{13}C NMR (100 MHz, DMSO-d_6) δ 22.2, 51.9, 104.7 (d, *J* = 23), 105.7 (d, *J* = 25), 110.1, 112.4, 117.4 (d, *J* = 20), 130.1 (d, *J* = 12), 146.1, 146.8, 149.2, 150.3, 166.5, 177.5.

IR 1429, 1732, 2722.

HRMS (ES-ToF) *m/z* found 446.1427 $[M+CH_3CN+H]^+$, $C_{21}H_{19}F_3N_5O_3$ requires 446.1440.

Compound 30: 1-(2,4-Difluorophenyl)-6-fluoro-7-(4-methylpiperazin-1-yl)-4-oxo-1,4-dihydro-1,8-naphthyridine-3-carboxylic acid, hydrochloride

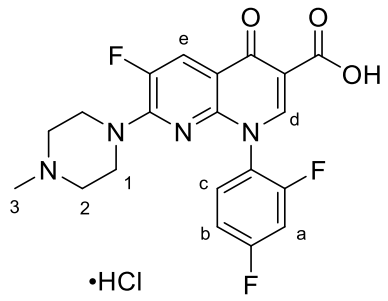

Prepared as described in General Procedure B using **15**, affording 0.022 g (72%) of **30** as a white solid.

^{1}H NMR (400 MHz, DMSO-d_6) δ 2.55 (s, 3H, **3**), 2.70 (t, *J* = 7.5, 4H, **2**), 3.69 (t, *J* = 7.5, 4H, **1**), 7.36 (td, *J* = 8.4, 2.7, 1H, **b** or **c**), 7.56–7.67 (m, 1H, **b** or **c**), 7.83 (td, *J* = 8.4, 5.8, 1H, **a**), 8.29 (d, *J* = 13.0, 1H, **e**), 8.93 (s, 1H, **d**), 11.0 (br s, 1H, OH).

^{13}C NMR (100 MHz, DMSO-d_6) δ 14.3, 22.2, 51.9, 104.8 (d, *J* = 24), 105.6 (d, *J* = 24), 109.7, 112.1, 119.6 (d, *J* = 21), 129.7 (d, *J* = 12), 146.1, 146.8, 149.2, 150.3, 166.5, 177.5.

^{19}F NMR (377 MHz, DMSO-d_6) δ -127.2 (d, *J* = 13.0), -115.5 (q, *J* = 9.9, 9.5), -106.8 (q, *J* = 8.1).

IR 1426, 1731, 2426.

HRMS (ES-ToF) *m/z* found 460.1317 $[M+CH_3CN+H]^+$ $C_{22}H_{21}F_3N_5O_3$ requires 460.1596.

Compound 31: 1-(2,4-Difluorophenyl)-6-fluoro-7-(piperidin-1-yl)-4-oxo-1,4-dihydro-1,8-naphthyridine-3-carboxylic acid, hydrochloride

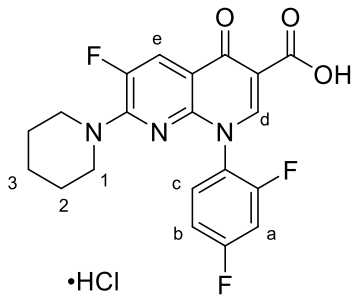

Prepared as described in General Procedure B using **16**, affording 0.045 g (36%) of **31** as a white solid.

^{1}H NMR (400 MHz, DMSO-d_6) δ 1.47–1.77 (m, 6H, **2** and **3**), 3.49–3.66 (m, 4H, **1**), 7.03–7.14 (m, 2H, **b** and **c**), 7.37–7.47 (m, 1H, **a**), 8.07 (d, *J* = 13.4, 1H, **e**), 8.66 (s, 1H, **d**), 14.93 (s, 1H).

^{13}C NMR (100 MHz, DMSO-d_6) δ 24.5, 25.9, 48.9, 104.8 (d, *J* = 24), 105.6 (d, *J* = 24), 109.9, 112.1, 119.6 (d, *J* = 21), 129.7 (d, *J* = 12), 146.1, 146.8, 148.7, 150.3, 166.5, 177.5.

IR 1431, 1724, 2859.

HRMS (ES-ToF) *m/z* found 404.1222 $[M+H]^+$, $C_{20}H_{17}F_3N_3O_3$ requires 404.1222.

Compound 32: 7-(Cyclohexylamino)-1-(2,4-difluorophenyl)-6-fluoro-4-oxo-1,4-dihydro-1,8-naphthyridine-3-carboxylic acid, hydrochloride

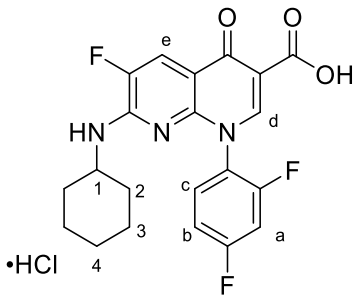

Prepared as described in General Procedure B using **17**, affording 0.027 g (36%) of **32** as a white solid.

^{1}H NMR (400 MHz, DMSO-d_6) δ 1.04–1.06 (m, 6H, **3** and **4**), 2.09 (m, 4H, **2**), 3.64 (t, *J*=6.8, 1H, **1**), 7.35 (t, *J* = 8.6, 1H, **b** or **c**), 7.61 (t, *J* = 9.5, 1H, **b** or **c**), 7.81 (q, *J* =7.9, 1H, **a**), 8.00 (d, *J* = 10.5, 1H, **e**), 8.23 (br s, 1H, NH), 8.83 (s, 1H, **d**), 15.31 (br s, 1H, OH).
^{13}C NMR (100 MHz, DMSO-d_6) δ 25.4, 25.5, 32.6, 50.5, 110.1 (d, *J* = 24), 112.5 (d, *J*=24), 115.7 117.1, 121.7, 123.2 (d, *J* = 21), 127.5 (d, *J* = 12), 142.3, 145.7, 150.0, 150.9, 158.0, 162.5, 165.2, 175.0.
IR 1429, 1721, 3319**.**
HRMS (ES-ToF) *m/z* found 418.1360 $[M+H]^+$, $C_{21}H_{19}F_3N_3O_3$ requires 418.1379.

Compound 33: 1-(2,4-Difluorophenyl)-6-fluoro-7-(methylamino)-4-oxo-1,4-dihydro-1,8-naphthyridine-3-carboxylic acid, hydrochloride

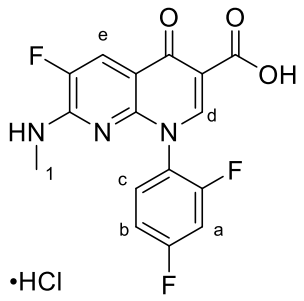

Prepared as described in General Procedure B using **18**, affording 0.017 g (38%) of **33** as a white solid.

^{1}H NMR (400 MHz, DMSO-d_6) δ 2.60 (s, 3H, **1**), 7.34 (t, *J* = 8.7, 1H, **b** or **c**), 7.60 (t, *J*=9.8, 1H, **b** or **c**), 7.82 (q, *J* = 7.8, 1H, **a**), 8.00 (d, *J* = 10.4, 1H, **e**), 8.36 (br s, 1H, NH), 8.79 (s, 1H, **d**), 15.28 (s, 1H, OH).

^{13}C NMR (100 MHz, DMSO-d_6) δ 27.1, 107.1 (d, *J* = 23), 112.2 (d, *J* = 24), 113.2, 116.7, 119.2, 123.5 (d, *J* = 21), 127.5 (d, *J* = 12), 144.6, 145.7, 150.7, 152.4, 158.0, 162.5, 165.2, 175.3.

IR 1475, 1725, 3321.

HRMS (ES-ToF) *m/z* found 350.0759 $[M+H]^+$, $C_{16}H_{11}F_3N_3O_3$ requires 350.0753.

Compound 34: 1-(2,4-Difluorophenyl)-6-fluoro-4-oxo-7-(propan-2-ylamino)-1,4-dihydro-1,8-naphthyridine-3-carboxylic acid, hydrochloride

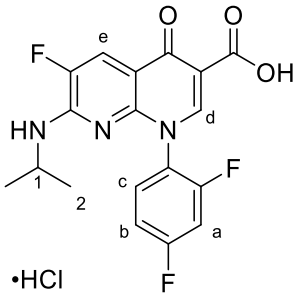

Prepared as described in General Procedure B using **19**, affording 0.030 g (48%) of **34** as a white solid.

^{1}H NMR (400 MHz, DMSO-d_6) δ 1.03 (d, *J* = 6.7, 6H, **2**), 3.63 (sept, *J* = 6.7, 1H, **1**), 7.34 (t, *J* = 8.5, 1H, **b** or **c**), 7.60 (t, *J* = 9.3, 1H, **b** or **c**), 7.82 (q, *J* = 7.7, 1H, **a**), 8.00 (d, *J*=10.6, 1H, **e**), 8.19 (br s, 1H, NH), 8.80 (s, 1H, **d**), 15.29 (s, 1H, OH).

^{13}C NMR (100 MHz, DMSO-d_6) δ 27.5, 31.2, 40.4, 105.3 (d, *J* = 23), 109.6 (d, *J* = 24), 112.7, 115.2, 123.5 (d, *J* = 21), 131.3 (d, *J* = 12), 145.1, 147.5, 147.9, 151.6, 152.4, 165.9, 177.5.

IR 1475, 1725, 3321.

HRMS (ES-ToF) *m/z* found 378.1022 $[M+H]^+$, $C_{18}H_{15}F_3N_3O_3$ requires 378.1066.

Compound 35: 1-(2,4-Difluorophenyl)-6-fluoro-4-oxo-7-(propylamino)-1,4-dihydro-1,8-naphthyridine-3-carboxylic acid, hydrochloride

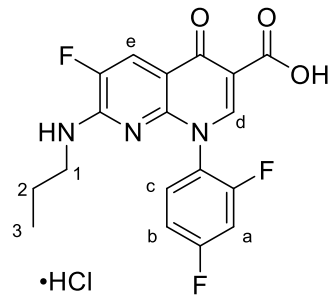

Prepared as described in General Procedure B using **20**, affording 0.019 g (34%) of **35** as a white solid.

^{1}H NMR (400 MHz, DMSO-d_6) δ 0.66 (t, *J* = 7.4, 3H, **3**), 1.22–1.38 (m, 2H, **2**), 3.00 (t, *J*=6.7, 2H, **1**), 7.35 (t, *J* = 8.5, 1H, **b** or **c**), 7.56–7.67 (m, 1H, **b** or **c**), 7.82 (td, *J* = 8.6, 5.7, 1H, **a**), 8.02 (d, *J* = 10.4, 1H, **e**), 8.49 (t, *J* = 5.8, 1H, NH), 8.81 (s, 1H, **d**), 15.30 (s, 1H).

^{13}C NMR (100 MHz, DMSO-d_6) δ 11.5, 21.7, 42.8, 110.2 (d, *J* = 23), 112.4 (d, *J* = 25), 115.7, 117.1, 121.0 (d, *J* = 21), 123.2, 127.5 (d, *J* = 13), 142.3, 144.9, 150.0, 151.6, 158.4, 162.2, 165.2, 175.5.

IR 1430, 1716, 3331.

HRMS (ES-ToF) *m/z* found 378.1072 $[M+H]^+$, $C_{18}H_{15}F_3N_3O_3$ requires 378.1066.

Compound 36: 7-(Cyclopropylamino)-1-(2,4-difluorophenyl)-6-fluoro-4-oxo-1,4-dihydro-1,8-naphthyridine-3-carboxylic acid, hydrochloride

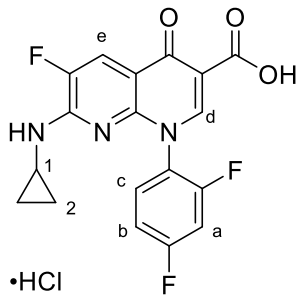

Prepared as described in General Procedure B using **21**, affording 0.011 g (23%) of **36** as a white solid.

^{1}H NMR (400 MHz, DMSO-d_6) δ 0.48 (d, *J* = 8.6, 2H, **2**) 0.57 (d, *J* = 6.5, 2H, **2**), 2.45 (m, 1H, **1**), 5.49 (br s, 1H, NH), 7.01–7.15 (m, 2H, **b** and **c**), 7.45 (td, *J* = 8.6, 5.8, 1H, **a**), 8.10 (d, *J* = 10.3, 1H, **e**), 8.44 (s, 1H, **d**).

^{13}C NMR (100 MHz, DMSO-d_6) δ 7.3, 26,1, 111.0 (d, *J* = 23), 112.4 (d, *J* = 25), 115.9, 117.1, 122.0 (d, *J* = 20), 123.2, 127.3 (d, *J* = 12), 143.3, 144.8, 149.0, 151.6, 158.4, 162.2, 165.5, 175.9.

IR 1447, 1712, 3323.

HRMS (ES-ToF) *m/z* found 376.0919 $[M+H]^+$, $C_{18}H_{13}F_3N_3O_3$ requires 376.0909.

Compound 37: 1-(2,4-Difluorophenyl)-6-fluoro-4-oxo-7-(pyrrolidin-1-yl)-1,4-dihydro-1,8-naphthyridine-3-carboxylic acid, hydrochloride

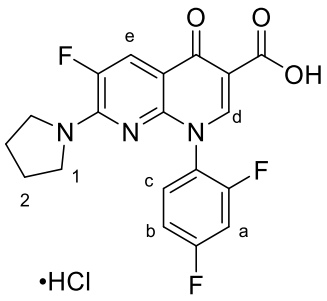

Prepared as described in General Procedure B using **22**, affording 0.045 g (53%) of **37** as a white solid.

^{1}H NMR (400 MHz, DMSO-d_6) δ 1.85 (br s, 4H, **2**), 3.55 (br s, 4H, **1**), 7.34 (td, *J* = 8.6, 2.9, 1H, **b** or **c**), 7.60 (td, *J* = 9.6, 2.8, 1H, **b** or **c**), 7.80 (td, *J* = 8.7, 5.9, 1H, **a**), 8.04 (d, *J* = 12.6, 1H, **e**), 8.80 (s, 1H, **d**), 15.22 (s, 1H).

^{13}C NMR (100 MHz, DMSO-d_6) δ 23.8, 48.9, 104.9 (d, *J* = 22), 109.2, 112.7 (d, *J* = 25), 113.9, 116.5, 117.7 (d, *J* = 20), 123.1, 131.2 (d, *J* = 12), 143.4, 146.9, 148.1, 151.6, 158.4, 162.2, 165.9, 177.4.

^{19}F NMR (377 MHz, DMSO-d_6) δ -133.3 (s), -115.2 (q, *J* = 9.3), -107.3 (q, *J* = 8.3).

IR 1423, 1712, 3077.

HRMS (ES-ToF) *m/z* found 390.1076 $[M+H]^+$, $C_{19}H_{15}F_3N_3O_3$ requires 390.1066.

Compound 38: 1-(2,4-Difluorophenyl)-6-fluoro-7-{[(2*R*)-1-hydroxybutan-2-yl]amino}-1,4-dihydro-4-oxo-1,8-naphthyridine-3-carboxylic acid, hydrochloride

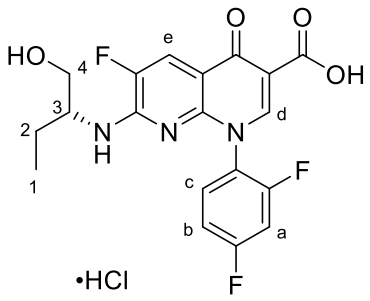

Prepared as described in General Procedure B using **23**, affording 0.030 g (59%) of **38** as a white solid.

^{1}H NMR (400 MHz, DMSO-d_6) δ 0.61 (t, *J* = 7.3, 3H, **1**), 0.69 (ta, *J* = 7.5, 2H, **2**), 1.23–1.47 (m, 3H, **3** and **4**), 7.34 (t, *J* = 8.6, 1H, **b** or **c**), 7.59 (t, *J* = 9.6, 1H, **b** or **c**), 7.73–7.87 (m, 1H, **a**), 7.97 (br s, 1H, NH), 8.00 (d, *J* = 10.4, 1H, **e**), 8.78 (s, 1H, **d**), 15.29 (s, 1H, OH).

^{13}C NMR (100 MHz, DMSO-d_6) δ 10.1, 23.9, 53.0, 62.5, 104.9, 112.3 (d, *J* = 22), 115.7, 117.0 (d, *J* = 25), 121.9 (d, *J* = 20), 123.1, 127.2 (d, *J* = 12), 142.0, 145.9, 150.4, 151.4, 158.1, 162.2, 165.9, 177.0.

IR 1448, 1694, 3337.

HRMS (ES-ToF) *m/z* found 408.1183 $[M+H]^+$, $C_{19}H_{17}F_3N_3O_4$ requires 408.1171.

Compound 39: 1-Cyclopropyl-6-fluoro-4-oxo-7-(piperazin-1-yl)-1,4-dihydro-1,8-naphthyridine-3-carboxylic acid, hydrochloride

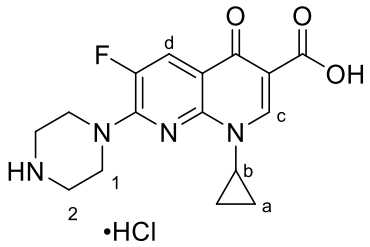

Prepared as described in General Procedure B using **24**, affording 0.040 g (52%) of **39** as a white solid.

^{1}H NMR (400 MHz, D_2O) δ 1.04 (dd, *J* = 6.3, 4.1, 2H, **a**), 1.24 (q, *J* = 7.4, 2H, **a**), 3.42 (t, *J* = 5.2, 4H, **1**), 3.66 (tt, *J* = 7.4, 4.1, 1H, **b**), 4.14 (t, *J* = 5.2, 4H, **2**), 7.80 (d, *J* = 13.1, 1H, **d**), 8.64 (s, 1H, **c**).

^{13}C NMR (100 MHz, D_2O) δ 6.6, 35.3, 43,0, 43.6, 110.6, 112.4, 119.0 (d, *J* = 20), 146.0, 147.9, 150.6, 152.7, 165.1, 175.5.

IR 1429, 1728, 2700.

HRMS (ES-ToF) *m/z* found 374.1635 $[M+CH_3CN+H]^{+\cdot}$ $C_{18}H_{21}FN_5O_3$ requires 374.1628.

Compound 40: 1-Cyclopropyl-6-fluoro-7-(4-methylpiperazin-1-yl)-4-oxo-1,4-dihydro-1,8-naphthyridine-3-carboxylic acid, hydrochloride

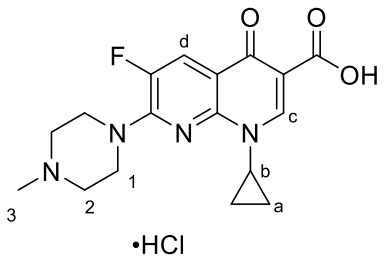

Prepared as described in General Procedure B using **25**, affording 0.065 g (80%) of **40** as a white solid.

^{1}H NMR (400 MHz, D_2O) δ 1.03 (dd, *J* = 6.3, 4.0, 2H, **a**), 1.23 (t, *J* = 6.8, 2H, **a**), 2.92 (s, 3H, **3**), 3.27 (tt, *J* = 12.3, 3.2, 1H, **b**), 3.51–3.67 (m, 4H, **1** or **2**), 4.74–4.79 (m, 4H, **1** or **2**), 7.81 (d, *J* = 12.9, 1H, **d**), 8.62 (s, 1H, **c**).

^{13}C NMR (100 MHz, D_2O) δ 6.6, 35.3, 43.0, 43.9, 52.9, 106.9, 112.4, 119.4 (d, *J* = 20), 146.7, 147.7, 151.6, 152.6, 163.9, 173.9.

IR 1450, 1725, 2457.

HRMS (ES-ToF) *m/z* found 347.1509 $[M+H]^+$, $C_{17}H_{20}FN_4O_3$ requires 347.1519.

Compound 41: 1-Cyclopropyl-6-fluoro-4-oxo-7-(piperidin-1-yl)-1,4-dihydro-1,8-naphthyridine-3-carboxylic acid, hydrochloride

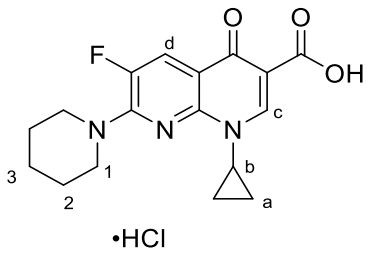

•HCl

Prepared as described in General Procedure B using **26**, affording 0.024 g (38%) of **41** as a white solid.

^{1}H NMR (400 MHz, DMSO-d_6) δ 1.04–1.26 (m, 4H, **a**), 1.68–1.76 (m, 6H, **2** and **3**), 3.71 (tt, *J* = 7.4, 4.1, 1H, **b**), 3.83–3.91 (m, 4H, **1**), 8.05 (d, *J* = 13.8, 1H, **d**), 8.61 (s, 1H, **c**), 15.29 (s, 1H).

^{13}C NMR (100 MHz, DMSO-d_6) δ 7.3, 24.6, 26.1, 35.6, 48.5, 106.5, 112.6, 118.7 (d, *J*=20), 146.7, 147.7, 151.5, 152.6, 163.9, 173.9.

IR 1440, 1721, 2939.

HRMS (ES-ToF) *m/z* found 332.1408 $[M+H]^+$, $C_{17}H_{18}FN_3O_3$ requires 332.1410.

Compound 42: 1-Cyclopropyl-6-fluoro-7-(methylamino)-4-oxo-1,4-dihydro-1,8-naphthyridine-3-carboxylic acid, hydrochloride

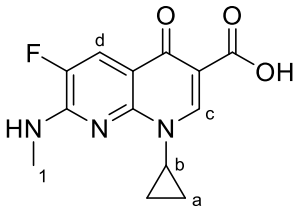

•HCl

Prepared as described in General Procedure B using **27**, affording 0.021 g (41%) of **42** as a white solid.

^{1}H NMR (400 MHz, DMSO-d_6) δ 1.06–1.16 (m, 2H, **a**), 1.16–1.25 (m, 2H, **a**), 2.80 (d, *J*=4.8, 3H, **1**), 3.05 (d, *J*=4.5, 3H, **1**), 3.68–3.80 (m, 1H, **b**), 7.94 (d, *J* = 10.6, 1H, **d**), 8.57 (s, 1H, **c**), 15.53 (s, 1H).

^{13}C NMR (100 MHz, DMSO-d_6) δ 7.5, 28.1, 35.6, 108.0, 112.6, 115.0 (d, *J* = 21), 145.1, 146.7, 148.6, 166.4, 176.9.

IR 1632, 1706, 3255.

HRMS (ES-ToF) *m/z* found 278.0943 $[M+H]^+$, $C_{13}H_{12}FN_3O_3$ requires 278.0941

Compound 43: 1-Cyclopropyl-6-fluoro-7-(4-hydroxypiperidin-1-yl)-4-oxo-1,4-dihydro-1,8-naphthyridine-3-carboxylic acid, hydrochloride

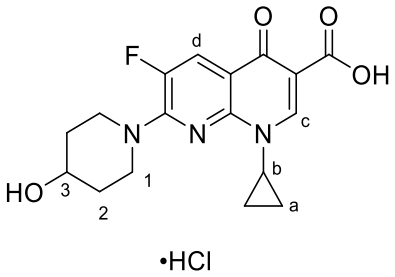

•HCl

Prepared as described in General Procedure B using **28**, affording 0.019 g (26%) of **43** as a white solid.

^{1}H NMR (400 MHz, DMSO-d_6) δ 1.06–1.13 (m, 2H, **a**), 1.18 (m, 2H, **a**), 1.52 (ddt, *J* = 13.4, 9.0, 4.4, 2H, **2**), 1.91 (ddt, *J* = 12.9, 6.5, 3.4, 2H, **2**), 3.56 (ddd, *J*=12.9, 6.5, 3.4, 2H, **1**), 3.70 (td, *J* =7.4, 3.8, 2H, **1**), 3.84 (tt, *J* = 8.1, 4.0, 1H, **3**), 3.90–3.94 (m, 1H, **b**), 4.85 (s, 1H), 8.06 (d, *J* = 13.7, 1H, **d**), 8.61 (s, 1H, **c**), 15.27 (s, 1H).

^{13}C NMR (100 MHz, DMSO-d_6) δ 7.3, 34.6, 35.4, 44.9, 65.7, 110.1, 112.5, 119.7 (d, *J*=19), 147.5, 147.9, 150.0, 152.4, 166.3, 176.9.

IR 1449, 1626, 1708, 3466.

HRMS (ES-ToF) *m/z* found 348.1367 $[M+H]^+$, $C_{17}H_{18}FN_3O_4$ requires 348.1360.

Compound 44: *tert*-Butyl 3-(2,6-dichloro-5-fluoropyridin-3-yl)-3-oxopropanoate

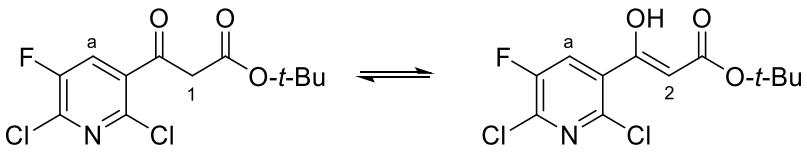

2,6-Dichloro-5-fluoronicotinic acid (13.0 g, 62.2 mmol) was dissolved in $SOCl_2$ (50 mL) and the mixture was heated at 80 °C for 2 h. The $SOCl_2$ was then removed by evaporation under reduced pressure yielding 2,6-dichloro-5-fluoronicotinyl chloride (**3**) as a yellowish oil. Mono-*tert*-butyl malonate (19 mL, 160.93 mmol) and biquinoline (5.0mg) were dissolved in 500 mL of dry THF and cooled to -30 °C. A solution of 2.5M *n*-butyllithium in hexane (100 mL) was added until a light pink colour remained at -5°C. The suspension was then cooled to -50 °C. **3** was then dissolved in 30 mL of dry THF and added to the suspension drop wise. After the addition, the dry ice bath was removed and the reaction allowed to stir at r.t. for 1 h. The reaction was acidified with 1 N HCl to approximately pH 1 and was extracted with ether. The ether fraction was washed with saturated aqueous Na_2CO_3 solution and then H_2O. The organic layer was dried ($MgSO_4$) and evaporated to dryness yielding a residue, which was then recrystallized in pentane to give 14.2 g (74%) of **44** (and its enol form) as a white solid.

R_f 0.67 (1:1 DCM/pentane).

^{1}H NMR (400 MHz, $CDCl_3$) δ 1.44 (s, 9H, CC$\underline{H}_3$), 1.55 (s, 9H, CC$\underline{H}_3$), 4.03 (s, 2H, **1**), 5.74 (s, 1H, **2**), 7.84 (m, 2H, a), 12.78 (s, 1H, OH).

^{13}C NMR (100 MHz, $CDCl_3$) δ 27.9, 28.2, 49.7, 82.6, 83.0, 96.4, 126.9 (d, *J* = 22), 127.5 (d, *J* = 22), 130.6, 134.0, 138.4 (d, *J* = 21), 140.5 (d, *J* = 22), 140.9, 141.5, 152.7 (d, *J*=21), 155.3 (d, *J* = 23), 164.6, 165.6, 172.2, 191.5.

Compound 45: *tert*-Butyl 2-[(2,6-dichloro-5-fluoropyridin-3-yl)carbonyl]-3-[(2,4-difluorophenyl)amino]prop-2-enoate

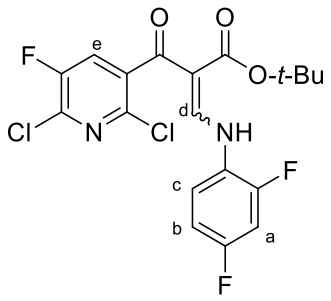

44 (3.0 g, 9.74 mmol) was dissolved in triethyl orthoformate (4.0 mL, 24.05 mmol) and Ac_2O (25 mL, 264.5 mmol), and the solution was heated at 130 °C for 1 h. The solution was evaporated under reduced pressure to a mobile oil, which was dissolved in DCM (25mL), and 2,4-difluoroaniline (2.3 mL, 22.6 mmol) was added. After stirring at r.t. for 0.5 h, the solution was evaporated to dryness and the product was purified by column chromatography (9:1 DCM/pentane), affording 4.61 g of **45** as a yellow oil in quantitative yield.

***R*$_f$** 0.82 (DCM).

^{1}H NMR (400 MHz, $CDCl_3$) δ 1.27 (s, 9H, CC$\underline{H}_3$), 1.31 (s, 9H, CC$\underline{H}_3$), 6.67–6.84 (m, 3H), 6.99–7.05 (m, 3H, **a**, **b** and **c**), 7.38–7.51 (m, 3H, **a**, **b** and **c**), 8.59 (dd, *J* = 13.5, 4.2, 2H, **e**), 11.47 (d, *J* = 13.9, 1H, **d**), 12.61 (d, *J* = 13.5, 1H, **d**).

^{13}C NMR (100 MHz, $CDCl_3$) δ 13.5, 14.0, 27.8, 27.9, 60.7, 81.5, 82.3, 103.8 (d, *J* = 26), 104.85–105.74 (m), 110.9 (d, *J* = 22), 112.0–112.7 (m), 116.8 (d, *J* = 9), 118.0–118.4 (m), 118.9 (d, *J* = 25), 124. 8 (d, *J* = 22), 125.3 (d, *J* = 22), 152.4, 152.7, 152.8, 153.9, 164.9, 189.5, 189.7.

Compound 46: *tert*-Butyl 3-(cyclopropylamino)-2-[(2,6-dichloro-5-fluoropyridin-3-yl)carbonyl]prop-2-enoate

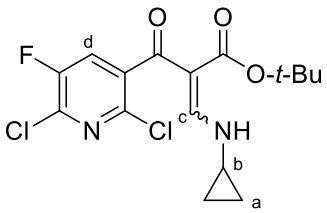

44 (2.6 g, 8.44 mmol) was dissolved in triethyl orthoformate (3.5 mL, 21.04 mmol) and Ac_2O (20 mL, 211.58 mmol), and the solution was heated at 130 °C for 1 h. The solution was evaporated under reduced pressure to a mobile oil, which was dissolved in DCM (20 mL), and cyclopropylamine (1.4 mL, 20.20 mmol) was added. After stirring at r.t. for 0.5h, the solution was evaporated to dryness and the product was purified by column chromatography (9:1 DCM/pentane), affording 1.68 g (53%) of **46** as a yellow oil.

***R*$_f$** 0.50 (DCM).

^{1}H NMR (400 MHz, $CDCl_3$) δ 0.82–1.01 (s, 9H, CC$\underline{H}_3$), 1.19 (s, 4H, **a**), 1.26 (s, 9H, CC$\underline{H}_3$), 3.01–3.07 (m, 1H, **b**), 5.32 (s, 1H,), 7.35 (dd, *J* = 7.1, 3.1, 1H, **d**), 7.41 (dd, *J*= 7.2, 2.9, 1H, **d**), 8.27 (d, *J* = 14.1, 1H), 8.31–8.39 (m, 1H), 9.81 (d, *J* = 15.3, 1H), 10.99 (d, *J*=15.2, 1H).

^{13}C NMR (100 MHz, $CDCl_3$) δ 6.6, 6.7, 14.0, 27.9, 28.0, 30.8, 30.9, 60.2, 80.7, 100.5, 101.2, 124.5 (d, *J* = 22), 136.2, 139.5, 161.2, 161.8 162.0, 165.4, 188.1.

Compound 47: *tert*-Butyl 7-chloro-1-(2,4-difluorophenyl)-6-fluoro-4-oxo-1,4-dihydro-1,8-naphthyridine-3-carboxylate

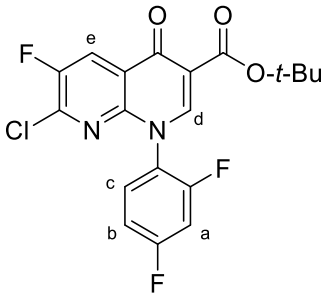

K_2CO_3 (2.0 g, 14.47 mmol) was added to a solution of **45** (5.46 g, 12.20 mmol) in acetonitrile (50 ml), and the solution was heated to reflux overnight. The solvent was then evaporated to dryness and the residue was dissolved in DCM, washed with H_2O twice, dried over $MgSO_4$, and purified by column chromatography (99:1 DCM/MeOH), affording 4.3 g (86%) of **47**, as a white solid.

***R**f* 0.89 (94:6 DCM/MeOH).

M.p. 209.7–211.5 ºC.

^{1}H NMR (400 MHz, $CDCl_3$) δ 1.61 (s, 9H, CC$\underline{H}_3$), 7.09–7.14 (m, 2H, **b** and **c**), 7.41–7.45 (m, 1H, **a**), 8.46 (s, 1H, **d**), 8.48 (d, *J* = 7.5, 1H, **e**).

^{13}C NMR (100 MHz, $CDCl_3$) δ 28.2, 82.2, 105.5 (d, *J* = 25), 112.5 (d, *J* = 24), 114.8, 123.2 (d, *J* = 20), 129.8 (d, *J* = 10), 142.8, 144.8, 148.8, 151.4, 154.0, 158.6, 162.1, 163.1, 170.1 173.5.

IR 1404, 1640, 1692, 2984.

HRMS (ES-ToF) *m/z* found 411.075 $[M+H]^+$, $C_{19}H_{15}ClF_3N_2O_3$ requires 411.0723.

Compound 48: *tert*-Butyl 7-chloro-1-cyclopropyl-6-fluoro-4-oxo-1,4-dihydro-1,8-naphthyridine-3-carboxylate

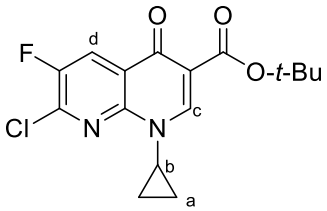

K_2CO_3 (0.74 g, 5.35 mmol) was added to a solution of **46** (1.68 g, 4.48 mmol) in acetonitrile (50 ml), and the solution was heated to reflux overnight. The solvent was then evaporated to dryness and the residue was dissolved in DCM, washed with H_2O twice, dried over $MgSO_4$, and purified by column chromatography (99:1 DCM/MeOH), affording 1.12 g (74%) of **48**, as a white solid.

***R**f* 0.77 (9:1 DCM/MeOH).

^{1}H NMR (400 MHz, $CDCl_3$) δ 1.02–1.08 (m, 2H, **a**), 1.33 (dd, *J* = 7.1, 1.6, 2H, **a**), 1.62 (s, 9H, CCH_3), 3.65 (tt, *J* = 7.1, 3.7, 1H, **b**), 8.44 (d, *J* = 7.2, 1H, **d**), 8.60 (s, 1H, **c**).

^{13}C NMR (100 MHz, $CDCl_3$) δ 7.7, 28.3, 34.3, 81.8, 113.4, 123.1 (d, *J* = 14), 123.9, 142.1, 145.9, 148.6, 151.3, 153.9, 163.7, 173.4.

IR 1405, 1642, 1697, 2979.

HRMS (ES-ToF) *m/z* found 339.0912 $[M+H]^+$, $C_{16}H_{17}ClFN_2O_3$ requires 339.0912.

Compound 49: *tert*-Butyl 1-(2,4-difluorophenyl)-6-fluoro-7-(4-hydroxypiperidin-1-yl)-4-oxo-1,4-dihydro-1,8-naphthyridine-3-carboxylate

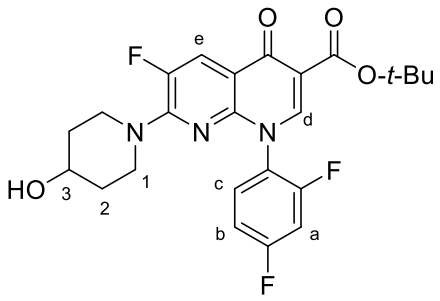

Prepared as described in General Procedure A, using **47** and 4-hydroxypiperidine, affording 0.096 g (69%) of **49** as a white solid.

***R*$_f$** 0.42 (92:8 DCM/MeOH).

^{1}H NMR (400 MHz, $CDCl_3$) δ 1.54 (d, *J* = 9.3, 2H, **2**), 1.61 (s, 9H, $CC\underline{H}_3$), 1.81–1.94 (m, 2H, **2**), 3.23–3.26 (m, 1H, **1**), 3.90–3.95 (m, 3H, **1** and **3**), 7.01–7.13 (m, 2H, **b** and **c**), 7.41 (td, *J* = 8.7, 5.8, 1H, **a**), 8.14 (d, *J* = 13.5, 1H, **e**), 8.33 (s, 1H, **d**).

^{13}C NMR (100 MHz, $CDCl_3$) δ 28.3, 33.9, 44.3, 67.2, 81.5, 104.9 (m), 111.9 (d, *J* = 26), 114.2, 115.5, 121.2 (d, *J* = 22), 124.9, 130.1 (d, *J* = 10), 145.0, 146.0, 146.8, 149.5, 149.6, 164.0, 173.9.

IR 1720, 2994.

Compound 50: *tert*-Butyl 1-(2,4-difluorophenyl)-6-fluoro-7-[(2*S*)-2-(hydroxymethyl)pyrrolidin-1-yl]4-oxo-1,4-dihydro-1,8-naphthyridine-3-carboxylate

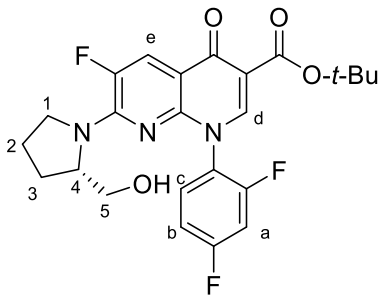

Prepared as described in General Procedure A, using **47** and (*S*)-(+)-2-pyrrolidinemethanol, affording 0.107g (77%) of **50** as a white solid.

***R*$_f$** 0.53 (92:8 DCM/MeOH).

^{1}H NMR (400 MHz, $CDCl_3$) δ 1.60 (s, 9H, CC$\underline{H}_3$), 1.81– 2.09 (m, 4H, **2** and **3**), 3.40–3.58 (m, 2H, **1**), 3.66–3.80 (m, 2H, **5**), 4.08 (br s, 1H, **4**), 7.03–7.15 (m, 2H, **b** and **c**), 7.40 (q, *J* = 7.5, 1H, **a**), 8.07 (d, *J* = 12, 1H, **e**), 8.27 (s, 1H, **d**).

^{13}C NMR (100 MHz, $CDCl_3$) δ 23.8, 27.5, 28.3, 49.5, 61.0, 64.5, 81.5, 105.1 (m), 112.1 (d, *J* = 19), 114.1, 115.5, 120.2 (m), 124.9, 130.2 (m), 145.2, 146.0, 146.6, 149.0, 149.6, 164.0, 174.3.

IR 1728, 2942.

Compound 51: *tert*-Butyl 1-(2,4-difluorophenyl)-6-fluoro-7-[(3*S*)-3-hydroxypyrrolidin-1-yl)-4-oxo-1,4-dihydro-1,8-naphthyridine-3-carboxylate

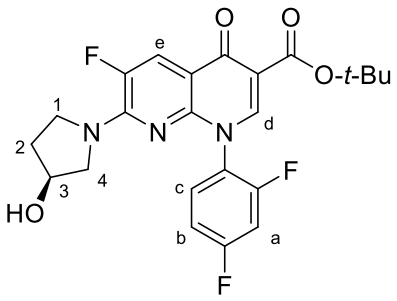

Prepared as described in General Procedure A, using **47** and (*S*)-3-pyrrolidinol, affording 0.103 g (76%) of **51** as a white solid.

***R*$_f$** 0.52 (92:8 DCM/MeOH).

^{1}H NMR (400 MHz, $CDCl_3$) δ 1.60 (s, 9H, $CC\underline{H}_3$), 1.94– 2.05 (m, 2H, **2**), 2.83 (t, *J* = 7.2, 2H, **1**), 3.58 (br s, 1H, **3**), 4.53 (d, *J* = 4.8, 2H, **4**), 7.06 (tq, *J* =7.9, 3.1, 2H, **b** and **c**), 7.37 (dt, *J* = 13.3, 6.7, 1H, **a**), 7.95 (d, *J* = 12.7, 1H, **e**), 8.28 (s, 1H, **d**).

^{13}C NMR (100 MHz, $CDCl_3$) δ 28.3, 33.4, 46.2, 56.7, 70.0, 81.6, 104.9 (m), 111.9 (d, *J*=22), 113.6, 113.9, 119.2 (d, *J* = 20), 124.9, 130.1 (d, *J* = 10), 144.8, 145.6, 146.5, 147.3, 148.5, 164.1, 174.1.

IR 1683, 2974.

Compound 52: *tert*-Butyl 1-(2,4-difluorophenyl)-6-fluoro-7-[(*trans*-4-hydroxycyclohexyl)amino]-4-oxo-1,4-dihydro-1,8-naphthyridine-3-carboxylate

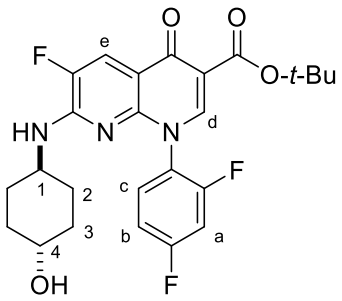

Prepared as described in General Procedure A, using **47** and *trans*-4-aminocyclohexanol, affording 0.125 g (70%) of **52** as a white solid.

R_f 0.38 (92:8 DCM/MeOH).

^{1}H NMR (400 MHz, $CDCl_3$) δ 1.16**–**1.25 (m, 4H, **2**), 1.61 (s, 9H, $CC\underline{H}_3$), 1.89–2.00 (m, 4H, **3**), 3.36 (ddq, *J* = 10.6, 7.3, 3.4, 1H, **1**), 3.63 (dt, *J* = 10.6, 5.8, 1H, **4**), 7.01**–**7.14 (m, 2H, **b** and **c**), 7.41 (td, *J* = 8.4, 5.6, 1H, **a**), 8.08 (d, *J* = 10.6 Hz, 1H, **e**), 8.31 (s, 1H, **d**).

^{13}C NMR (100 MHz, $CDCl_3$) δ 28.3, 30.0, 33.7, 49.8, 69.6, 81.6, 104.8 (d, *J* = 24), 111.9 (m), 114.1, 117.4 (d, *J* = 15), 124.8, 130.2 (d, *J* = 10), 144.2, 145.6, 146.5, 147.3, 149.1, 164.1, 174.0.

IR 1722, 2930.

Compound 53: *tert*-Butyl 7-(cyclohexylamino)-1-cyclopropyl-6-fluoro-4-oxo-1,4-dihydro-1,8-naphthyridine-3-carboxylate

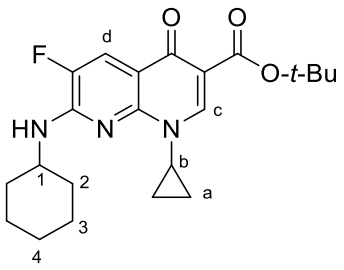

Prepared as described in General Procedure A, using **48** and cyclohexylamine, affording 0.068 g (40%) of **53** as a white solid.

***R*$_f$** 0.52 (92:8 DCM/MeOH).

^{1}H NMR (400 MHz, $CDCl_3$) δ 0.99–1.08 (m, 2H, **a**), 1.12–1.24 (m, 2H, **a**), 1.24–1.52 (m, 2H, **4**), 1.62 (s, 9H, $CC\underline{H}_3$), 1.85 (dq, *J* = 13.0, 4.0, 2H, **3**), 2.17 (dt, *J* = 11.1, 3.8, 2H, **3**), 3.51 (tt, *J* = 7.5, 4.1, 1H, **b**), 3.76–3.84 (m, 4H, **2**), 4.04 (t, *J* = 6.9, 1H, **1**), 8.05 (d, *J*=10.9, 1H, **d**), 8.44 (s, 1H, **c**).

^{13}C NMR (100 MHz, $CDCl_3$) δ 7.4, 25.0, 25.7, 28.4, 32.7, 33.9, 50.3, 81.1, 112.7, 114.5, 117.2 (d, *J* = 17), 146.5, 147.1, 148.9, 149.1, 164.9, 173.8.

IR 1685, 2962.

Compound 54: *tert*-Butyl 1-cyclopropyl-6-fluoro-4-oxo-7-(propan-2-ylamino)-1,4-dihydro-1,8-naphthyridine-3-carboxylate

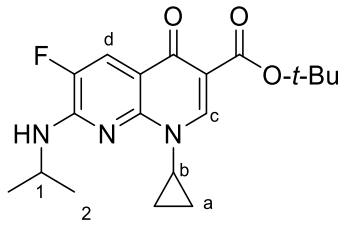

Prepared as described in General Procedure A, using **48** and 2-propylamine, affording 0.090 g (70%) of **54** as a white solid.

***R*$_f$** 0.61 (92:8 DCM/MeOH).

^{1}H NMR (400 MHz, $CDCl_3$) δ 0.99–1.08 (m, 2H, **a**), 1.14–1.26 (m, 2H, **a**), 1.37 (d, *J* = 6.5, 6H, **2**), 1.62 (s, 9H, $CC\underline{H}_3$), 3.49–3.59 (m, 1H, **b**), 4.36 (h, *J* = 6.5, 1H, **1**), 5.14 (dd, *J*=7.0, 2.9, 1H, NH), 8.06 (d, *J* = 10.7, 1H, **d**), 8.44 (s, 1H, **e**).

^{13}C NMR (100 MHz, $CDCl_3$) δ 7.4, 22.5, 28.4, 33.9, 43.2, 81.1, 112.8, 117.8 (d, *J* = 17), 146.4, 146.7, 148.4, 149.0, 164.9, 173.8.

IR 1718, 2910.

Compound 55: *tert*-Butyl 1-cyclopropyl-6-fluoro-4-oxo-7-(propylamino)-1,4-dihydro-1,8-naphthyridine-3-carboxylate

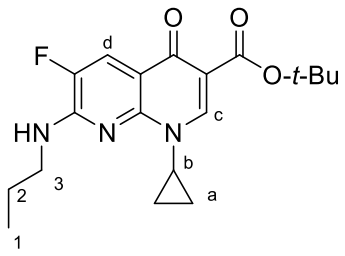

Prepared as described in General Procedure A, using **48** and *n*-propylamine, affording 0.077 g (60%) of **55** as a white solid.

***R*$_f$** 051 (92:8 DCM/MeOH).

^{1}H NMR (400 MHz, $CDCl_3$) δ 0.99–1.08 (m, 5H, **a** and **1**), 1.14–1.26 (m, 2H, **a**), 1.62 (s, 9H, CCH_3), 1.77 (dt, *J* = 14.6, 7.3, 2H, **2**), 3.49–3.63 (m, 3H, **b** and **3**), 5.37 (t, *J* = 5.9, 1H, NH), 8.06 (d, *J* = 10.8, 1H, **d**), 8.44 (s, 1H, **c**).

^{13}C NMR (100 MHz, $CDCl_3$) δ 7.4, 11.5, 22.6, 28.4, 33.9, 43.0, 81.1, 112.8, 117.3 (d, *J*=17), 146.5, 147.8, 148.4, 149.9, 164.9, 173.8.

Compound 56: *tert*-Butyl 1-cyclopropyl-7-(cyclopropylamino)-6-fluoro-4-oxo-1,4-dihydro-1,8-naphthyridine-3-carboxylate

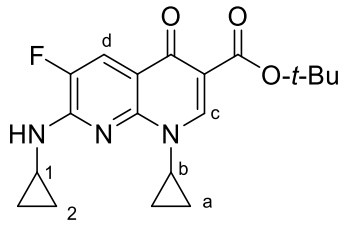

Prepared as described in General Procedure A, using **48** and cyclopropylamine, affording 0.085 g (67%) of **56** as a white solid.

***R*$_f$** 0.49 (92:8 DCM/MeOH).

^{1}H NMR (400 MHz, $CDCl_3$) δ 0.64–0.73 (m, 2H, **a**), 0.90 (t, *J* = 6.9, 2H, **2**), 1.01–1.09 (m, 2H, **a**), 1.18–1.26 (m, 2H, **2**), 1.62 (s, 9H, CC$\underline{H}_3$), 2.87–2.98 (m, 1H, **1**), 3.59 (td, *J* = 7.4, 3.8, 1H, **b**), 5.50 (s, 1H, NH), 8.07 (d, *J* = 10.6, 1H, **d**), 8.46 (s, 1H, **c**).

^{13}C NMR (100 MHz, $CDCl_3$) δ 7.2, 7.5, 23.9, 28.4, 34.0, 81.1, 112.8, 115.3, 117.4 (d, *J*=17), 144.2, 146.6, 148.4, 149.9, 164.8, 173.9.

Compound 57: *tert*-Butyl 1-cyclopropyl-6-fluoro-4-oxo-7-(pyrrolidin-1-yl)-1,4-dihydro-1,8-naphthyridine-3-carboxylate

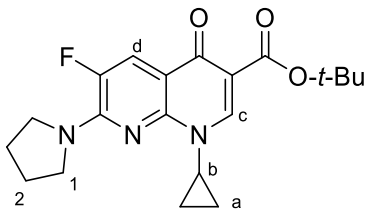

Prepared as described in General Procedure A, using **48** and pyrrolidine, affording 0.069 g (52%) of **57** as a white solid.

***R*$_f$** 0.67 (92:8 DCM/MeOH).

^{1}H NMR (400 MHz, $CDCl_3$) δ 0.96–1.06 (m, 2H, **a**), 1.12–1.24 (m, 2H, **a**), 1.62 (s, 9H, $CC\underline{H}_3$), 2.03 (t, *J* = 6.4, 4H, **2**), 3.51 (t, *J* = 6.0, 1H, **b**), 3.81 (t, *J* = 6.4, 4H, **1**), 8.05 (d, *J*=13.0, 1H, **d**), 8.41 (s, 1H, **c**).

^{13}C NMR (100 MHz, $CDCl_3$) δ 7.3, 28.4, 33.7, 48.6, 81.0, 112.5, 114.2, 119.4 (d, *J* = 21), 146.5, 147.4, 148.4, 149.9, 165.0, 173.8.

Compound 58: *tert*-Butyl 1-cyclopropyl-6-fluoro-7-[(2*S*)-2-(hydroxymethyl)pyrrolidin-1-yl]-4-oxo-1,4-dihydro-1,8-naphthyridine-3-carboxylate

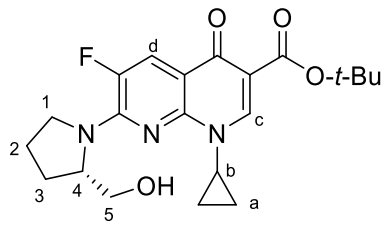

Prepared as described in General Procedure A, using **48** and (*S*)-(+)-2-pyrrolidinemethanol, affording 0.078 g (55%) of **58** as a white solid.

***R*$_f$** 0.57 (92:8 DCM/MeOH).

^{1}H NMR (400 MHz, $CDCl_3$) δ 0.96–1.11 (m, 2H, **a**), 1.21–1.28 (m, 2H, **a**), 1.62 (s, 9H, $CC\underline{H}_3$), 1.97– 2.21 (m, 4H, **2** and **3**), 3.37–3.51 (m, 2H, **1**), 3.79–3.81 (m, 2H, **5**), 3.96–4.02 (m, 1H, **b**), 4.62–4.63 (m, 1H, **4**), 8.00 (d, *J* = 13.5, 1H, **d**), 8.40 (s, 1H, **c**).

^{13}C NMR (100 MHz, $CDCl_3$) δ 7.6, 24.2, 27.8, 28.4, 33.9, 49.9, 61.6, 65.3, 81.2, 112.7, 114.7, 120.2 (d, *J* = 21), 146.3, 146.7, 147.2, 149.9, 164.7, 173.4.

Compound 59: *tert*-Butyl 1-cyclopropyl-6-fluoro-7-[(3*S*)-3-hydroxypyrrolidin-1-yl]-4-oxo-1,4-dihydro-1,8-naphthyridine-3-carboxylate

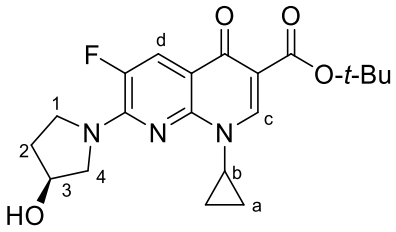

Prepared as described in General Procedure A, using **48** and (*S*)-3-pyrrolidinol, affording 0.070 g (51%) of **59** as a white solid.

***R*$_f$** 0.43 (92:8 DCM/MeOH).

^{1}H NMR (400 MHz, $CDCl_3$) δ 0.94–1.03 (m, 2H, **a**), 1.13–1.23 (m, 2H, **a**), 1.62 (s, 9H, CCH_3), 2.12 (pt, *J* = 8.9, 4.0, 2H, **2**), 3.04 (d, *J* = 4.0 0, 1H, **3**), 3.47 (tt, *J* = 7.5, 4.1, 1H, **b**), 3.82–3.98 (m, 4H, **2** and **4**), 4.63 (s, 1H), 7.91 (d, *J* = 12.9, 1H, **d**), 8.38 (s, 1H, **c**).

^{13}C NMR (100 MHz, $CDCl_3$) δ 7.3, 28.4, 33.8, 46.4, 57.0, 81.2, 112.5, 114.1, 119.4 (d, *J*=20), 146.4, 146.7, 147.2, 148.3, 164.8, 173.8.

Compound 60: *tert*-Butyl 1-cyclopropyl-6-fluoro-7-{[(2*R*)-1-hydroxybutan-2-yl]amino}-1,4-dihydro-4-oxo-1,8-naphthyridine-3-carboxylate

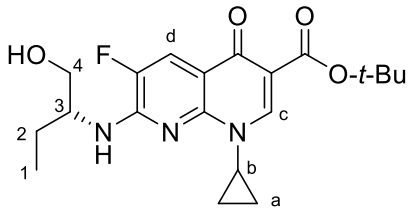

Prepared as described in General Procedure A, using **48** and (*R*)-2-amino-1-butanol, affording 0.12 g (72%) of **60** as a white solid.

***R*$_f$** 0.63 (92:8 DCM/MeOH).

^{1}H NMR (400 MHz, $CDCl_3$) δ 0.98–1.11 (m, 5H, **1** and **a**), 1.17–1.28 (m, 2H, **a**), 1.62 (s, 9H, $CC\underline{H}_3$), 1.73–1.84 (m, 2H, **2**), 3.20 (s, 1H), 3.50 (tt, *J* = 7.5, 4.1, 1H, **b**), 3.81 (d, *J*=6.5, **4**), 3.92 (d, *J* = 6.0, 1H, **4**), 4.21 (dq, *J* = 6.4, 6.0, 1H, **3**), 8.02 (d, *J* = 10.7, 1H, **d**), 8.41 (s, 1H, **c**).

^{13}C NMR (100 MHz, $CDCl_3$) δ 7.4, 10.7, 24.3 28.3, 34.0, 55.1, 64.8, 81.2, 112.8, 114.7, 117.5 (d, *J* = 17), 144.3, 146.4, 146.8, 150.0, 164.6, 173.7.

Compound 61: *tert*-Butyl 1-cyclopropyl-6-fluoro-7-[(*trans*-4-hydroxycyclohexyl)amino]-4-oxo-1,4-dihydro-1,8-naphthyridine-3-carboxylate

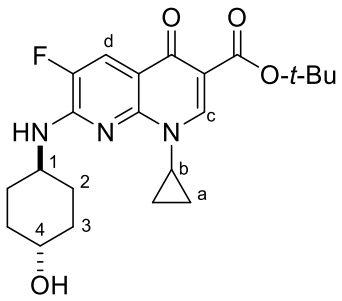

Prepared as described in General Procedure A, using **48** and *trans*-4-aminocyclohexanol, affording 0.066 g (32%) of **61** as a white solid.

***R*$_f$** 0.40 (92:8 DCM/MeOH).

^{1}H NMR (400 MHz, $CDCl_3$) δ 0.99–1.09 (m, 2H, **a**), 1.20 (d, *J* = 6.8 Hz, 2H, **a**), 1.37**–**1.54 (m, 4H, **2**), 1.79 (s, 9H, $CC\underline{H}_3$), 2.06–2.16 (m, 2H, **3**), 2.27 (dt, *J* = 11.6, 4.3, 2H, **3**), 3.51 (tt, *J* = 6.8, 4.0, 1H, **b**), 3.76 (dt, *J* = 10.2, 4.3, 1H, **1**), 4.03 (dtd, *J* = 10.9, 6.9, 3.5, 1H, **4**), 8.05 (d, *J* = 10.7, 1H, **d**), 8.44 (s, 1H, **c**).

^{13}C NMR (100 MHz, $CDCl_3$) δ 7.5, 28.4, 30.4, 34.0, 49.8, 69.7, 81.2, 112.8, 114.7, 117.4 (d, *J* = 17), 144.2, 146.6, 147.0, 149.0, 164.7, 173.8.

Compound 62: 1-(2,4-Difluorophenyl)-6-fluoro-7-(4-hydroxypiperidin-1-yl)-4-oxo-1,4-dihydro-1,8-naphthyridine-3-carboxylic acid, hydrochloride

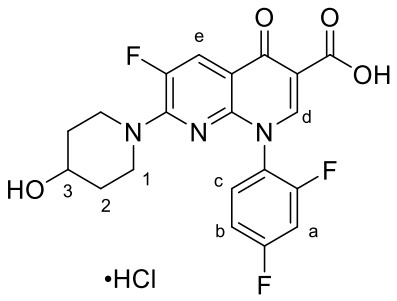

Prepared as described in General Procedure C using **49**, affording 0.041 g (48%) of **62** as a white solid.

^{1}H NMR (400 MHz, DMSO-d_6) δ 1.31 (dt, *J* = 12.0, 8.0, 2H, **2**), 1.66–1.75 (m, 2H, **2**), 3.28 (dq, *J* = 14.4, 5.1, 4.6, 3H, **3** and **1**), 3.67–3.88 (m, 2H, **1**), 7.35 (dd, *J* = 10.0, 6.9, 1H, **b** or **c**), 7.62 (td, *J* = 9.7, 2.9, 1H,**b** or **c**), 7.82 (td, *J* = 8.7, 5.7, 1H,**a**), 8.12 (d, *J*=13.4, 1H, **e**), 8.86 (s, 1H, **f**), 15.03 (s, 1H).

^{13}C NMR (100 MHz, DMSO-d_6) δ 33.3, 44.7, 65.4, 104.4–106.4 (m), 109.3, 112.7 (d, *J*=26), 119.8 (d, *J* = 22), 124.5, 131.3 (d, *J* = 10), 146.0, 146.5, 148.5, 148.7, 150.1, 165.7, 177.5.

IR 1429, 1722, 3545.

HRMS (ES-ToF) *m/z* found 420.1189 $[M+H]^+$, $C_{20}H_{17}F_3N_3O_4$ requires 420.1171.

Compound 63: 1-(2,4-Difluorophenyl)-6-fluoro-7-[(2*S*)-2-(hydroxymethyl)pyrrolidin-1-yl]4-oxo-1,4-dihydro-1,8-naphthyridine-3-carboxylic acid, hydrochloride

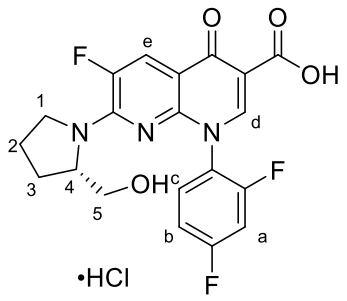

Prepared as described in General Procedure C, using **50**, affording 0.014 g (28%) of **63** as a white solid.

^{1}H NMR (400 MHz, DMSO-d_6) δ 1.82–1.94 (m, 4H, **2** and **3**), 3.40–3.58 (m, 2H, **1**), 3.66–3.80 (m, 3H, **4** and **5**), 7.33 (t, *J* = 8.6, 1H, **b** or **c**), 7.52–7.62 (m, 1H, **b** or **c**), 7.79 (tdd, *J* = 8.8, 5.9, 3.1, 1H, **a**), 8.06 (d, *J* = 13.0, 1H, **e**), 8.81 (s, 1H, **d**), 15.21 (s, 1H).

^{13}C NMR (100 MHz, DMSO-d_6) δ 24.9, 30.1, 51.5, 62.0, 62.6, 109.1 (m), 112.1 (d, *J*=19), 114.9, 116.9, 121.4 (m), 124.9, 130.0 (m), 145.9, 146.0, 146.4, 149.9, 151.4, 158.0, 164.0, 174.9.

IR 1432, 1732, 3342**.**

HRMS (ES-ToF) *m/z* found 420.1168 $[M+H]^+$, $C_{20}H_{17}F_3N_3O_4$ requires 420.1171.

Compound 64: 1-(2,4-Difluorophenyl)-6-fluoro-7-[(3*S*)-3-hydroxypyrrolidin-1-yl)-4-oxo-1,4-dihydro-1,8-naphthyridine-3-carboxylic acid, hydrochloride

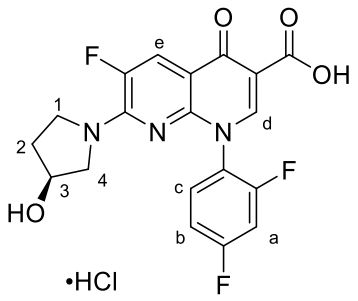

Prepared as described in General Procedure C using **51**, affording 0.020 g (30%) of **64** as a white solid.

^{1}H NMR (400 MHz, DMSO-d_6) δ 2.35 (m, 2H, **2**), 2.40 (br s, 1H, OH), 3.22 (br s, 1H, **4**), 3.76 (m, 3H, **1** and **4**), 4.30 (s, 1H, **3**), 6.97 (td, *J* =8.5, 2.7, 1H, **b** or **c**), 7.50 (td, *J* = 9.7, 2.8, 1H, **b** or **c**), 7.91 (td, *J* = 8.7, 5.9, 1H, **a**), 8.15 (d, *J* = 12.6, 1H, **e**), 8.90 (s, 1H, **d**), 14.60 (s, 1H, OH).

^{13}C NMR (100 MHz, DMSO-d_6) δ 47.0, 57.1, 104.9 (m), 109.2, 110.6, 112.6 (d, *J* = 22), 117.8 (d, *J* = 21), 124.7, 131.2 (d, *J* = 10), 146.9, 148.1, 149.2, 156.4, 158.9, 161.8, 165.9, 177.4.

IR 1413, 1630, 1703, 3419.

HRMS (ES-ToF) *m/z* found 406.1018 $[M+H]^+$, $C_{19}H_{15}F_3N_3O_4$ requires 406.1015.

Compound 65: 1-(2,4-Difluorophenyl)-6-fluoro-7-[(*trans*-4-hydroxycyclohexyl)amino]-4-oxo-1,4-dihydro-1,8-naphthyridine-3-carboxylic acid, hydrochloride

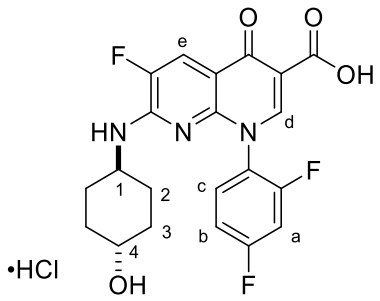

Prepared as described in General Procedure C using **52**, affording 0.051 g (46%) of **65** as a white solid.

^{1}H NMR (400 MHz, DMSO-d_6): δ 1.76–1.81 (m, 4H, **2** and **3**), 1.95–2.00 (m, 4H, **2** and **3**), 3.00 (br s, 1H, OH), 3.56 (m, 1H, **4**), 3.87 (m, 1H, **1**), 7.04 (td, *J* =8.8, 2.5, 1H, **b** or **c**), 7.25 (td, *J* = 9.6, 2.8, 1H, **b** or **c**), 7.66 (td, *J* = 8.7, 6.0, 1H, **a**), 8.16 (d, *J* = 12.0, 1H, **e**), 8.90 (s, 1H, **d**), 14.64 (s, 1H, OH).

^{13}C NMR (100 MHz, DMSO-d_6) δ 29.6, 34.5, 50.2, 68.9, 104.8 (d, *J* = 24), 109.3, 111.9 (m), 112.6, 117.4 (d, *J* = 17), 124.8, 130.2 (d, *J* = 10), 144.2, 145.6, 147.9, 149.5, 158.0, 162.3, 165.2, 175.0.

IR 1437, 1637, 1732, 3298.

HRMS (ES-ToF) *m/z* found 434.1317 $[M+H]^+$, $C_{21}H_{19}F_3N_3O_4$ requires 434.1328.

Compound 66: 7-(Cyclohexylamino)-1-cyclopropyl-6-fluoro-4-oxo-1,4-dihydro-1,8-naphthyridine-3-carboxylic acid, hydrochloride

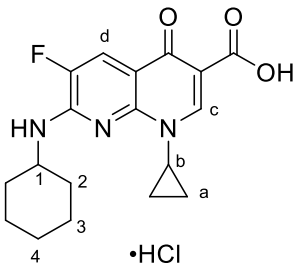

Prepared as described in General Procedure C using **53**, affording 0.026 g (50%) of **66** as a white solid.

^{1}H NMR (400 MHz, DMSO-d_6) δ 1.05–1.23 (m, 6H, **a** and **3**), 1.27–1.48 (m, 4H, **a** and **4**), 1.73–1.84 (m, 2H, **2**), 2.01 (d, *J* = 9.7, 2H, **2**), 3.69 (tt, *J* = 7.2, 4.1, 1H, **b**), 3.95–4.12 (m, 1H, **1**), 7.93 (d, *J* = 10.7, **d**), 8.18 (d, *J* = 7.4, 1H, OH), 8.57 (s, 1H, **c**), 15.52 (s, 1H).

^{13}C NMR (100 MHz, DMSO-d_6) δ 7.4, 25.4, 25.7, 32.1, 35.5, 51.0, 108.0, 110.6, 115.4 (d, *J* = 17), 146.8, 147.1, 148.5, 149.1, 166.4, 173.8.

IR 1431, 1631, 1721, 2933, 3322.

HRMS (ES-ToF) *m/z* found 346.1575 $[M+H]^+$, $C_{18}H_{21}FN_3O_3$ requires 346.1567.

Compound 67: 1-Cyclopropyl-6-fluoro-4-oxo-7-(propan-2-ylamino)-1,4-dihydro-1,8-naphthyridine-3-carboxylic acid, hydrochloride

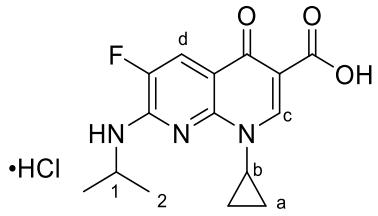

Prepared as described in General Procedure C using **54**, affording 0.037 g (39%) of **67** as a white solid.

^{1}H NMR (400 MHz, DMSO-d_6) δ 1.05–1.23 (m, 4H, **a**), 1.30 (d, *J* = 6.6, 6H, **2**), 3.71 (tt, *J*=7.3, 4.2, 1H, **b**), 4.41 (h, *J* = 6.6, 1H, **1**), 7.93 (d, *J* = 10.7, 1H, **d**), 8.17 (d, *J* = 7.4, 1H, OH), 8.57 (s, 1H, **c**), 15.53 (s, 1H).

^{13}C NMR (100 MHz, DMSO-d_6) δ 7.5, 22.1, 35.5, 43.4, 112.8, 115.1–115.6 (m), 146.4, 146.7, 148.4, 149.0, 164.9, 173.8.

IR 1432, 1633, 1726, 3289**.**

HRMS (ES-ToF) *m/z* found 306.1268 $[M+H]^+$, $C_{15}H_{17}FN_3O_3$ requires 306.1254.

Compound 55: 1-Cyclopropyl-6-fluoro-4-oxo-7-(propylamino)-1,4-dihydro-1,8-naphthyridine-3-carboxylic acid, hydrochloride

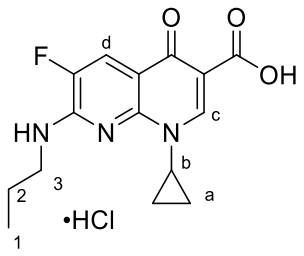

Prepared as described in General Procedure C using **55**, affording 0.044 g (47%) of **68** as a white solid.

^{1}H NMR (400 MHz, DMSO-d_6) δ 0.93 (t, J = 7.4, 3H, **1**), 1.10 (ta, J = 4.7, 2H, **a**), 1.12–1.22 (m, 2H, **a**), 1.67–1.70(m, 2H, **2**), 3.49 (t, J = 6.6, 2H, **3**), 3.70 (tt, J = 7.5, 4.1, 1H, **b**), 7.93 (d, J = 12, 1H, **d**), 8.43 (t, J = 4, 1H), 8.56 (s, 1H, **c**).

^{13}C NMR (100 MHz, DMSO-d_6) δ 7.0, 11.4, 21.6, 35.0, 42.5, 107.5, 110.2, 114.6 (d, J=17), 144.4, 148.1, 150.8, 150.9, 166.0, 176.3.

IR 1423, 1634, 1725, 3261**.**

HRMS (ES-ToF) *m/z* found 306.1267 $[M+H]^+$, $C_{15}H_{17}FN_3O_3$ requires 306.1254.

Compound 69: 1-Cyclopropyl-7-(cyclopropylamino)-6-fluoro-4-oxo-1,4-dihydro-1,8-naphthyridine-3-carboxylic acid, hydrochloride

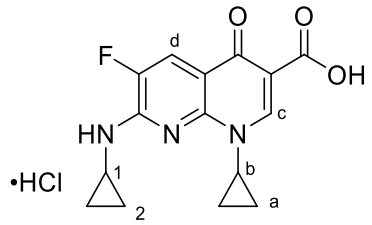

Prepared as described in General Procedure C using **56**, affording 0.061 g (56%) of **69** as a white solid.

^{1}H NMR (400 MHz, DMSO-d_6) δ 0.69 (p, *J* = 4.0, 2H, **2**), 0.84 (td, *J* = 7.8, 4.0 Hz, 2H, **2**), 1.12 (dd, *J* = 7.7, 5.3, 2H, **a**), 1.20 (p, *J* = 7.7, 2H, **a**), 3.03 (tq, *J* = 7.8, 4.0, 1H, **1**), 3.75 (tt, *J* = 7.7, 4.4, 1H, **b**), 7.94 (d, *J* = 10.6, 1H, **d**), 8.59 (s, 1H, **c**), 15.50 (s, 1H).

^{13}C NMR (100 MHz, DMSO-d_6) δ 7.7, 15.6, 35.5, 55.4, 65.4, 107.8, 111.5, 116.4 (d, *J*=17), 144.6, 146.7, 148.7, 153.0, 166.3, 176.8.

IR 1439, 1634, 1724, 3291.

HRMS (ES-ToF) *m/z* found 304.1109 $[M+H]^+$, $C_{15}H_{15}FN_3O_3$ requires 304.1097.

Compound 70: 1-Cyclopropyl-6-fluoro-4-oxo-7-(pyrrolidin-1-yl)-1,4-dihydro-1,8-naphthyridine-3-carboxylic acid, hydrochloride

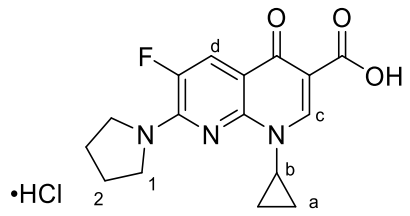

Prepared as described in General Procedure C using **57**, affording 0.035 g (73%) of **70** as a white solid.

^{1}H NMR (400 MHz, $CDCl_3$) δ 1.08 (qd, *J* = 5.9, 2.4, 2H, **a**), 1.16–1.31 (m, 2H, **a**), 2.07 (br s, 4H, **2**), 3.64 (tt, *J* = 7.5, 4.2, 1H, **b**), 3.86 (br s, 4H, **1**), 5.32 (s, 1H), 7.97 (d, *J* = 12.5, 1H), 8.68 (s, 1H), 15.29 (s, 1H).

^{13}C NMR (100 MHz, $CDCl_3$) δ 7.5, 15.3, 34.6, 65.9, 108.6, 111.4, 117.8 (d, *J* = 21), 145.2, 145.8, 147.6, 149.4, 167.2, 176.9.

IR 1428, 1633, 1718, 2960.

HRMS (ES-ToF) *m/z* found 318.1270 $[M+H]^+$, $C_{16}H_{17}FN_3O_3$ requires 318.1254.

Compound 71: 1-Cyclopropyl-6-fluoro-7-[(2*S*)-2-(hydroxymethyl)pyrrolidin-1-yl]-4-oxo-1,4-dihydro-1,8-naphthyridine-3-carboxylic acid, hydrochloride

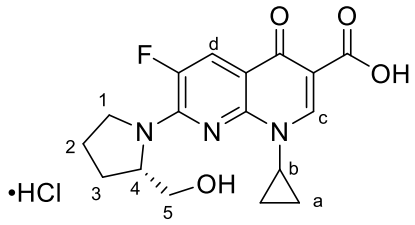

Prepared as described in General Procedure C using **58**, affording 0.012 g (20%) of **71** as a white solid.

^{1}H NMR (400 MHz, DMSO-d_6) δ δ 0.95–1.11 (m, 2H, **a**), 1.19–1.27 (m, 2H, **a**), 1.79–2.17 (m, 4H, **2** and **3**), 3.40–3.55 (m, 2H, **1**), 3.63–3.83 (m, 2H, **4** and **5**), 3.96–4.02 (m, 1H, **b**), 8.00 (d, *J* = 13.5, 1H, **d**), 8.40 (s, 1H, **c**).

^{13}C NMR (100 MHz, $CDCl_3$) δ 7.4, 24.2, 27.8, 28.4, 33.9, 49.9, 61.6, 65.3, 112.7, 114.7, 120.2 (d, *J* = 21), 146.3, 146.7, 147.2, 149.9, 164.7, 173.4.

IR 1455, 1631, 1688, 3393**.**

HRMS (ES-ToF) *m/z* found 348.1366 $[M+H]^+$, $C_{17}H_{19}FN_3O_4$ requires 348.1360.

Compound 72: 1-Cyclopropyl-6-fluoro-7-[(3*S*)-3-hydroxypyrrolidin-1-yl]-4-oxo-1,4-dihydro-1,8-naphthyridine-3-carboxylic acid, hydrochloride

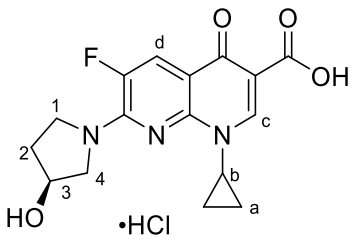

Prepared as described in General Procedure B using **59**, affording 0.040 g (49%) of **72** as a white solid.

^{1}H NMR (400 MHz, DMSO-d_6) δ 1.02–1.13 (m, 2H, **a**), 1.13–1.25 (m, 2H, **a**), 2.02 (br s, 2H, **2**), 3.90–3.99 (m, 1H, **b**), 3.86 (br s, 2H, **1**), 4.44 (br s, 2H, **4**), 5.14 (br s, 1H, **3**), 7.96 (d, *J* = 12.7, 1H, **d**), 8.56 (s, 1H, **c**).

^{13}C NMR (100 MHz, DMSO-d_6) δ 7.3, 35.3, 46.3, 49.6, 107.8, 111.0, 117.6 (d, *J* = 20), 145.2, 146.9, 147.9, 149.3, 166.4, 176.7.

^{19}F NMR (377 MHz, DMSO-d_6) δ -134.3.

IR 1443, 1633, 1716, 3362**.**

HRMS (ES-ToF) *m/z* found 334.1216 $[M+H]^+$, $C_{16}H_{17}FN_3O_4$ requires 334.1203.

Compound 73: 1-Cyclopropyl-6-fluoro7-{[(2*R*)-1-hydroxybutan-2-yl]amino}-4-oxo-1,4-dihydro-1,8-naphthyridine-3-carboxylic acid, hydrochloride

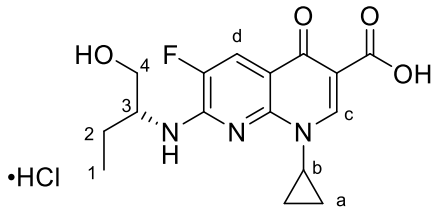

Prepared as described in General Procedure C using **60**, affording 0.058 g (55%) of **73** as a white solid.

^{1}H NMR (400 MHz, DMSO-d$_6$) δ 0.92 (t, *J* = 7.4, 3H, **1**), 1.02–1.30 (m, 4H, **a**), 1.52–1.82 (m, 2H, **2**), 3.54 (tt, *J* = 10.9, 5.6, 1H, **b**), 3.62 (dd, *J* = 10.9, 5.8, 1H, **4**), 3.69 (tt, *J* = 7.5, 4.2, 1H, **4**), 4.22 (tq, *J* = 10.1, 6.7, 6.2, 1H, **3**), 7.95 (m, 1H, **d**), 8.56 (s, 1H, **c**), 15.54 (s, 1H).

^{13}C NMR (100 MHz, DMSO-d$_6$) δ 7.4, 11.2, 23.7, 35.5, 55.4, 62.6, 107.9, 111.0, 118.0 (d, *J* = 21), 145.1, 146.7, 147.7, 149.0, 166.4, 176.7.

IR 1447, 1636, 1724, 3347**.**

HRMS (ES-ToF) *m/z* found 336.1376 $[M+H]^+$, $C_{16}H_{19}FN_3O_4$ requires 336.1360.

Compound 74: 1-Cyclopropyl-6-fluoro7-[(*trans*-4-hydroxycyclohexyl)amino]-4-oxo-1,4-dihydro-1,8-naphthyridine-3-carboxylic acid, hydrochloride

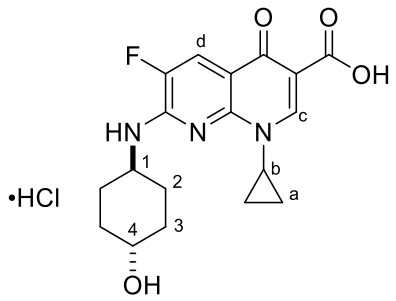

Prepared as described in General Procedure C using **61**, affording 0.035 g (52%) of **74** as a white solid.

^{1}H NMR (400 MHz, DMSO-d$_6$) δ 1.02–1.22 (m, 4H, **a**), 1.22–1.37 (m, 2H, **2**), 1.46 (qd, *J*= 12.8, 12.2, 3.1, 2H, **2**), 1.80–2.08 (m, 4H, **3**), 3.41–3.50 (m, 1H, **1**), 3.69 (t, *J* = 7.1, 1H, **4**), 4.00 (tt, *J* = 7.3, 3.8, 1H, **b**), 7.90 (d, *J* = 10.6, **d**), 8.16 (d, *J* = 7.3), 8.56 (s, 1H, **c**), 15.73 (s, 1H).

^{13}C NMR (100 MHz, DMSO-d$_6$) δ 7.4, 11.2, 23.7, 35.5, 55.4, 62.6, 107.9, 111.0, 118.0 (d, *J* = 21), 145.1, 146.7, 147.7, 149.0, 166.4, 176.7.

IR 1445, 1636, 1716, 3350**.**

HRMS (ES-ToF) *m/z* found 362.1503 $[M+H]^+$, $C_{18}H_{21}FN_3O_3$ requires 362.1516.

Compound 75: *tert*- Butyl 7-{4-[(*tert*-butoxycarbonyl)amino]piperidin-1-yl}-1-(2,4-difluorophenyl)-6-fluoro-4-oxo-1,4-dihydro-1,8-naphthyridine-3-carboxylate

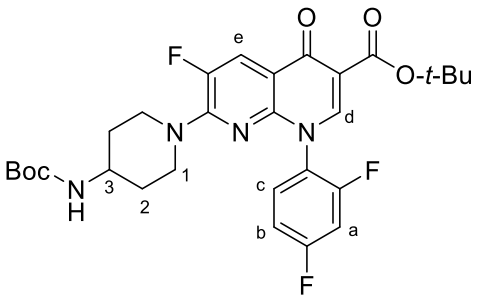

Prepared as described in General Procedure A, using **47** and 4-(*N*-boc-amino)piperidine, affording 0.13 g (90%) of **75** as a white solid.

***R*$_f$** 0.59 (92:8 DCM/MeOH).

^{1}H NMR (400 MHz, $CDCl_3$) δ 1.46 (s, 9H, Boc $(CH_3)_3$), 1.59 (s, 9H, CCH_3), 1.94 (d, *J*=14.2, 4H, **2**), 2.98 (da, *J* = 14.2, 4H, **1**), 3.67 (s, 1H, **3**), 7.07 (tdd, *J* = 8.9, 6.1, 3.2, 2H, **b** and **c**), 7.33–7.45 (m, 1H, **a**), 8.15 (d, *J* = 13.2, 1H, **e**), 8.33 (s, 1H, **d**).

^{13}C NMR (100 MHz, $CDCl_3$) δ 28.3, 28.4, 32.3, 46.0, 47.8, 57.1, 81.6, 105.0 (d, *J* = 26), 112.0 (d, *J* = 23), 112.5, 121.3 (d, *J* = 22), 130.0 (d, *J* = 10), 146.9, 148.9, 150.0, 150.2, 155.0, 157.9, 161.7, 164.0, 173.9.

Compound 76: (7-(4-Aminopiperidin-1-yl)-1-(2,4-difluorophenyl)-6-fluoro-4-oxo-1,4-dihydro-1,8-naphthyridine-3-carboxylic acid, methanesulfonate

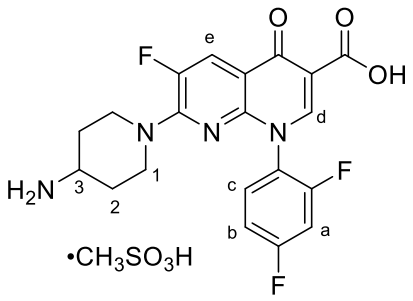

Prepared as described in General Procedure D using **75**, affording 0.041 g (30%) of **76** as a white solid.

^{1}H NMR (400 MHz, DMSO-d_6) δ 1.41 (ta, *J* = 12.6, 2H, **2**), 1.88 (ta, *J* = 12.6, 2H, **2**), 2.32 (s, 3H, SO_3CH_3), 2.93–3.22 (m, 1H, **3**), 3.32 (t, *J* = 5.0, 2H, **1**), 4.11 (t, *J* = 5.0, 2H, **1**), 7.29–7.43 (m, 1H, **b** or **c**), 7.62 (ddd, *J* = 10.3, 9.0, 2.8, 1H, **b** or **c**), 7.84 (td, *J* = 7.9, 7.1, 5.2, 1H, **a**), 8.21 (d, *J* = 13.2, 1H, **e**), 8.91 (s, 1H, **d**).

^{13}C NMR (100 MHz, DMSO-d_{63}) δ 29.7, 45.2, 47.5, 105.5 (m), 109.5, 112.8 (d, *J*=23), 120.2 (d, *J* = 22), 124.4, 131.4 (d, *J* = 11), 140.9, 148.8, 149.0, 150.2, 156.4, 158.7, 165.7, 177.6.

^{19}F NMR (377 MHz, DMSO-d_6) δ -127.0 (d, *J* = 13), -115.00–117.06 (m), -107.1 (q, *J*=8).

IR 1432, 1629, 1735, 3055.

HRMS (ES-ToF) *m/z* found 460.1386 $[M+CH_3CN+H]^+$, $C_{22}H_{21}F_3N_5O_3$.

Compound 77: 1-(2,4-Difluorophenyl)-6-fluoro-7-(piperazin-1-yl)-4-oxo-1,4-dihydro-1,8-naphthyridine-3-carboxylic acid, methanesulfonate

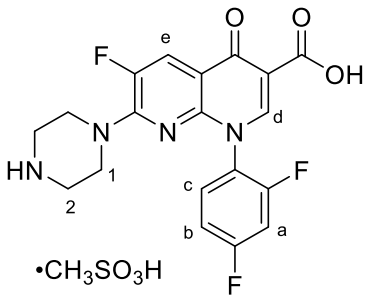

Prepared as described in General Procedure D using **14**, affording 0.069 g (65%) of **77** as a white solid.

^{1}H NMR (400 MHz, DMSO-d_6) δ 2.39 (br s, 8H, **1** and **2**), 3.15 (s, 3H, SO_3CH_3), 7.36 (tt, *J* = 8.9, 1.9, 1H, **b** or **c**), 7.61 (ddd, *J* = 10.4, 8.9, 2.8, 1H, **b** or **c**), 7.83 (td, *J* = 8.7, 5.9, 1H, **a**), 8.27 (d, *J* = 13.1, 1H, **e**), 8.92 (s, 1H, **d**).

^{13}C NMR (100 MHz, DMSO-d_6) δ 42.6, 43.9 (2), 105.4 (m), 109.6, 112.8 (d, *J*=23), 113.3, 120.4 (d, *J* = 22), 124.3, 131.3 (d, *J* = 10), 145.7, 146.4, 149.0, 150.2, 156.4, 158.7, 165.6, 177.6.

^{19}F NMR (377 MHz, DMSO-d_6) δ -127.2 (d, *J* = 13), -115.5 (d, *J* = 9), -106.8 (d, *J* = 8).

IR 1432, 1629, 1735, 3052.

HRMS (ES-ToF) *m/z* found 405.1171 $[M+H]^+$, $C_{19}H_{16}F_3N_4O_3$ requires 405.1175.

Compound 78: 1-(2,4-Difluorophenyl)-6-fluoro-7-(piperidin-1-yl)-4-oxo-1,4-dihydro-1,8-naphthyridine-3-carboxylic acid, methanesulfonate

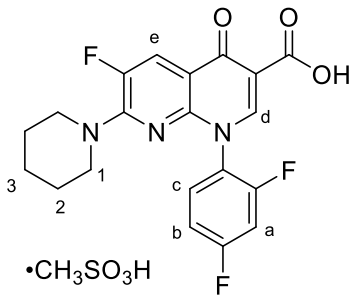

Prepared as described in General Procedure D using **16**, affording 0.064 g (66%) of **78** as a white solid.

^{1}H NMR (400 MHz, DMSO-d_6) δ 1.54–1.78 (m, 10H, **1**,**2** and **3**), 3.14 (s, 3H, SO_3CH_3), 7.35 (t, *J* = 7.7, 1H, **b** or **c**), 7.69–7.53 (m, 1H, **b** or **c**), 7.83 (td, *J* = 8.7, 5.7, 1H, **a**), 8.12 (d, *J* = 13.5, 1H, **e**), 8.86 (s, 1H, **d**).

^{13}C NMR (100 MHz, DMSO-d_6) δ 24.3, 25.9, 48.2, 48.3, 104.5 (m), 109.3, 111.8, 112.7 (d, *J* = 22), 119.7 (d, *J* = 23), 131.3 (d, *J* = 11), 146.0, 146.3, 148.5, 150.1, 156.4, 158.7, 161.9, 165.8, 177.4.

IR 1430, 1629, 1723, 2921.

HRMS (ES-ToF) *m/z* found 404.1227 $[M+H]^+$, $C_{20}H_{17}F_3N_3O_3$ requires 404.1222.

Compound 79: *tert*-Butyl 7-{4-[(*tert*-butoxycarbonyl)amino]piperidin-1-yl}-1-cyclopropyl-6-fluoro-4-oxo-1,4-dihydro-1,8-naphthyridine-3-carboxylate

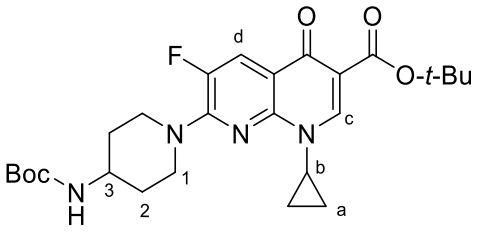

Prepared as described in General Procedure A, using **48** and 4-(*N*-boc-amino)piperidine, affording 0.086 g (58%) of **79** as a white solid.

***R*$_f$** 0.42 (92:8 DCM/ MeOH).

^{1}H NMR (400 MHz, $CDCl_3$) δ 0.96–1.08 (m, 2H, **a**), 1.11–1.23 (m, 2H, **a**), 1.48 (s, 9H, Boc $(CH_3)_3$), 1.62 (s, 9H, CCH_3), 1.67 (br s, 4H, **2**), 2.10 (t, *J* = 12.7, 2H, **1**), 3.10 (s, 3H, SO_3CH_3), 3.20 (t, *J* = 12.7, 2H, **1**), 3.50 (tt, *J* = 7.5, 4.1, 1H, **b**), 3.78 (br s, 1H, **3**), 8.12 (d, *J* = 13.5, 1H, **d**), 8.46 (s, 1H, **c**).

^{13}C NMR (100 MHz, DMSO-d_6) δ 7.4, 28.3, 28.4, 32.5, 33.8, 46.2, 47.8, 57.1, 81.6, 109.7, 113.8, 121.3 (d, *J* = 22), 147.0, 148.7, 149.5, 150.9, 155.7, 164.0, 173.9.

Compound 80: 7-(4-Aminopiperidin-1-yl)-1-cyclopropyl-6-fluoro-4-oxo-1,4-dihydro-1,8-naphthyridine-3-carboxylic acid, methanesulfonate

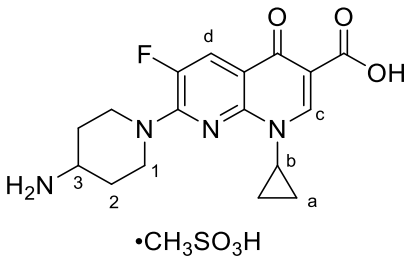

Prepared as described in General Procedure D using **79**, affording 0.041 g (92%) of **80** as a white solid.

^{1}H NMR (400 MHz, DMSO-d_6) δ 1.06–1.15 (m, 2H, **a**), 1.16–1.27 (m, 2H, **a**), 1.63 (da, *J*=12.4, 4.0, 2H, **2**), 2.08 (d, *J* = 11.9, 2H, **2**), 3.15 (s, 3H, SO_3CH_3), 3.20 (t, *J* = 11.8, 2H, **1**), 3.72 (m, 1H, **b**), 3.78 (br s, 1H, **3**), 4.57 (d, *J* = 13.6, 2H, **1**), 8.12 (d, *J* = 13.5, 1H, **d**), 8.46 (s, 1H, **c**).

^{13}C NMR (100 MHz, DMSO-d_6) δ 7.4, 30.0, 35.4, 45.5, 47.8,108.1, 113.0, 120.0 (d, *J*=23), 148.7, 150.1, 150.9, 155.7, 166.2, 177.0.

^{19}F NMR (377 MHz, DMSO-d_6) δ -127.4 (d, *J* = 13).

HRMS (ES-ToF) *m/z* found 347.1511 $[M+H]^+$, $C_{17}H_{20}FN_4O_3$ requires 347.1519.

Compound 81: 1-Cyclopropyl-6-fluoro-4-oxo-7-(piperazin-1-yl)-1,4-dihydro-1,8-naphthyridine-3-carboxylic acid, methanesulfonate

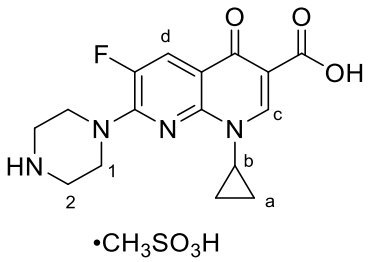

•CH_3SO_3H

Prepared as described in General Procedure D using **24**, affording 0.088 g (100%) of **81** as a white solid.

^{1}H NMR (400 MHz, DMSO-d_6) δ 0.97–1.31 (m, 4H, **a**), 2.83 (t, *J* = 5.1, 4H, **2**), 3.18 (s, 3H, SO_3CH_3), 3.72 (m, 1H, **b**), 4.06 (t, *J* = 5.1, 4H, **1**), 8.10 (d, *J* = 13.0, 1H, **d**), 8.64 (s, 1H, **c**).

^{13}C NMR (100 MHz, DMSO-d_6) δ 7.3, 35.5, 43.0, 44.1, 108.2, 113.6, 120.3 (d, *J* = 22), 146.3, 147.9, 150.0, 149.5, 166.0, 177.0.

IR 1437, 1626, 1718, 2832.

HRMS (ES-ToF) *m/z* found 333.1367 $[M+H]^+$, $C_{16}H_{18}FN_4O_3$ requires 333.1363.

Compound 82: 1-Cyclopropyl-6-fluoro-4-oxo-7-(piperidin-1-yl)-1,4-dihydro-1,8-naphthyridine-3-carboxylic acid, methanesulfonate

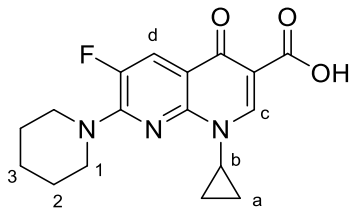

•CH_3SO_3H

Prepared as described in General Procedure D using **25**, affording 0.066 g (66%) of **82** as a white solid.

^{1}H NMR (400 MHz, DMSO-d_6) δ 0.95–1.32 (m, 4H, **a**), 1.67 (br s, 6H, **2** and **3**), 3.12 (s, 3H, SO_3CH_3), 3.14 (p, *J* = 1.6, 4H, **1**), 3.68 (tt, *J* = 7.4, 4.2, 1H, **b**), 8.01 (d, *J* = 13.8, 1H, **d**), 8.61 (s, 1H, **c**).

IR 1440, 1626, 1721, 2852.

HRMS (ES-ToF) *m/z* found 332.1419 $[M+H]^+$, $C_{17}H_{19}FN_3O_3$ requires 332.1410.

It was not possible to run a suitable ^{13}C NMR due to poor solubility in chosen solvent.

Compound 83: *tert*-Butyl 7-{(1α,5α,6α)-6-[(*tert*-butoxycarbonyl)amino]-3-azabicyclo[3.1.0]hexan-3-yl}-1-cyclopropyl-6-fluoro-4-oxo-1,4-dihydro-1,8-naphthyridine-3-carboxylate

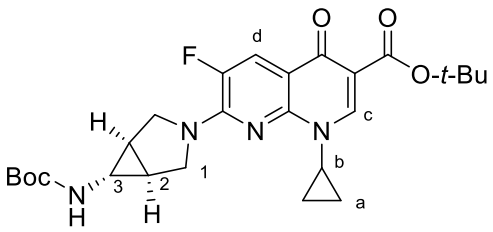

Prepared as described in General Procedure A and further purified by column chromatography (96:4 DCM/MeOH), using **48** and **11**, affording 0.11 g (58%) of **83** as a white solid.

^{1}H NMR (400 MHz, $CDCl_3$) δ 0.92–1.04 (m, 2H, **a**), 1.10–1.24 (m, 2H, **a**), 1.48 (s, 9H, Boc $(CH_3)_3$), 1.57 (s, 9H, CCH_3), 1.71 (br s, 1H, **2**), 1.91 (br s, 1H, **2**), 2.41 (q, *J* = 5.6, 1H, **3**), 3.47 (tt, *J* = 7.4, 4.1, 1H, **b**), 3.93 – 3.72 (m, 2H, **1**), 4.20 (d, *J* = 11.7, 2H, **1**), 8.06 (d, *J* = 13.0 Hz, 1H, **d**), 8.42 (s, 1H, **c**).

^{13}C NMR (100 MHz, $CDCl_3$) δ 7.3, 24.8, 28.4, 33.8, 50.5, 80.0, 81.1, 120.0 (d, *J* = 20), 146.4, 146.7, 148.2, 151.3, 156.2, 160.7, 164.8, 173.8.

Compound 84: 7-[(1α,5α,6α)-)-6-Amino-3-azabicyclo[3.1.0]hexan-3-yl]-1-cyclopropyl-6-fluoro-4-oxo-1,4-dihydro-1,8-naphthyridine-3-carboxylic acid, methanesulfonate

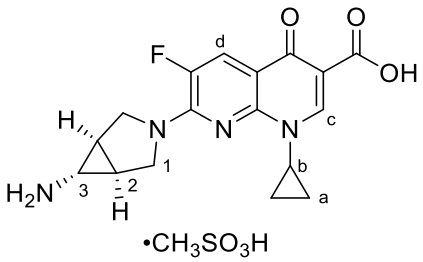

Prepared as described in General Procedure D using **83**, affording 0.038 g (43%) of **84** as a white solid.

^{1}H NMR (400 MHz, DMSO-d_6) δ 1.15–1.00 (m, 2H, **a**), 1.20 (h, *J* = 5.4, 1H, **a**), 2.22–2.14 (m, 1H, **2**), 2.60 (br s, 1H, **2**), 3.10 (s, 3H, SO_3CH_3), 3.68 (tt, *J* = 7.5, 4.2, 1H, **b**), 3.92 (t, *J* = 12.0, 2H, **1**), 4.10 (dd, *J* = 12.0, 3.2, 2H, **1**), 4.20 (br s, 1H, **3**), 7.98 (d, *J* = 12.7, 1H, **d**), 8.56 (s, 1H, **c**).

^{13}C NMR (100 MHz, DMSO-d_6) δ 7.3, 31.8, 35.4, 50.6 (2), 107.9, 111.5, 118.1 (d, *J* =21), 147.2, 147.4, 149.2, 160.7, 166.2, 176.7.

IR 1464, 1628, 1704, 3051**.**

HRMS (ES-ToF) *m/z* found 345.1367 $[M+H]^+$, $C_{17}H_{18}FN_4O_3$ requires 345.1363.

Compound 85: 2,4-Difluorobenzene-1-diazonium

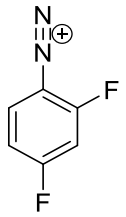

A solution of $NaNO_2$ (2.24 g, 32.41 mmol) in H_2O (10 mL) was added to a solution of 2,4-difluoroaniline (3 mL, 29.46 mmol) in HCl 20% (15 mL) at 0 ºC. After 1 h stirring at 0ºC, the mixture was used in the next step without further purification.

Compound 86: *tert*-Butyl 3-(2,6-dichloro-5-fluoropyridin-3-yl)-2-[2-(2,4-difluorophenyl)hydrazinylidene]-3-oxopropanoate

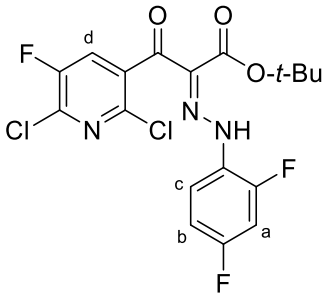

To a vigorously stirred solution of **44** (5.7 g, 18.5 mmol) and NaOAc (7.6 g, 92.65 mmol) in EtOH (25 mL), H_2O (25 mL) and $CHCl_3$ (25 mL), **85** (in solution) was added at once at below 10 ºC and stirred for further 4 h at 15 ºC. After addition of H_2O (50 mL), the mixture was extracted with DCM. The combined organic layers were dried over $MgSO_4$ and evaporated to dryness yielding a residue, which was then purified by column chromatography (75:25 DCM/petroleum ether), affording 5.89 g (71%) of **86** as a yellow solid.

***R*$_f$** 0.68 (98:2 DCM/MeOH).

^{1}H NMR (400 MHz, DMSO-d_6) δ 1.59 (s, 9H, CCH_3), 6.85–6.98 (m, 2H, **b** and **c**), 7.19 (td, *J* = 8.9, 5.6, 1H, **a**), 7.64 (d, *J* = 7.1, 1H, **d**).

^{13}C NMR (100 MHz, DMSO-d_6) δ 28.1, 84.7, 104.4 (m), 112.5 (d, *J* = 22), 116.9 (d, *J* = 10), 126.7 (d, *J* = 21), 136.7, 138.5, 141.0, 152.8, 162.5, 170.8, 178.5, 185.1.

Compound 87: *tert*-Butyl 7-chloro-1-(2,4-difluorophenyl)-6-fluoro-4-oxo-1,4-dihydropyrido[2,3-*c*]pyridazine-3-carboxylate

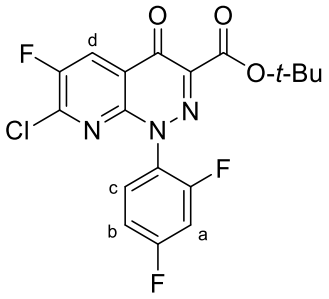

K_2CO_3 (2.4 g, 17.36 mmol) was added to a solution of **86** (5.9 g, 13.16 mmol) in acetonitrile (80 mL) and the solution was heated to reflux overnight. The solvent was evaporated to dryness and the residue was taken up with DCM, washed with H_2O twice, dried over MgSO4, and purified by column chromatography (98:2 DCM/MeOH), affording 4.34 g (80%) of **87** as a yellow solid:

***R**f* 0.30 (98:2 DCM/MeOH).

^{1}H NMR (400 MHz, $CDCl_3$) δ 1.64 (s, 9H, CCH_3), 7.00–7.18 (m, 2H, **b** and **c**), 7.54 (td, *J*=8.5, 5.7, 1H, **a**), 8.35 (d, *J* = 6.6, 1H, **d**).

^{13}C NMR (100 MHz, $CDCl_3$) δ 28.1, 84.1, 105.1 (dd, *J* = 27, 23), 112.3 (dd, *J* = 23, 4), 121.2 (d, *J* = 21), 129.9 (d, *J* = 10), 143.2, 145.9, 151.4, 154.0, 156.3, 158.9, 161.2, 162.2, 164.6, 168.0.

IR 1141, 1407, 1648, 1718, 2982**.**

HRMS (ES-ToF) *m/z* found 412.0691 $[M+H]^+$, $C_{18}H_{14}ClF_3N_3O_3$ requires 412.0676.

Compound 88: *tert*-Butyl 1-(2,4-difluorophenyl)-6-fluoro-4-oxo-7-(piperidin-1-yl)-1,4-dihydropyrido[2,3-*c*]pyridazine-3-carboxylate

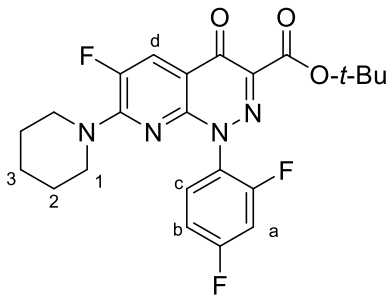

Prepared as described in General Procedure A, using **87** and piperidine, affording 0.116 g (80%) of **88** as a white solid.

^{1}H NMR (400 MHz, $CDCl_3$) δ 1.53–1.74 (m, 11H, CCH_3 and **2**), 1.93 (p, *J* = 5.6, 2H, **2**), 3.16 (t, *J* = 5.6, 2H, **3**), 3.59 (t, *J* = 5.3, 4H, **1**), 7.02 (dtd, *J* = 25.1, 9.1, 2.7, 2H, **b** and **c**), 7.49 (td, *J* = 8.4, 5.7, 1H, **a**), 7.94 (d, *J* = 13.3, 1H, **d**).

^{13}C NMR (100 MHz, $CDCl_3$) δ 22.6, 25.9, 28.1, 44.5, 83.3, 102.3–105.0 (m), 111.7 (d, *J*=23), 113.5, 118.8 (d, *J* = 22), 130.0 (d, *J* = 10), 143.3, 146.3, 146.9, 148.9, 152.0, 162.5, 162.2, 164.6, 167.2.

Compound 89 *tert*-Butyl 1-(2,4-difluorophenyl)-6-fluoro-7-{[(2*R*)-1-hydroxybutan-2-yl]amino}-4-oxo-1,4-dihydropyrido[2,3-*c*]pyridazine-3-carboxylate

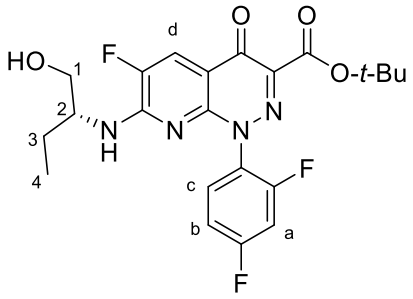

Prepared as described in General Procedure A, using **87** and (*R*)-2-aminobutan-1-ol, affording 0.081 g (55%) of **89** as a white solid.

^{1}H NMR (400 MHz, $CDCl_3$) δ 0.85 (t, *J* = 7.4, 3H, **4**), 1.58–1.62 (m, 11H, **3** and CCH_3), 1.80 (br s, 1H, **2**), 3.57–3.77 (m, 2H, **1**), 5.77 (d, *J* = 6.6, 1H, NH), 6.93–7.15 (m, 2H, **b** and **c**), 7.50 (td, *J* = 8.5, 5.8, 1H, **a**), 7.93 (d, *J* = 10.0, 1H, **d**).

^{13}C NMR (100 MHz, $CDCl_3$) δ10.4, 23.8, 28.1, 54.6, 63.5, 83.5, 104.5 (m), 111.1 (d, *J*=22), 113.6, 115.2 (d, *J* = 18), 130.2 (d, *J* = 10), 144.5, 144.9, 147.7, 151.9, 152.5, 162.4, 162.2, 164.6, 167.6.

Compound 90: 1-(2,4-Difluorophenyl)-6-fluoro-4-oxo-7-(piperidin-1-yl)-1,4-dihydropyrido[2,3-*c*]pyridazine-3-carboxylic acid, methanesulfonate

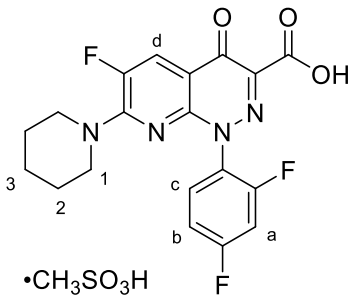

Prepared as described in General Procedure D, using **88**, affording 0.053 g (38%) of **90** as a white solid.

^{1}H NMR (400 MHz, DMSO-d_6) δ 1.52 (tt, *J* = 6.2, 4.1, 4H, **2**), 1.61 (q, *J* = 6.2, 2H, **3**), 3.12 (s, 3H, SO_3CH_3), 3.60 (t, *J* = 4.1, 4H, **1**), 7.37 (td, *J* = 8.6, 8.1, 2.8, 1H, **b** or **c**), 7.63 (ddd, *J* = 11.2, 9.0, 2.8, 1H, **b** or **c**), 7.78 (td, *J* = 8.7, 5.9, 1H, **a**), 8.06 (d, *J* = 13.4, 1H, **d**).

^{13}C NMR (100 MHz, DMSO-d_6) δ 24.2, 26.0, 48.4, 105.1 (m), 112.9 (d, *J* = 35), 118.5 (d, *J* = 23), 126.2, 131.3 (d, *J* = 11), 146.8, 147.7, 150.6, 163.2, 168.9.

^{19}F NMR (377 MHz, DMSO-d_6) δ -123.8 (d, *J* = 13), -115.5 (d, *J* = 10), -106.4–107.4 (m).

IR 1432, 1615, 1741, 2948.

HRMS (ES-ToF) *m/z* found 405.1181[M+H]$^+$, $C_{19}H_{16}F_3N_4O_3$ requires 405.1175.

Compound 91: 1-(2,4-Difluorophenyl)-6-fluoro-7-{[(2*R*)-1-hydroxybutan-2-yl]amino}-4-oxo-1,4-dihydropyrido[2,3-*c*]pyridazine-3-carboxylic acid, methanesulfonate

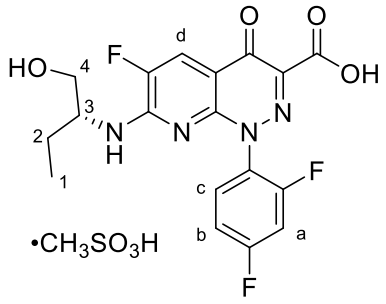

Prepared as described in General Procedure D, using **89**, affording 0.050 g (70%) of **91** as a light brown solid.

^{1}H NMR (400 MHz, DMSO-d_6) δ 0.69 (t, *J* = 7.4, 3H, **1**), 1.42 (ddq, *J* = 7.4, 6.8, 2H, **2**), 2.04–2.10 (m, 1H, **3**), 3.12 (s, 3H, SO_3CH_3), 3.57–3.60 (m, 2H, **4**), 7.37 (td, *J* =8.7, 2.7, 1H, **b** or **c**), 7.62 (td, *J* = 9.7, 2.8, 1H, **b** or **c**), 7.77 (td, *J* = 8.7, 5.9, 1H, **a**), 7.99 (d, *J*=10.1, 1H, **d**).

^{13}C NMR (101 MHz, DMSO-d_6) δ 10.9, 23.4, 55.9, 61.9, 105.1 (d, *J* = 25), 112.7 (d, *J*=23), 114.2 (d, *J* = 18), 126.4, 131.2 (d, *J* = 10), 145.9, 148.5, 149.0, 152.0, 156.2, 158.8, 161.8, 163.2, 169.3.

^{19}F NMR (377 MHz, DMSO-d_6) δ -132.7 (d, *J* = 10.4), -115.9, -106.9 (q, *J* = 8.0).

IR 1481, 1631, 1718, 3308, 3467**.**

HRMS (ES-ToF) *m/z* found 409.1120 $[M+H]^+$, $C_{18}H_{16}F_3N_4O_4$ requires 409.1124.

4.3. Biology general procedures

Common Buffers

10x TBST: 40 mL Tween 20, 616 mL 1 M Tris-HCl, 184 mL 1 M Tris-Base, 320 g NaCl, qs to 4 L with dH_2O.

4x Tris/SDS Buffer: 6.05 g of Tris-Base, 60 mL dH_2O, pH to 6.8, qs to 100 mL with dH_2O, 0.4 g of SDS.

6x SDS/Sample Buffer: 35 mL 4x Tris/SDS Buffer, 5 g SDS, 4.65 g DTT, 6 mg Bromophenol Blue, 15 mL glycerol, qs to 50 mL with dH_2O.

6x Hot Lysis Buffer: 35 mL 4x Tris/SDS Buffer, 5 g SDS, 15 mL glycerol, qs to 50 mL with dH_2O.

Kinase buffer (KB): 9 parts of 10x kinase mix (25 mM HEPES, 150 mM NaCl, 5 mM β-glycerophosphate, 1.5 mM DTT, 30 mM $MgCl_2$, pH 7.4) and 1 part of 10x BSA (10% BSA in PBS).

Lysis buffer: 50 mM NaH_2PO_4, 300 mM NaCl, 10 mM imidazole, 10% glycerol, pH 8, PIC, 10 µg/mL of leupeptin, 1 mM PMSF, 0.01% β-ME, 2 mM Na_2VO_3).

Wash buffer I: 50 mM NaH_2PO_4, 500 mM NaCl, 10 mM imidazole, 10% glycerol, pH 8, 5 µg/mL of leupeptin,1 mM PMSF, 0.01% β-ME.

Wash buffer II: 50 mM NaH_2PO_4, 300 mM NaCl, 10 mM imidazole, 10% glycerol, pH 8, 5 µg/mL of leupeptin, 1 mM PMSF, 0.01% β-ME.

Elution buffer: 50 mM NaH_2PO_4, 300 mM NaCl, 250 mM imidazole, 10% glycerol, pH 8, PIC; 5 µg/mL of leupeptin, 0.01% β-ME.

Dialysis buffer: 20 mM HEPES, 300 mM NaCl,10 mM β-glycerophosphate,1 mM EGTA, 1 mM DTT, 10% glycerol, pH 7.4, 2.1 µg/mL of aprotinin.

Storage buffer: 20 mM HEPES, 300 mM NaCl, 10 mM β-glycerophosphate, 1 mM EGTA, 1 mM DTT, 50% glycerol, pH 7.4.

Common reagents and antibodies

Monoclonal rabbit phospho-p90RSK(Ser380) antibody (Cell Signaling Technology, #12032).

Polyclonal rabbit RAN antibody (Cell Signaling Technology, #4462).

Monoclonal rabbit GFP antibody (Cell Signaling Technology, #2956).

Anti-mouse IgG, HRP-linked antibody (Cell Signaling Technology, #7076).

Anti-rabbit IgG, HRP-linked antibody (Cell Signaling Technology, #7074).

Polyclonal rabbit phospho-p90RSK(Thr359/Ser363) antibody (Cell Signaling Technology, #9344S).

Monoclonal anti-V5 tag antibody (ThermoFisher Scientific, #37-7500).

Polyclonal rabbit anti-ACTIVE® MAPK (pTEpY) (Promega, #V8031).

Monoclonal rabbit phospho-ERα(Ser167) antibody (Cell Signaling Technology, #5587).

Polyclonal mouse IgG (H+L) Cross-Adsorbed Secondary Antibody, Alexa Fluor 488 (ThermoFisher Scientific, #A-11059).

U0126 (Tocris), BI-D1870 (Enzo), Epidermal Growth Factor from murine submaxillary gland (Sigma), GDC-0994 (Selleckchem)

Western Blots

Samples (20 µg of protein) were added to 6x SDS/Sample buffer and dH_2O, and boiled at 95 °C for 3 min before being resolved by gel electrophoresis (SDS-PAGE), using 7.5% SDS-polyacrylamide gels or Novex™ 8% Tris-Glycine pre-cast gels (Invitrogen). Proteins were transferred to nitrocellulose membranes using wet transfer or to nitrocellulose transfer stacks (iBlot™, Tranfer Stack, nitrocellulose, mini, ThermoFisher Scientific) membranes using a standard 7-minute protocol (ThermoFisher iBlot 2 Dry Blotting System). Membranes were blocked in 5% skim milk in TBST for 0.5 h at r.t., and then incubated with the relevant antibody in 5% BSA in TBST. Membranes were washed 3 times with TBST before incubation with the relevant secondary antibody (HRP) in 5% BSA in TBST. Membranes were washed 3 times with TBST, before they were developed

(ECL Western Blotting Detection Reagents) and imaged for chemiluminescence using films or imaging systems ChemiDoc (BioRad) and ImageQuant LAS 4000 mini (GE Life Sciences).

Kinase assays

Kinase, inhibitors and ATP solutions were prepared in KB. All assays measured initial reaction velocity. Antibodies solutions were prepared in 3% BSA in PBS. HRP activity was measured using Western Lightning Plus-ECL (PerkinElmer Life Sciences, Waltham, MA).

4.4. Biochemical assay

4.4.1. ERK2: expression, purification, and activity confirmation

Isolation of plasmid DNA

Plasmid pET-His6-ERK2-MEK1_R4F_coexpression was a gift from Melanie Cobb (Addgene plasmid #39212). Plasmid was striped against a Luria broth (LB) agar plate (containing ampicillin, 1:1000) and incubated overnight at 37 ºC. One single colony was picked from the plate and added into a test tube containing liquid LB (containing ampicillin, 1:1000), that was incubated overnight with vigorous shaking at 37 ºC. A glycerol stock was made from liquid culture (500 µL was added into 500 µL of 50% glycerol in dH2O in a 2-mL cryovial, gently mixed and stored at -80 ºC). To isolate plasmid DNA, a QIAprep Spin Miniprep kit was used and the experiment was carried out according to the manufacturer's instructions. The concentration of plasmid DNA was measured using Nanodrop (46.1 ng/µL).

DNA transformation

A frozen cryovial containing BL21(DE3) cells (65 µL) was thawed in ice for 10 min. Plasmid DNA of ERK2 (5 µL) was added and mixed by flicking the tube 4-5 times. The mixture was placed in ice for 0.5 h, heat shocked at 42 ºC for 30 s and placed on ice for a further 5 min. 1 mL of LB at r.t. was added and the tube incubated at 37 ºC for 0.5 h. 100 µL of the mixture was loaded and spread onto an agar plate. The remaining mixture was centrifuged for 30 s and then 800 µL of supernatant discarded. The pellet was resuspended in the remaining liquid, loaded and spread onto another agar plate. Both plates were incubated overnight at 37 ºC. Transformation efficiency was measured in 6.5×10^2 CFU/µg of DNA.

ERK2 expression

From the incubated agar plates, a single colony was picked and incubated in 2 mL of LB (containing carbenicillin, 1:1000) at 30 ºC overnight. After 12 h, a glycerol stock was made (500 µL of liquid culture was added into 500 µL of 50% glycerol in dH2O in a 2 mL cryovial, gently mixed and stored at -80 ºC). 100 µL of the liquid culture was added to a 1-L conical flask containing 150 mL of LB (containing carbenicillin, dilution 1:1000), and incubated at 30 ºC. Samples were collected every hour to measure the optical density (OD) of the mixture. When it reached 0.6 (after 5 h approximately), IPTG was added to induce expression (375 µL, final concentration 0.25 mM) and the mixture was incubated for another 16 hours at 30 ºC. Finally, flasks were cooled down in an ice bath, followed by centrifugation (8000 rpm, 35 min, 4 ºC). The supernatant was removed and pellets were frozen at -80 ºC.

ERK2 purification

Pellets (from previous step) were thawed in ice, resuspended in 40 mL of lysis buffer and disrupted using Emulsiflex (between 10000 and 15000 psi). Disrupted cells were then transferred to two centrifuge tubes and centrifuged (10000 rpm, 0.5 h, 4 ºC). The supernatant was collected and centrifuged again. In the meantime, 1.2 mL of Ni-NTA agarose in ethanol was transferred to a falcon tube and left resting for 0.5 h. The supernatant (ethanol) was then removed from the beads and 10 mL of lysis buffer was added and left to equilibrate for another 0.5 h. Then the buffer was removed and beads were resuspended in 2 mL of lysis buffer. After centrifuging, supernatant fractions were collected and the Ni beads were added to the combined fractions and left rotating at 4ºC for 1 h. After, a tube containing a cocktail of protease inhibitors (PIC) was added to the lysate. (Next steps were carried at 4 ºC). The lysate was filtered using a column and the unbound protein was collected. The column was washed twice with 10 mL of wash buffer I and twice with 10 mL of wash buffer II. The protein was then eluted using elution buffer in 5 fractions of 1.5 mL each. E5 was stored at -20 °C. The other four fractions, E1 to E4,

were transferred into dialysis cassettes (Slide-A-Lyzer Dialysis Cassette, 3500 MWCO, 0.5 – 3 mL), and left floating and stirring for 1 h in 1 L of dialysis buffer. After 1 h, dialysis buffer was replaced by storage buffer and the cassettes were left floating and stirring for another 7 hours. Samples were then removed out of the cassettes, transferred to appropriate tubes and stored at -20 °C. Protein concentration was measured using Nanodrop Protein A280: E1= 0.85–1.19 mg/mL; E2= 0.17–0.24 mg/mL; E3= 0.09 mg/mL; E4= 0.05 mg/mL.

Preparing ERK2 kinase assay plates

A 20 µg/mL dilution of GST-MBPtide in 50 mM Na_2CO_3, pH 9.6, was made (30 mL). 50µL of this dilution was added to each well of a Luminunc 96-well plate (with Maxisorp surface treatment). Each plate was covered with Microplate Adhesive Film, incubated at 37 °C for 0.5 h and then stored at 4 °C overnight. Adhesives were then removed and the solution was aspirated using a plate washer. 200 µL of 3% tryptone in PBS was added to each well. Plates were sealed again and placed in the incubator at 37 °C for 0.5 h and then stored at 4 °C overnight. Adhesives were then removed and the blocking solution was aspirated using a plate washer. Plates were stored at r.t. and in the dark for 24 h or until they were completely dry. Plates were then sealed again and stored at 4 °C, ready to be used.

ERK2 kinase assay with inhibitor GDC-0994

50 µL of kinase (5 nM) and 25 µL of GDC-0994 in KB at the indicated concentrations were added to each well and incubated for 2 h. The reactions were initiated by adding 25 µL of ATP (final concentration 10 µM) and terminated 20 min later by addition of 0.5M EDTA, pH 8.0. The plates were extensively washed and phosphorylation of substrate was detected using purified monoclonal mouse anti-phospho-MBP (UBI) antibody and HRP-conjugated donkey anti-mouse antibody.

4.4.2. RSK4: expression, purification, and activity confirmation

Isolation of plasmid DNA

Plasmid R777-E296 Hs.RPS6KA6-nostop was a gift from Dominic Esposito (Addgene plasmid #70580). Plasmid was striped against a LB agar plate (containing spectinomycin, 1:2000 dilution) and incubated overnight at 37 ºC. One single colony was picked from the plate and added into a test tube containing liquid LB (containing spectinomycin, 1:2000 dilution), that was incubated overnight with vigorous shaking at 37 ºC. To isolate plasmid DNA, a QIAprep Spin Miniprep kit was used and the experiment was carried out according to the manufacturer's instructions. The concentration of plasmid DNA was measured using Nanodrop (109.3 ng/µL). The generated clone was sequenced and checked using BLAST.

DNA transformation

A frozen cryovial containing DH5α cells (15 µL) was thawed in ice for 10 min. Plasmid DNA of RSK4 (2 µL) was added and mixed by flicking the tube 4-5 times. The mixture was placed in ice for 0.5 h, heat shocked at 42 ºC for 30 s and placed in ice for a further 5 min. 1 mL of LB (at r.t.) was added into the mixture and the tube incubated at 37 ºC for 0.5 h. 100 µL of the mixture was loaded and spread onto an agar plate and incubated overnight at 37 ºC.

Generating an entry clone for RSK4

From the incubated agar plate, one single colony was picked and incubated in 2 mL of LB (containing spectinomycin, dilution 1:2000) at 37 ºC overnight. 100 µL of the liquid culture was added to a 1-L conical flask containing 150 mL of LB (containing spectinomycin, dilution 1:1000), and incubated at 37 ºC overnight. The contents were then centrifuged (7000 rpm, 0.5 h, 4 °C). To isolate plasmid DNA, a NucleoBond Xtra Midi Macherey-Nagel kit was used and the experiment was carried out according to the

manufacturer's instructions. The concentration of plasmid DNA was measured using Nanodrop (3248.1 ng/µL).

LR recombinant reaction with RSK4/analysis by PCR

Reagents and procedures were provided in the BaculoDirect™ C-Term Expressing Kit (ThermoFisher Scientific, #12562-013). Briefly, to a vial containing BaculoDirect Linear DNA (10 µL), 300 ng of entry clone and 5 µL of 1XTE Buffer were added. A tube containing LR Clonase II Enzyme mix was thawed in ice for 2 min and 4 µL of this enzyme mix was added to the vial containing the entry close. The content was mixed well by tapping the tube several times. The reaction was incubated at 27 °C for 1 h and then at r. t. for 18 hours. It was then analysed by PCR. 0.5 µL of the BaculoDNA was diluted 200-fold. 2 µL of this dilution was added to 34 µL of dH_2O, 10 µL of Q5 5x buffer, 1 µL of dNTP, 2.5 µL of forward primer (polyhedron promoter) and 0.5 µL of Q5 enzyme. 23.75 µL of this mixture was transferred into two PCR tubes. To the first one, 1.25 µL of hRSK4-int1R was added and to the other tube 1.25 µL of V5 reverse primer was added. 25 µL of each sample and a molecular weight marker was loaded onto a 1% agarose gel and ran according to the cycle parameters described below. It was analysed under the UV light.

Step	Time	Temperature	Cycles
Initial denaturation	5 minutes	95 ºC	1X
Denaturation	45 seconds	94 ºC	25X
Annealing	1 minute	52 ºC	
Extension	1.5 minutes	72 ºC	
Final extension	10 minutes	72 ºC	1X

Sf9 cell culture

Sf9 cells were obtained from Invitrogen (lot no. 1846945) and cultured in the appropriate dishes sizes with 1) Membrane-filtered Grace's Insect Medium, Supplemented with 10% FBS, 5% Penicillin-Streptomycin and 0.25 µg/mL of Amphotericin B (complete growth medium) or 2) Membrane-filtered Sf-900 SFM II with 5% Penicillin-Streptomycin and 0.25 µg/mL of Amphotericin B; or a mixture containing these two (proportions stated), unless otherwise stated. Incubation temperature was 27 ºC.

Transfection of baculovirus into Sf9 cells and generating high titer stock

Reagents and procedures were provided in the BaculoDirect™ C-Term Expressing Kit (ThermoFisher Scientific, #12562-013). Briefly, 2 mL of Grace's Insect medium, Unsupplemented was added to a 35-mm dish and $8x10^5$ cells were seeded into the dish. The following solutions were prepared: I) 8 µL of Cellfectin reagent with 100 µL of Grace's Insect medium, Unsupplemented; II) 10 µL of LR recombination reaction with 100 µL of Grace's Insect medium, Unsupplemented. Solutions I and II were combined, gently mixed and incubated at r. t. for 35 min. The transfection mix was then added dropwise onto to the dish and incubated at 27 ºC. After 5 h, the medium was replaced with 2 ml of complete growth medium complemented with 100 µM ganciclovir. After 6 days incubating at 27 °C, cells were showing signs of infection. Supernatant (denominated P1 viral stock) was collected in a falcon tube, centrifuged, transferred to a new tube and kept at 4 ºC, protected from light. Frozen stocks of P1 were made (1 mL of P1 viral stock was centrifuged at 3500 rpm for 5 min and 20 x 50 µL aliquots were made and kept at -80 °C). Cells were resuspended in PBS (1 mL), transferred into an Eppendorf and centrifuged. Supernatant was removed and the pellet was resuspended in 500 µL of 1xSDS and kept at -20 °C. P2 culture was started by adding 100 µL of P1 into 10 mL of Grace's Insect medium, Unsupplemented on a 10-cm dish. After 72 h, cells were showing signs of infection. Supernatant (denominated P2 viral stock) was collected in a falcon tube, centrifuged, transferred to a new tube and kept at 4 ºC, protected from light. Frozen

stocks of P2 were made (0.4 mL of P2 viral stock was centrifuged at 3500 rpm for 5 min and 8 x 50 µL aliquots were made and kept at -80 °C). Cells were resuspended in PBS (1 mL) and transferred into an Eppendorf tube that was centrifuged. Supernatant was removed, and pellet was resuspended in 500 µL of 1xSDS and kept at -20 °C. P3 culture was started by adding 100 µL of P2 into 10 mL of complete growth medium on a 10-cm dish. After 72 h, cells were showing signs of infection. Supernatant (denominated P3 viral stock) was collected in a falcon tube, centrifuged, transferred to a new tube and kept at 4 ºC, protected from light. Cells were resuspended in PBS (1 mL) and transferred into an Eppendorf tube that was centrifuged. Supernatant was removed and the pellet was resuspended in 500 µL of 1xSDS and kept at -20 °C. P1, P2 and P3 cell lysates were analysed by Western blot for protein expression.

Optimising expression with high titer viral stocks.

Using a 6-well tissue culture plate, $1x10^6$ cells were added to each well containing 2 mL of complete growth medium each. The plate was incubated for 1 h allowing cells to fully attach to the bottom of the plate. Viral stock was then added to each well according to the specific MOIs of 1 (10 µL), 2 (20 µL), 5 (50 µL), 10 (100 µL) and 20 (200 µL) (volumes calculated with the equation below, P3 titer was assumed to be of $1x10^8$ pfu/mL, from BaculoDirect™ guidelines). The cells were incubated for 48 h then harvested, transferred to 15-mL falcon tubes and centrifuged (2000 rpm, 3 min). The medium was aspirated and pellets resuspended in 4% PFA (0.5 mL). After 20 min, pellets were washed with PBS followed by a wash with 0.5% Triton/PBS. After 10 min, tubes were again centrifuged, the medium removed and pellets washed with 10% BSA/0.5% Triton in PBS. After 1 h, tubes were again centrifuged, the medium removed and pellets resuspended in a solution of anti-V5 antibody (1:5000 dilution in 1% BSA in PBS) and incubated for 2h. The tubes were centrifuged, and the pellets were then washed with 0.1% Triton/PBS (3x) then incubated with the secondary antibody Alexa 488 (1:1000 dilution in 1% BSA) for 2 h. They were centrifuged, and the pellets were then washed with 0.1% Triton/PBS

(3x). Pellets were then resuspended in Hoechst (1:500 dilution in PBS) and incubated for 20 min. Tubes were then centrifuged and the pellets washed with 0.1% Triton/PBS. Pellets were then resuspended in PBS, plated on microscopy slides and figures were taken using a confocal microscope.

$$\text{Inoculum required (mL)} = \frac{\text{MOI (pfu/cell)} \times \text{number of cells}}{\text{viral titer (pfu/mL)}}$$

RSK4 expression

In a spinner flask, $3x10^7$ cells were added and incubated with 75 mL of a mixture of SFM-900 II medium (75%) and complete growth medium (25%) with stirring at 27 ºC. After 48h, 3.5 mL of P3 viral stock was added into the flask and incubated for further 48 h. With 2 h left, infected cells were divided into two spinner flasks and U0126 (10 μM final concentration) was added to one of them. At the end of the 48 h, cells were harvested (10000 rpm, 0.5 h) and pellets frozen.

RSK4 purification

Same procedure as for ERK2 purification. Protein concentration was measured using Nanodrop Protein A280: E1 0.43 mg/mL (without UO0126); E2 0.02 mg/mL (without U0126); E1 0.12 mg/mL (with U0126); E2 0.09 mg/mL (with U0126).

RSK4 kinase assay plates preparation

Glutathione-S-transferase (GST)-fusion protein (1 μg) containing the ERα-Ser167 sequence-RLASTND was adsorbed in the wells of LumiNunc 96-well polystyrene plates (MaxiSorp surface treatment). The wells were blocked with sterile 3% tryptone in PBS (see ERK2 kinase plates preparation for full procedure).

4.5. Cell-based assay

HEK-293T cell culture

HEK-293T cells were obtained from a frozen stock and cultured in the appropriate dishes sizes with Dulbecco's Modified Eagle Medium, supplemented with 10% FBS, 5% Penicillin-Streptomycin. Incubation temperature was 37 ºC. 0.5 % Trypsin-EDTA (Gibco®) was used for cell digestion.

Transduction of HEK-293T cells with RSK4 lentivirus

To $3x10^5$ HEK-293T cells in a 15-mL falcon tube, 90 µL of RSK4 lentivirus was added. Then 1.5 mL of culture medium was added and mixed. The contents of the tube were then divided into 3 wells of a 12-well tissue culture plate and incubated at 37 ºC for 72 h. The cells were passed and combined on a 15-cm plate containing 20 mL of medium and incubated for another 24 h. Transduced and non-transduced cells were sorted using Fluorescence-Activated Cell Sorting (FACS). Sorted cells ($5x10^4$ cells) were then plated on a single well of a 12-well tissue culture plate and incubated for 72 h. Cells were then passaged and transferred to 3 wells of the same 12-well tissue culture plate. After another 72 h, the cells were passaged and transferred to 10-cm plates and kept for expansion.

General cell-based assay protocol

Using 35-mm dishes, 10^6 transduced cells were seeded and incubated overnight. Inhibitors and controls were added at the relevant concentration and incubated for 2 hours. 20 minutes prior to collecting lysates, cells were further stimulated with EGF (final concentration 20 nM). After the end of EGF incubation, medium was removed by suction, plates washed twice with PBS and 40 µL of hot lysis buffer was added and cells were scrapped. Samples were collected in Eppendorf tubes and boiled at 95 °C for 10 min and further stored at -20 ºC. Concentration of lysates were measured with Nanodrop or

calculated using the DC™ Protein Assay (Bio-Rad). Analysis was carried out using general method for Western blots.

Western blot quantification with ImageJ

After developing the western blots, images were saved as JPEG in grayscale. Using ImageJ, measurements were set for “mean gray value” only. A Region of Interest (ROI) was defined for each row of protein. Measurements were taken for each lane of the same row of protein with the same ROI, including for the background of each lane (below or above each band). For each value (protein band and background), the inverted value (255 - X) was calculated. The net protein was then calculated by deducting the inverted background from the inverted band value. The final relative quantification values are the ratio of the net protein band to the net loading control band of each lane.

In-gel digestion

Samples (20 µg of protein) were added to 6x SDS/Sample buffer and dH_2O, and boiled at 95 °C for 3 min before being resolved by gel electrophoresis (SDS-PAGE), using Novex™ 8% Tris-Glycine pre-cast gels (Invitrogen). The gels were washed twice for 5 minutes with dH_2O and stained with Simply Blue Safe Stain (Life Technologies) for 20 minutes before being destained in dH_2O overnight. The gels were imaged and each lane was cut out and further destained in 50% methanol in dH_2O. Each lane was cut into approximately 1 mm^3 pieces and in-gel digestion was performed based on Schevchenko et al[108]. Briefly, gel pieces were dehydrated with 150 µL of acetonitrile for 10 minutes which was aspirated before the addition of 50 µL mM dithiothreitol in 0.1 M ammonium bicarbonate buffer (AmBic) for 0.5 h at 56 ºC. Excess reagent was removed and the pieces dehydrated again with acetonitrile before the addition of 40 µL mM iodoacetamide in 0.1M AmBic for 20 minutes at r. t. in the dark. The gels were subsequently dehydrated once more and washed with 150 µL of 0.1 M AmBic for 15 minutes, followed by another dehydration addition before the addition of 40 µL of modified porcine trypsin (Promega)

(12.5 ng/L) for 45 minutes at 37 ºC. A further 10 µL of 0.1 M AmBic was added and left overnight at 37 ºC. During peptide extraction, all solutions were retained and pooled. Trypsin was removed the following morning and 20 µL of 25 mM AmBic was added and incubated for 15 min at 37 ºC to wash before dehydration with 20 µL of acetonitrile for 15 min at 37 ºC. The supernatants for each sample were removed and pooled before adding 20 µL of extraction buffer (1% formic acid, 2% acetonitrile in dH_2O) for 15 min at 37 ºC. Supernatants were collected and pooled for each sample and extraction repeated once more. Samples were then dried in a vacuum centrifuge and stored at -80 ºC until ready for analysis by LC-MS.

References

1. Wong, M. C. S., Lao, X. Q., Ho, K., Goggins, W. B. & Tse, S. L. A. Incidence and mortality of lung cancer : global trends and association with socioeconomic status. *Sci. Rep.* 1–9 (2017). doi:10.1038/s41598-017-14513-7
2. Alberg, A. J., Brock, M. V, Ford, J. G., Samet, J. M. & Spivack, S. D. Epidemiology of Lung Cancer 3rd ed : American College of Chest Physicians Evidence-Based Clinical Practice Guidelines. *Chest* **143,** 1–29 (2013).
3. Herbst, R. S., Morgensztern, D. & Boshoff, C. The biology and management of non-small cell lung cancer. *Nature* **553,** 446–454 (2018).
4. Sutherland, K. D. & Berns, A. Cell of origin of lung cancer. *Mol. Oncol.* **4,** 397–403 (2010).
5. Hanahan, D. & Weinberg, R. A. Hallmarks of Cancer: The Next Generation. *Cell* **144,** 646–674 (2011).
6. He, X. Efficacy and safety of docetaxel for advanced non-small-cell lung cancer : a meta-analysis of Phase III randomized controlled trials. 2023–2031 (2015).
7. Burris, H. A. Shortcomings of current therapies for non-small-cell lung cancer: Unmet medical needs. *Oncogene* **28,** S4–S13 (2009).
8. Shaw, A. T. *et al.* Crizotinib versus Chemotherapy in Advanced ALK-Positive Lung Cancer. *N. Engl. J. Med.* **368,** 2385–2394 (2013).
9. Huang, L. & Fu, L. Mechanisms of resistance to EGFR tyrosine kinase inhibitors. *Acta Pharm. Sin. B* **5,** 390–401 (2015).
10. Manning, G., Whyte, D. B., Martinez, R. & Hunter, T. The Protein Kinase Complement of the Human Genome. *Science (80-.).* **298,** 1912–1934 (2002).
11. Ma, H., Deacon, S. & Horiuchi, K. The challenge of selecting protein kinase assays for lead discovery optimization. *Expert Opin. Drug Discov.* **1,** 607–621 (2008).
12. Ubersax, J. A. & Ferrell, J. E. Mechanisms of specificity in protein phosphorylation.

Nat. Rev. Mol. Cell Biol. **8,** 530–541 (2007).

13. Sebolt-Leopold, J. S. & Herrera, R. Targeting the mitogen-activated protein kinase cascade to treat cancer. *Nat. Rev. Cancer* **4,** 937–947 (2004).
14. Rubinfeld, H. & Seger, R. The ERK Cascade: A Prototype of MAPK Signaling. *Mol. Biotechnol.* **31,** 151–174 (2005).
15. Meloche, S. & Pouysségur, J. The ERK1/2 mitogen-activated protein kinase pathway as a master regulator of the G1- to S-phase transition. *Oncogene* **26,** 3227–39 (2007).
16. Melnikova, I. & Golden, J. Targeting protein kinases. *Nat. Rev. Drug Discov.* **3,** 993–994 (2004).
17. Zhang, J., Yang, P. L. & Gray, N. S. Targeting cancer with small molecule kinase inhibitors. *Nat. Rev. Cancer* **9,** 28–39 (2009).
18. Cohen, P. & Alessi, D. R. Kinase drug discovery - What's next in the field? *ACS Chem. Biol.* **8,** 96–104 (2013).
19. Wenthur, C. J., Gentry, P. R., Mathews, T. P. & Lindsley, C. W. Drugs for allosteric sites on receptors. *Annu Rev Pharmacol Toxicol* **54,** 165–184 (2014).
20. Pettinger, J., Jones, K. & Cheeseman, M. D. Lysine-Targeting Covalent Inhibitors. *Angew. Chemie - Int. Ed.* **56,** 15200–15209 (2017).
21. Liu, Q. *et al.* Developing irreversible inhibitors of the protein kinase cysteinome. *Chem. Biol.* **20,** 146–159 (2013).
22. Romeo, Y., Zhang, X. & Roux, P. P. Regulation and function of the RSK family of protein kinases. *Biochem. J.* **441,** 553–569 (2012).
23. Chrestensen, C. a & Sturgill, T. W. Characterization of the p90 ribosomal S6 kinase 2 carboxyl-terminal domain as a protein kinase. *J. Biol. Chem.* **277,** 27733–41 (2002).
24. Malakhova, M. *et al.* Structural diversity of the active N-terminal kinase domain of p90 ribosomal S6 kinase 2. *PLoS One* **4,** e8044 (2009).
25. Carriere, A., Ray, H., Blenis, J. & Roux, P. P. The RSK factors of activating the

Ras/MAPK signaling cascade. *Front. Biosci.* **13,** 4258–4275 (2008).

26. Anjum, R. & Blenis, J. The RSK family of kinases: Emerging roles in cellular signalling. *Nat. Rev. Mol. Cell Biol.* **9,** 747–758 (2008).
27. Yntema, H. G. *et al.* A novel ribosomal S6-Kinase is commonly deleted in patients with complex X-linked mental retardation. *Genomics* **62,** 332–343 (1999).
28. Dummler, B. A. *et al.* Functional characterization of human RSK4, a new 90-kDa ribosomal S6 kinase, reveals constitutive activation in most cell types. *J. Biol. Chem.* **280,** 13304–13314 (2005).
29. Lara, R., Seckl, M. J. & Pardo, O. E. The p90 RSK family members: common functions and isoform specificity. *Cancer Res.* **73,** 5301–8 (2013).
30. Jensen, C. J. *et al.* 90-kDa Ribosomal S6 Kinase Is Phosphorylated and Activated by 3-Phosphoinositide-dependent Protein Kinase-1*. *J. Biol. Chem* **274,** 27168–27176 (1999).
31. Favata, M. F. *et al.* Identification of a Novel Inhibitor of Mitogen-activated Protein Kinase Kinase *. *J. Biol. Chem.* **273,** 18623–18632 (1998).
32. Ludwik, K. A. & Lannigan, D. A. Ribosomal S6 kinase (RSK) modulators: a patent review. *Expert Opin. Ther. Pat.* **26,** 1061–1078 (2016).
33. Moon, H. G. *et al.* Phosphorylation of p90RSK is associated with increased response to neoadjuvant chemotherapy in ER-positive breast cancer. *BMC Cancer* **12,** 1 (2012).
34. Stratford, A. L. *et al.* Targeting p90 ribosomal S6 kinase eliminates tumor-initiating cells by inactivating Y-box binding protein-1 in triple-negative breast cancers. *Stem Cells* **30,** 1338–1348 (2012).
35. Smith, J. A. *et al.* Identification of the first specific inhibitor of p90 ribosomal S6 kinase (RSK) reveals an unexpected role for RSK in cancer cell proliferation. *Cancer Res.* **65,** 1027–1034 (2005).
36. Clark, D. E. *et al.* The serine/threonine protein kinase, p90 ribosomal S6 kinase, is an important regulator of prostate cancer cell proliferation. *Cancer Res.* **65,**

3108–3116 (2005).

37. Cho, Y.-Y. *et al.* RSK2 as a key regulator in human skin cancer. *Carcinogenesis* **33,** 2529–2537 (2012).

38. Kang, S. *et al.* p90 ribosomal S6 kinase 2 promotes invasion and metastasis of human head and neck squamous cell carcinoma cells. *J. Clin. Invest.* **120,** 1165–1177 (2010).

39. Lopez-Vincente, L. *et al.* Regulation of replicative and stress-induced senescence by RSK4, which is down-regulated in human tumors. *Clin. Cancer Res.* **15,** 4546–4553 (2009).

40. Lopez-Vincente, L. *et al.* RSK4 inhibition results in bypass of stress-induced and oncogene-induced senescence. *Carcinogenesis* **32,** 470–476 (2011).

41. Thakur, A. *et al.* Aberrant expression of X-linked genes RbAp46, Rsk4, and Cldn2 in breast cancer. *Mol. Cancer Res.* **5,** 171–181 (2007).

42. Thakur, A. *et al.* Anti-invasive and antimetastatic activities of ribosomal protein S6 kinase 4 in breast cancer cells. *Clin. Cancer Res.* **14,** 4427–4436 (2008).

43. Serra, V. *et al.* RSK 3/4 mediate resistance to PI3K pathway inhibitors in breast cancer. *J. Cinical Investig.* **123,** 2551–2563 (2013).

44. Fan, L. *et al.* Ribosomal s6 protein kinase 4: a prognostic factor for renal cell carcinoma. *Br. J. Cancer* **109,** 1137–46 (2013).

45. Lara, R. *et al.* An siRNA screen identifies RSK1 as a key modulator of lung cancer metastasis. *Oncogene* **30,** 3513–3521 (2011).

46. Zhou, Y. *et al.* Crucial roles of RSK in cell motility by catalysing serine phosphorylation of EphA2. *Nat. Commun.* **6,** 1–12 (2015).

47. Cohen, M. S., Zhang, C., Shokat, K. M. & Taunton, J. Structural bioinformatics-based design of selective, irreversible kinase inhibitors. *Science (80-.).* **308,** 1318–1321 (2005).

48. Smith, J. A. *et al.* Identification of the First Specific Inhibitor of p90 Ribosomal S6 Kinase (RSK) Reveals an Unexpected Role for RSK in Cancer Cell Proliferation.

Cancer Res. 1027–1034 (2005).

49. Sapkota, G. P. *et al.* BI-D1870 is a specific inhibitor of the p90 RSK (ribosomal S6 kinase) isoforms in vitro and in vivo. *Biochem. J.* **401,** 29–38 (2007).

50. Aronchik, I. *et al.* Novel Potent and Selective Inhibitors of p90 Ribosomal S6 Kinase Reveal the Heterogeneity of RSK Function in MAPK-Driven Cancers. *Mol. Cancer Res.* **12,** 803–812 (2014).

51. Nguyen, T. Targeting RSK: An Overview of Small Molecule Inhibitors. *Anticancer. Agents Med. Chem.* **8,** 710–716 (2008).

52. Lesher, G. Y., Froelich, E. J., Gruett, M. D., Bailey, J. H. & Brundage, R. P. 1,8-Naphthyridine Derivatives. A New Class of Chemotherapeutic Agents. *J. Med. Chem.* **5,** 1063–1065 (1962).

53. Bisacchi, G. S. Origins of the Quinolone Class of Antibacterials: An Expanded 'Discovery Story'. *J. Med. Chem.* **58,** 4874–4882 (2015).

54. Andriole, V. T. The Quinolones : Past , Present , and Future. *Clin. Infect. Dis.* **41,** 113–119 (2005).

55. Wolfson, J. S. & Hooper, D. C. Fluoroquinolone Antimicrobial Agents. *Clin. Microbiol. Rev.* **2,** 378–424 (1989).

56. Zhanel, G. G. *et al.* The New Fluoroquinolones: A Critical Review. *Can. J. Infect. Dis.* **10,** 207–238 (1999).

57. Aldred, K. J., Kerns, R. J. & Osherof, N. Mechanism of Quinolone Action and Resistance. *Biochemistry* **53,** 1565–1574 (2014).

58. Domagala, J. M. Structure-activity and structure-activity-side-effect relationships for the quinolone antibacterials. *J. Antimicrob. Chemother.* **33,** 685–706 (1994).

59. Chu, D. T. & Fernandes, P. B. Structure-Activity Relationships of the Fluoroquinolones. *Antimicrob. Agents Chemother.* **33,** 131–135 (1989).

60. Brighty, K. E. Azabicyclo Quinolone and Naphthyridinone Carboxylic Acids. (1992). doi:US005485919A

61. Brighty, K. E. & Gootz, T. D. The chemistry and biological profile of trovafloxacin.

J. Antimicrob. Chemother. **39 Suppl B,** 1–14 (1997).

62. Briggs-Gooding, B. & Jones, R. N. In vitro antimicrobial activity of CP-99,219, a novel azabicyclo-naphthyridone. *Antimicrob.Agents Chemother.* **37,** 349–353 (1993).

63. Eliopoulos, G. M., Klimm, K., Eliopoulos, C. T., Ferraro, M. J. & Moellering, R. C. In vitro activity of CP-99,219, a new fluoroquinolone, against clinical isolates of gram-positive bacteria. *Antimicrob. Agents Chemother.* **37,** 366–370 (1993).

64. Girard, A. E., Girard, D., Gootz, T. D., Faiella, J. A. & Cimochowski, C. R. In vivo efficacy of trovafloxacin (CP-99 , 219), a new quinolone with extended activities against gram-positive pathogens , Streptococcus pneumoniae , and Bacteroides fragilis . In Vivo Efficacy of Trovafloxacin (CP-99 , 219), a New Quinolone with Ext. *Antimicrob. Agents Chemother.* **39,** 2210–2216 (1995).

65. Spangler, S. K., Jacobs, M. R. & Appelbaum, P. C. Activity of CP 99,219 compared with those of ciprofloxacin, grepafloxacin, metronidazole, cefoxitin, piperacillin, and piperacillin-tazobactam against 489 anaerobes. *Antimicrob. Agents Chemother.* **38,** 2471–2476 (1994).

66. Teng, R., Girard, D., Gootz, T. D., Foulds, G. & Liston, T. E. Pharmacokinetics of trovafloxacin (CP-99,219), a new quinolone, in rats, dogs, and monkeys. *Antimicrob. Agents Chemother.* **40,** 561–566 (1996).

67. Teng, R., Liston, T. E. & Harris, S. C. Multiple-dose pharmacokinetics and safety of trovafloxacin in healthy volunteers. *J. Antimicrob. Chemother.* **37,** 955–963 (1996).

68. Teng, R. *et al.* Pharmacokinetics and safety of CP-99,219, a new quinolone antibiotic, following administration of single oral doses to healthy male volunteers. *J. Antimicrob. Chemother.* **36,** 385–394 (1995).

69. Bertino, J. & Fish, D. The Safety Profile of the Fluoroquinolones. *Clin. Ther.* **22,** 798–817 (2000).

70. Shaw, P. J., Ganey, P. E. & Roth, R. A. Idiosyncratic drug-induced liver injury and

the role of inflammatory stress with an emphasis on an animal model of trovafloxacin hepatotoxicity. *Toxicol. Sci.* **118,** 7–18 (2010).

71. Shaw, P. J. *et al.* Trovafloxacin enhances TNF-induced inflammatory stress and cell death signaling and reduces TNF clearance in a murine model of idiosyncratic hepatotoxicity. *Toxicol. Sci.* **111,** 288–301 (2009).
72. Shaw, P. J., Ganey, P. E. & Roth, R. A. Tumor Necrosis Factor alpha Is a Proximal Mediator of Synergistic Hepatotoxicity from Trovafloxacin / Lipopolysaccharide Coexposure. *J. Pharmacol. Exp. Ther.* **328,** 62–68 (2009).
73. Shaw, P. J., Hopfensperger, M. J., Ganey, P. E. & Roth, R. A. Lipopolysaccharide and trovafloxacin coexposure in mice causes idiosyncrasy-like liver injury dependent on tumor necrosis factor-alpha. *Toxicol. Sci.* **100,** 259–266 (2007).
74. Chu, D. T., Fernandes, P. B., Claiborne, A. K., Gracey, E. H. & Pernet, A. G. Synthesis and Structure-Activity Relationships of New Arylfluoronaphthyridine Antibacterial Agents. *J. Med. Chem.* **29,** 2363–2369 (1986).
75. Chu, D. T. W. *et al.* Synthesis and structure-activity relationships of novel arylfluoroquinolone antibacterial agents. *J. Med. Chem.* **28,** 1558–1564 (1985).
76. Matsumoto, J. *et al.* 1,4-Dihydro-4-oxopyridinecarboxylic acids as antibacterial agents. 2. Synthesis and structure-activity relationships of 1,6,7-trisubstituted 1,4-dihydro-4-oxo-1,8-naphthyridine-3-carboxylic acids, including enoxacin, a new antibacterial agent. *J. Med. Chem.* **27,** 292–301 (1984).
77. Remuzon, P. *et al.* Fluoronaphthyridines and -quinolones as Antibacterial Agents. 3. Synthesis and Structure-Activity Relationships of New 1-(1,1-Dimethyl-2-fluoroethyl), 1-[1-Methyl-1-(fluoromethyl)-2-fluoroethyl], and 1-[1,1-(Difluoromethyl) -2-fluoroethyl] Substituted De. *J. Med. Chem.* **34,** 29–37 (1991).
78. Norris, T. *et al.* Synthesis of trovafloxacin using various (1α,5α,6α)-3-azabicyclo[3.1.0]hexane derivatives. *J. Chem. Soc. Perkin Trans. 1* **4,** 1615–1622 (2000).
79. Lebel, H., Marcoux, J. F., Molinaro, C. & Charette, A. B. Stereoselective

Cyclopropanation Reactions. *Chem. Rev.* **103,** 977–1050 (2003).

80. Ballini, R., Fiorini, D. & Palmieri, A. A General Procedure for the One-pot Preparation of Polyfunctionalized Nitrocyclopropanes. *Synlett* 1704–1706 (2003).

81. Braish, T. F. *et al.* Construction of the (1a,5a,6a)-6-Amino-3-Azabiyclo[3.1.0]hexane Ring System. *Synlett* 1100–1102 (1996).

82. Madhusudhan, G., Balraju, V., Rajesh, T., Narayana, B. V. & Reddy, R. N. Synthesis of an amino moiety in trovafloxacin by using an in-expensive amidine base, N, N-diethylacetamidine. *Indian J. Chem.* **48,** 569–573 (2009).

83. Brighty, K. E. & Castaldi, M. Synthesis of (1α,5α,6α)-6-amino-3-azabicyclo[3.1.0]hexane, a novel chiral diamine. *Synlett* 1097–1099 (1996). doi:10.15713/ins.mmj.3

84. Handanyan, L. A., Morris, T. A., Hendrickson, P. J. J. & Norris, T. Crystal form of anhydrous 7-([1a,5a,6a]-6-amno-3-azabicyclo[3.1.0]hex-3-yl)-6-fluoro-1-(2,4-difluorophenyl)-1,4-dihydro-4-oxo-1,8 naphthyridne-3- carboxylic acid, methanesulfonic acid salt. (1998). doi:USOO5763454A

85. Yadav, J. S., Balanarsaiah, E., Raghavendra, S. & Satyanarayana, M. Chemoselective hydrolysis of tert-butyl esters in acetonitrile using molecular iodine as a mild and efficient catalyst. *Tetrahedron Lett.* **47,** 4921–4924 (2006).

86. Wu, Y., Limburg, D. C., Wilkinson, D. E., Vaal, M. J. & Hamilton, G. S. A mild deprotection procedure for tert -butyl esters and tert -butyl ethers using ZnBr 2 in methylene chloride. *Tetrahedron* **41,** 2847–2849 (2000).

87. Li, B. *et al.* Aqueous phosphoric acid as a mild reagent for deprotection of tert-butyl carbamates, esters, and ethers. *J. Org. Chem.* **71,** 9045–9050 (2006).

88. Florindo, C. *et al.* Novel organic salts based on fluoroquinolone drugs: Synthesis, bioavailability and toxicological profiles. *Int. J. Pharm.* **469,** 179–189 (2014).

89. Hoegenauer, K. *et al.* Discovery of novel pyrrolidineoxy-substituted heteroaromatics as potent and selective PI3K delta inhibitors with improved physicochemical properties. *Bioorganic Med. Chem. Lett.* **26,** 5657–5662 (2016).

90. Miyamoto, T. & Matsumoto, J. Fluorinated pyrido[2,3-c]pyridazines. II. Synthesis and antibacterial activity of 1,7-disubstituted-6-fluoro-4(1H)-oxopyrido[2,3-c]pyridazine-3-carboxylic acids. *Chem. Pharm. Bull.* **38,** 3359–3365 (1990).

91. Terstappen, G. C., Schlüpen, C., Raggiaschi, R. & Gaviraghi, G. Target deconvolution strategies in drug discovery. *Nat. Rev. Drug Discov.* **6,** 891–903 (2007).

92. Eder, J., Sedrani, R. & Wiesmann, C. The discovery of first-in-class drugs: Origins and evolution. *Nat. Rev. Drug Discov.* **13,** 577–587 (2014).

93. Khokhlatchev, A. *et al.* Reconstitution of Mitogen-activated Protein Kinase Phosphorylation Cascades in Bacteria. *J. Biol. Chem.* **272,** 11057–11062 (1997).

94. Robarge et al. Discovery of GDC-0994, a potent and selective ERK1/2 inhibitor in early clinical development. in *AACR Annual Meeting 2014* (2014).

95. Sivashanmugam, A. *et al.* Practical protocols for production of very high yields of recombinant proteins using Escherichia coli. *Protein Sci.* **18,** 936–948 (2009).

96. Kost, T. A., Condreay, J. P. & Jarvis, D. L. Baculovirus as versatile vectors for protein expression in insect and mammalian cells. *Nat. Biotechnol.* **23,** 567–575 (2005).

97. Joel, P. B. *et al.* pp90rsk1 Regulates Estrogen Receptor-Mediated Transcription through Phosphorylation of Ser-167. *Mol. Cell. Biol.* **18,** 1978–1984 (1998).

98. Mrozowski, R. M. *et al.* De novo synthesis and biological evaluation of C6″-substituted C4″-amide analogues of SL0101. *Org. Lett.* **16,** 5996–5999 (2014).

99. Hacker, D. L. & Balasubramanian, S. Recombinant protein production from stable mammalian cell lines and pools. *Curr. Opin. Struct. Biol.* **38,** 129–136 (2016).

100. Wurm, F. M. Production of recombinant protein therapeutics in cultivated mammalian cells. *Nat. Biotechnol.* **22,** 1393–1398 (2004).

101. Büssow, K. Stable mammalian producer cell lines for structural biology. *Curr. Opin. Struct. Biol.* **32,** 81–90 (2015).

102. Mancia, F. *et al.* Optimization of protein production in mammalian cells with a

coexpressed fluorescent marker. *Structure* **12,** 1355–1360 (2004).

103. Smith, G. K. & Wood, E. R. Cell-based assays for kinase drug discovery. *Drug Discov. Today* **7,** e13–e19 (2010).

104. Lipinski, C. A., Lombardo, F., Dominy, B. W. & Feeney, P. J. Experimental and computational approaches to estimate solubility and permeability in drug discovery and development settings. *Adv. Drug Deliv. Rev.* **46,** 3–26 (2001).

105. Veber, D. F. *et al.* Molecular properties that influence the oral bioavailability of drug candidates. *J. Med. Chem.* **45,** 2615–2623 (2002).

106. Ertl, P., Rohde, B. & Selzer, P. Fast calculation of molecular polar surface area as a sum of fragment-based contributions and its application to the prediction of drug transport properties. *J. Med. Chem.* **43,** 3714–3717 (2000).

107. Zhang, Y., Fonslow, B. R., Shan, B., Baek, M. C. & Yates, J. R. Protein Analysis by Shotgun / Bottom-up Proteomics. *Chem. Rev.* **113,** 2343–2394 (2013).

108. Shevchenko, A., Wilm, M., Vorm, O. & Mann, M. Mass spectrometric sequencing of proteins from silver-stained polyacrylamide gels. *Anal. Chem.* **68,** 850–858 (1996).